AFML-TR-71-142

MANUFACTURING METHODS AND TECHNOLOGY FOR PROCESSING COBALT-SAMARIUM MAGNETS

M. G. Benz, et al.

Technical Report AFML-TR-71-142

July 1971

AIR FORCE MATERIALS LABORATORY
AIR FORCE SYSTEMS COMMAND
WRIGHT-PATTERSON AIR FORCE BASE, OHIO 45433

UNCLASSIFIED

Security Classification

DOCUMENT CONTROL DATA - R & D

(Security classification of title, body of abstract and indexing annotation must be entered when the overall report is classified)

1. ORIGINATING ACTIVITY (Corporate author) General Electric Company Research and Development Center Schenectady, New York	2a. REPORT SECURITY CLASSIFICATION Unclassified 2b. GROUP

3. REPORT TITLE

MANUFACTURING METHODS AND TECHNOLOGY FOR PROCESSING COBALT-SAMARIUM MAGNETS

4. DESCRIPTIVE NOTES (Type of report and inclusive dates)

Technical Report AFML-TR-71-142 November 15, 1969 to May 15, 1971

5. AUTHOR(S) (First name, middle initial, last name)

Mark G. Benz et al.

6. REPORT DATE	7a. TOTAL NO. OF PAGES	7b. NO. OF REFS
July 1971	178	28

8a. CONTRACT OR GRANT NO.	9a. ORIGINATOR'S REPORT NUMBER(S)
F33615-70-C-1098	
b. PROJECT NO. 612-9A	S-71-1102
c.	9b. OTHER REPORT NO(S) (Any other numbers that may be assigned this report) AFML-TR-71-142
d.	

10. DISTRIBUTION STATEMENT

Approved for Public Release -- Distribution Unlimited.

11. SUPPLEMENTARY NOTES	12. SPONSORING MILITARY ACTIVITY
--	Air Force Materials Laboratory (MATE) Wright-Patterson Air Force Base, Ohio 45433

13. ABSTRACT Alternative manufacturing methods, processes, and techniques for fabrication of cobalt-samarium magnets have been evaluated.

A pre-production pilot line capable of producing cobalt-samarium magnets has been established.

The properties of magnets produced on this pre-production pilot line exceed : $(BH)_{max}$ 15 MGOe, B_r 8.2 kG, H_c 6.5 kOe, H_d (at $B/H = -1/2$) -5.0 kOe, and the irreversible loss (at $B/H = -1/2$) on exposure to 150°C less than 10%.

The cost of magnets produced on this pre-production pilot line was approximately one fourth the cost the same size magnet would be if fabricated from cobalt-platinum.

Magnets produced on this pilot line have been used to successfully fabricate five traveling wave tubes.

The performance of these tubes indicates that cobalt-samarium magnets are suitable for fabrication of traveling wave tubes; and, in fact, that they will allow further advances in the state-of-the-art in the design of such tubes.

DD FORM 1 NOV 1473

UNCLASSIFIED

Security Classification

NOTICE

When Government drawings, specifications, or other data are used for any purpose other than in connection with a definitely related Government procurement operation, the United States Government thereby incurs no responsibility nor any obligation whatsoever; and the fact that the government may have formulated, furnished, or in any way supplied the said drawings, specifications, or other data, is not to be regarded by implication or otherwise as in any manner licensing the holder or any other person or corporation, or conveying any rights or permission to manufacture, use, or sell any patented invention that may in any way be related thereto.

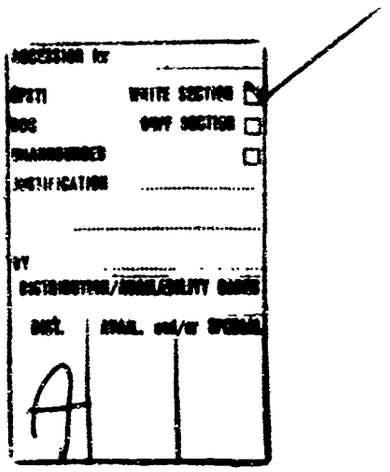

Copies of this report should not be returned unless return is required by security considerations, contractual obligations, or notice on a specific document.

KEY WORDS	LINK A		LINK B		LINK C	
	ROLE	WT	ROLE	WT	ROLE	WT
Magnufacturing Methods						
Permanent Magnets						
Rare Earth Magnets						
Cobalt-Samarium Magnets						
Traveling Tube Magnets						
Microwave Tube Magnets						

MANUFACTURING METHODS AND TECHNOLOGY FOR PROCESSING COBALT-SAMARIUM MAGNETS

General Electric Company
Research and Development Center
Schenectady, New York

ABSTRACT

Alternative manufacturing methods, processes, and techniques for fabrication of cobalt-samarium magnets have been evaluated.

A pre-production pilot line capable of producing cobalt-samarium magnets has been established.

The properties of magnets produced on this pre-production pilot line exceed: $(BH)_{max}$ 15 MGOe, B_r 8.2 kG, H_c -6.5 kOe, H_d (at B/H = -1/2) -5.0 kOe, and the irreversible loss (at B/H = -1/2) on exposure to 150°C less than 10%.

The cost of magnets produced on this pre-production pilot line was approximately one fourth the cost the same size magnet would be if fabricated from cobalt-platinum.

Magnets produced on this pilot line have been used to successfully fabricate five traveling wave tubes.

The performance of these tubes indicates that cobalt-samarium magnets are suitable for fabrication of traveling wave tubes; and, in fact, that they will allow further advances in the state-of-the-art in the design of such tubes.

FOREWORD

This report was prepared by the Properties Branch of the Metallurgy and Ceramics Laboratory, Research and Development Center, General Electric Company, Schenectady, New York, under USAF Contract No. F33615-70-C-1098. The contract was initiated under Project No. 612-9A. The work was administered under the direction of R. J. Charles, Properties Branch Manager and the Air Force Material Laboratory, Manufacturing Technology Division, Mr. H. K. Trinkle, project engineer.

Contributors to the work presented in this report are: M. G. Benz, R. E. Cech, R. P. Laforce, D. L. Martin, J. M. Reynolds, W. A. Reed, A. C. Rockwood, and C. E. Van Buren of the Research and Development Center, General Electric Company, Schenectady, New York; F. G. Jones and R. J. Parker of the Magnetic Materials Business Section, General Electric Company, Edmore, Michigan; and T. P. Carlisle, J. E. Grant, J. Kennedy, R. H. LeBorgne, and other members of the staff of the Electron Dynamics Division of Hughes Aircraft Company, Torrance, California.

The above contributors would like to acknowledge the assistance of J. T. Geertsen, R. T. Laing, and W. F. Moore of GE Corporate Research and Development, and K. D. Camp, R. B. Downs, A. G. Guy, H. E. Lehman, J. E. Macklin, G. H. Ravell, and E. B. Sinclair of the Magnetics Materials Business Section, General Electric Company, Edmore, Michigan. This report covers work from 15 November 1969 to 15 May 1971.

This technical report has been reviewed and is approved.

JULES I. WITTEBORT
Chief, Electronics Branch
Manufacturing Technology Division

CONTENTS

Contents (cont'd.)

LIST OF ILLUSTRATIONS

LIST OF TABLES

SECTION I

INTRODUCTION

The specific objective of this program is to establish manufacturing methods, processes, techniques, and special equipment for fabrication of cobalt-samarium magnets in production quantities. Although various research studies at the General Electric Research and Development Center have shown several procedures suitable for fabrication of high performance magnets, the one selected for further work on this manufacturing methods program is the procedure based on liquid-phase sintering of samarium-rich Co_5Sm to a closed pore structure. A copy of the paper, "Cobalt-Samarium Permanent Magnets Prepared by Liquid Phase Sintering"[1] outlining this approach, is included as the next section of this report.

The manufacturing methods program has proceeded as follows. Alternative unit operations which could be used for each step of the fabrication sequence have been evaluated during Phase I--Analysis. Traveling wave tube, and magnet dimensions and performance characteristics have also been established during this phase. Final reports for this phase are included in the section entitled Phase I--Analysis.

Processes and techniques for use in the pilot line have been selected and are discussed in the section entitled Phase II--Determination of Manufacturing Process.

A pre-production pilot line has been established and is discussed in the sections entitled Phase III (Part 1)--Pre-production Pilot Line: Powder and Phase III (Part 2)--Pre-production Pilot Line: Magnets.

Traveling wave tubes have been fabricated and evaluated. These are discussed in the section entitled Phase IV--Microwave Device Application of Co_5Sm Magnets.

---

1. M.G. Benz and D.L. Martin, Appl. Phys. Letters 17, 176 (1970).

SECTION II

PREPRINT: M.G. Benz and D.L. Martin, Appl. Phys. Letters 17, 176 (1970).

COBALT-SAMARIUM PERMANENT MAGNETS PREPARED BY LIQUID PHASE SINTERING*

M.G. Benz and D.L. Martin

Research and Development Center
General Electric Company
Schenectady, New York 12301

ABSTRACT

The preparation and measurement of magnetic properties of cobalt-samarium permanent magnets prepared by liquid phase sintering are discussed. Energy products in excess of 15 x 10^6 gauss-Oe were observed. Long-time exposure to air at 150°C did not degrade the samples.

---

*Note: The work described in this paper was completed prior to this manufacturing methods program. It was part of a program of research funded by the General Electric Company.

COBALT-SAMARIUM PERMANENT MAGNETS PREPARED BY LIQUID PHASE SINTERING

M.G. Benz and D.L. Martin

The preparation of cobalt-rare earth permanent magnets has received the attention of several authors.[1-4] As noted in these studies, two problem areas relating to coercive force have been identified. The first is loss of coercive force for stoichiometric Co_5Sm during sintering. It has been observed that the intrinsic coercive force drops from 12 to 2 kOe during sintering at 1150°C.[4] The second is loss of coercive force during long-time exposure to air at slightly elevated temperatures.[1] Both of these problem areas have been eliminated by the approach outlined in this paper, i.e., liquid-phase sintering of samarium-rich Co_5Sm to a closed pore structure.

SAMPLE PREPARATION

A melt of essentially Co_5Sm was prepared by induction melting. This was crushed to coarse powder in a mortar and pestle. It was then further reduced to an average particle diameter of 6μ to 8μ by processing in a fluid energy mill using nitrogen as the working gas. A second melt of Co + 60 weight percent samarium was processed in a similar manner. This composition was selected as one of a series of compositions that would have a liquid phase component at the sintering temperature of 1100°C. Samples for chemical analysis indicated 66.7% cobalt for the first powder and 40% cobalt for the second. The two powders were blended by tumbling to an average composition of 62.6% This composition is in the range which produces maximum densification during sintering as disclosed by Cech.[5] Portions of this powder were placed in rubber tubes 3/8 inch (0.98 cm) in diameter and 1 3/4 inches (4.45 cm) long and packed to a density of 3.5 g/cm^3. These tubes of powder were placed in an axial magnetic field of 60,000 to 100,000 Oe in order to align the powder. After aligning, the rubber tubes were evacuated and then the samples were subsequently hydrostatically pressed to 200,000 psi. The pressed density was approximately 6.9 g/cm^3. The resultant bars were then ground to cylinders 1/4 inch (0.64 cm) in diameter by 1 1/4 inches (3.18 cm) long. Subsequent sinetering for one-half hour at 1100 degrees in high-purity argon increased the density to approximately 7.7 g/cm^3. Metallographic examination of the sintered bars showed approximately 10% void volume. These voids were of the noninterconnecting type.

MEASUREMENT OF MAGNETIC PROPERTIES

Cobalt-samarium magnets are difficult to measure because of the need for extremely high fields for saturation and demagnetization. Hysteresigraphs built for measuring the properties of Alnico and barium oxide ferrite magnets are limited to about 25,000 Oe, a field too low for Co-Sm magnet testing. We have used a 100,000 Oe, niobium-tin superconducting solenoid for our measurements.

The magnetization and demagnetization measurements were made at a number of constant field levels between ±100,000 Oe by withdrawing the sample from a close-fitting, calibrated search coil. The magnetization was calculated from the relation

$$4\pi J = \frac{C}{1-K} \frac{10^8 \int Edt}{N_c A_s}, \text{ Gauss} \qquad \text{(II-1)}$$

where C is the coil coupling coefficient,
K is the demagnetization factor,
N_c is the number of turns in the coil,
A_s is the sample area, cm^2, and
$\int Edt$ is the time integrated voltage, volt-sec measured for withdrawal of the specimen.

The applied field, H_A, was determined by measuring the $\int Edt$ when an axial coil of known $N_c A_c$ is removed from the solenoid field. H_A is calculated from the relation

$$H_A = \frac{10^8 \int Edt}{N_c A_c}, \qquad \text{(II-2)}$$

where A_c is the area of the coil, cm^2.

The internal field, H, was determined from the relation

$$H = H_A - K\,4\pi J \qquad \text{(II-3)}$$

The demagnetization factor, K, used in the above equations was calculated from the magnet radius, R, and length, L, and the equation

$$K = \frac{1}{1 + \frac{L}{R^2}\sqrt{R(R+L)}} . \qquad \text{(II-4)}$$

This equation is based on Evershed's polar radiation model, and assumes a reversible permeability of one.[6]

Data gathered in this manner for several sintered cobalt-samarium magnets are listed in Table I. The demagnetization curves for one sample before and after exposure to air at 150°C for 1145 hours are shown in Fig. 1. The slight difference in properties before and after 150°C aging is not considered significant, being less than the estimated measurement error at the time of this study.

TABLE I

Summary of Magnetic Properties

Sample No.	Density (g/cm^3)	Saturation Measured at 100 kOe (kGauss)	B_r (kGauss)	$_BH_c$ (kOe)	$_MH_c$ (kOe)	$(BH)_{max}$ (MGOe)
A	7.56	9.47	8.05	-7.70	-15.7	15.7
B	7.56	9.41	7.98	-7.80	-14.8	15.7
C	7.58	9.50	8.06	-7.70	-16.2	15.7
D	7.62	9.42	8.06	-7.70	-16.4	15.7
D	7.62	9.37	7.98	-7.40	-16.4	15.4

After 1145 hours at 150°C in air.

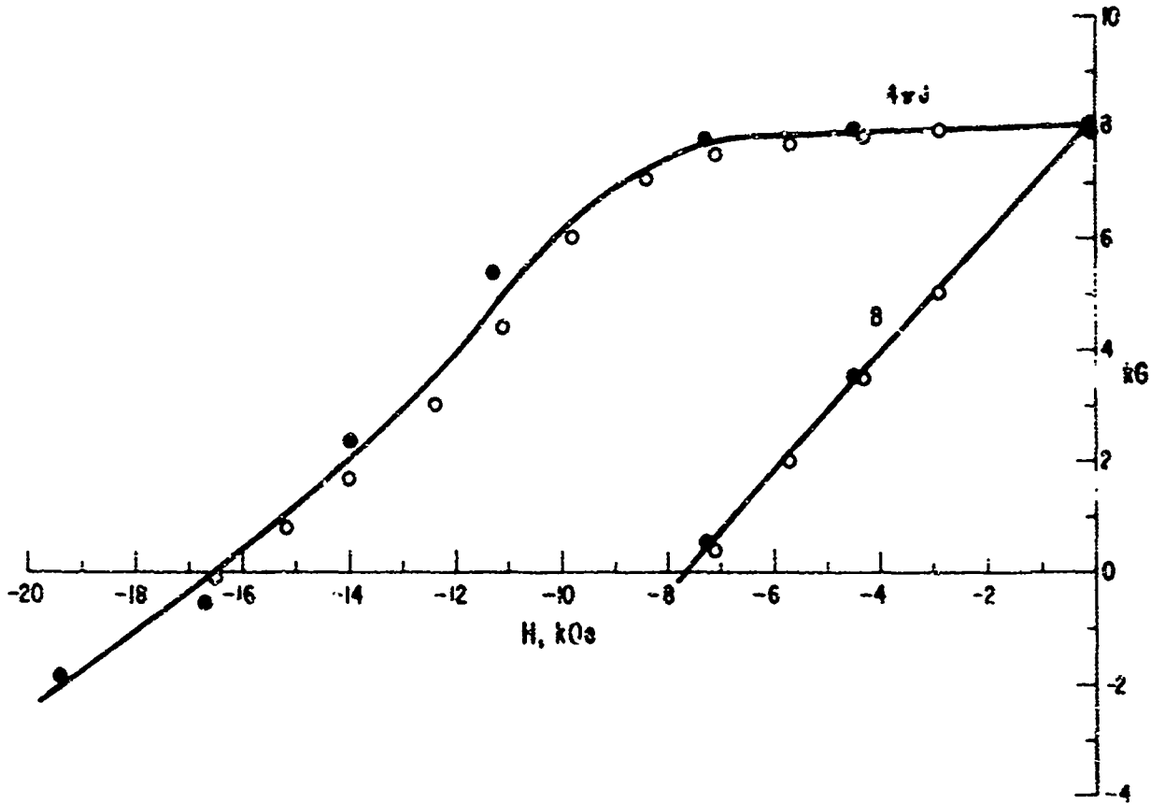

Figure 1 Magnetization and induction curves for sample D. Data represented by closed circles were taken before aging for 1145 hours at 150°C in air, and data represented by open circles were taken after.

SUMMARY AND CONCLUSIONS

1. Liquid phase sintering of cobalt-samarium is effective for preparation of high coercive force, high energy product magnets.

2. Sintering to a closed pore structure eliminates the loss of magnetic properties during long-time exposure to air at elevated temperatures normally observed for open pore structures.

3. Energy products in excess of 15 MGOe are reported in this paper. By improvements in alignment and packing, subsequent samples with energy products in excess of 20 MGOe have been realized.

ACKNOWLEDGMENTS

The authors would like to acknowledge the assistance of J.T. Geertsen, R.T. Laing, W.F. Moore, and A.C. Rockwood during this entire study, and the assistance of R.P. Laforce during the final portion of the study.

REFERENCES

1. J.J. Becker, Technical Report AFML-TR-67-28, Air Force Materials Laboratory, Dayton, Ohio (March 1967).

2. K.H.J. Buschow, W. Luiten, P.A. Naastepad, and F.F. Westendorp, Philips Tech. Rev., 29, 336 (1968).

3. D.K. Das, IEEE Trans. Magnetics, MAG 5, 214 (September 1969).

4. D.L. Martin (unpublished); also Fig. 34 in J.J. Becker, R.E. Cech, and D.L. Martin, "Research to Investigate Fundamental Magnetic Interactions in Selected Materials," Technical Report AFML-TR-70-76, Air Force Materials Laboratory (April 1970).

5. R.E. Cech, J. Appl. Phys., 41, 5247 (1970); also Fig. 44 in J.J. Becker, R.E. Cech, and D.L. Martin, ibid.

6. R.J. Parker and R.J. Studders, Permanent Magnets and Their Application, John Wiley and Sons, Inc., New York (1962), pp. 163-165.

SECTION III

Phase I--Analysis

As stated in Exhibit A of the contract work statement, the objective, criteria, and approach for this phase are:

• Objective. The objective of this phase is to analyze the problems associated with the establishment of manufacturing methods for the economical fabrication of cobalt-samarium magnets in production quantities, and to formulate a production plan for providing Co_5Sm magnets.

• Criteria and Approach

1. The effort under Phase I will be directed toward evaluation of the unit operations involved in manufacturing high-quality Co_5Sm magnets with respect toward their economics, reproducibility, and ease of transition into the magnet producing industry.

2. The work in this phase shall be divided into the following tasks:

Task 1--Raw Materials
Task 2--Melting and Casting
Task 3--Crushing
Task 4--Milling and Classifying
Task 5--Powder Storage
Task 6--Mixing Additives
Task 7--Magnetizing and Aligning Powder
Task 8--Pressing
Task 9--Sintering
Task 10--Shaping
Task 11--Magnetization
Task 12--Shipping

In addition to the above, the following Phase I--Supplementary Studies were conducted:

Supplementary Study

1. Multi-task Interaction Study
2. 150°C Aging Study
3. Temperature Coefficient Study Reversible and Irreversible Losses
4. Electrical and Mechanical Properties
5. Preparation and evaluation of Sample (1/2 Scale) TWT Magnets
6. Safety

A. Selection of Microwave Device

The traveling wave tube to be used in the evaluation of the Co_5Sm magnet shall be tube number, Hughes 641H. The performance characteristics of this tube shall be specified.

B. Magnet Characterization

1. Target Specifications (see Table II).

2. A complete specification of performance capability of the specified Co_5Sm magnet to be produced on this program, both by itself and in a periodic permanent magnet stack arrangement, shall be made at the end of this phase.

Pre-production Samples. Phase I--Pre-production samples in accordance with Exhibit A, paragraph B.1.d(2) specifications will be delivered at the completion of Phase I--Analysis.

All Phase I studies have been completed. Final Reports on each study are included in the following subsections. A description of the standard test bar utilized for many of these studies is included in Table III. Definitions for the symbols used in this report are listed in Table IV.

Task 1--Raw Materials (D.L. Martin and R.P. Laforce)

Two types of powder have been evaluated during this Phase I study. One type was prepared by melting cobalt and samarium to form a Co-Sm ingot which was converted into powder by crushing and milling. The other type powder was prepared from cobalt-samarium made by the alkaline hydride reduction process (i.e., the RD process).

The evaluation was based on magnetic properties measured on a standard, sintered test bar. In addition to the normal unit properties: B_S, B_r, H_c, H_{ci}, and $(BH)_{max}$, the demagnetizing field corresponding to a load line of slope-1/2 was also determined. This parameter (H_d at $B/H = -1/2$) is particularly useful for evaluating materials for use in the traveling wave tube selected by the Electron Dynamics Division of Hughes Aircraft Co. for Phase III evaluation of magnets.

Part 1--Powder from Ingot

High-purity, 99.9% samarium is available from numerous vendors. Because of a large variability in market price ($115 to $260 per pound), it was considered worthwhile to evaluate different sources.

TABLE II

Target Specification

Residual Induction (B_r)	> 7500 gauss
Coercive Force (H_c)	> 7500 Oe
Intrinsic Coercive Force (H_{ci})	> 12,000 Oe
Energy Product (BH_{max})	15×10^6 gauss-Oe
Temperature Stability	0.05% per °C
Magnet Life	Flux variation of > 5% over 1000 hours at 150°C for a magnet with load line of minus 1
Curie Point	> 700°C
Mechanical Properties	
Integrity	> 3% weight loss during normal handling (during shipping and assembly of TWT's)
Hardness	$R_c \cong 50$
Impact Strength	Capable of withstanding normal handling, assembly, and operation of TWT tubes consistent with MIL-5400 Class II environmental requirements
Flexural Strength	> 5000 psi
MIL-B-5400 Tests	
Corrosion	None
Temperature Extremes	Within 95° of original (-55° to 250°C) room temp properties

Note: See Table XXXIV for final specifications of typical properties of cobalt-samarium magnets to be fabricated during Phase III of this program.

TABLE III

Procedure for Making Standard Test Bars

1. Pack Co-Sm powder into a 3/8-inch-diameter by 1 3/4-inch-long rubber tube to a density of 3.5 g/cm^3
2. Align in a 60 kOe field. Vibrate the tube for 1 minute. Then evacuate tube* or advance end plungers to increase density to 4.5 g/cm^3 before removing sample from the field
3. Press the tube hydrostatically at 200,000 psi
4. Grind sample to a cylindrical shape suitable for magnetic testing (e.g., 0.330 inch in diameter by 1 inch long)
5. Sinter in an argon atmosphere
6. Measure B_s, the second quadrant demagnetization curve, weight, and volume. Peak magnetizing field of 100 kOe
7. Tabulate B_s, B_r, H_k, H_d at B/H = -1/2,

   H_c, H_{ci} $(BH)_{max}$, density, Packing (P), and Alignment (A)

*Most of the test samples were made using the evacuation technique. Near the end of the Phase I studies, samples were made by the moving-plunger technique.

TABLE IV

Definition of Symbols

B_s	Saturation magnetization. Taken as equal to the value of magnetization ($4\pi J$) at 100 kOe divided by the magnetic packing fraction P, in most cases
$4\pi J$	Magnetization
B_r	Remanent magnetization at zero field
B	Magnetic induction
H_k	The demagnetizing field required to drop the magnetization ($4\pi J$) 10% below remanence (B_r)
H_d at $B/H = -1/2$	The demagnetizing field required for $H = 2B$
H_c	The demagnetizing field required for the induction (B) to be zero
H_{ci}	The demagnetizing field required for the magnetization ($4\pi J$) to be zero
$(BH)_{max}$	Maximum energy product
Density	Weight divided by volume
P	Magnetic packing fraction. Equal to density (g/cm^3) divided 8.6 for cobalt-samarium
A	Alignment factor. Defined as remanent magnetization (B_r) divided by magnetization ($4\pi J$) at 100 kOe

Samarium of nominal 99.9% purity was purchased from four vendors: American Potash and Chemical, Atomergic Chemical, Michigan Chemical, and Research Chemical. In addition, a second lot of 99.9% metal from one of the four vendors was also available, as well as a 99.8% pure grade made from a 95% oxide. Altogether 5 lots of 99.9% pure and 1 lot of 99.8% pure metals were evaluated. A typical chemical analysis, as reported by the vendor for Lot B, is as follows: Gd, Eu, Y, Si, Fe, Mg, Ca, and Al under 0.01%. All the other rare earth metals were less than the spectrographic limits. The 99.8% grade contained slightly higher amounts of Gd, Y, Ca, and Mn to lower the purity slightly. Electrolytic cobalt of nominal 99.6% Co, with 0.35% nickel being the major impurity, was used for melting stock in making the Co-Sm alloys.

Samarium from each lot was melted with cobalt in an inert atmosphere induction furnace, and cast into copper molds. The ingots were ground into powder, mixed with a sintering agent, aligned in a magnetic field, and sintered into bars suitable for magnetic testing.

The initial results showed a great variability between vendors, or so it seemed. However, the variability was related to inadequate process control and not to samarium variability, since high-energy acceptable magnets were eventually made from each lot of samarium, including the 99.8% purity metal. This study has shown that the liquid-phase sintering process is one that requires careful control of the processing variables.

The results are summarized in Table V. Note that for each lot the properties obtained meet the goal of -5000 Oe value for H_d at $B/H = -1/2$. The initial batch made from lot D samarium had to be modified to 63.5% Co, 36.5% Sm in order to make a magnet which met the -5000 Oe goal for H_d at $B/H = -1/2$.

The conclusion to be made from this study is that high-energy product, high coercive force magnets can be made with 99.9% samarium from four vendors, but that success is greatly dependent upon close control of the processing variables. Thus, 99.9% samarium from any source should prove acceptable for making Co-Sm magnets by the powder-from-ingot process.

Part 2--RD Process Powder

The RD Process* involves reduction of samarium oxide by calcium in the presence of cobalt to form a Co-Sm alloy powder. The calcium oxide is removed by acid leaching, and the resulting Co-Sm powder is available for

*A GE process developed by R.E. Cech, General Electric Research and Development Center, Schenectady, N.Y. This investigator supplied the RD powder used in this study.

TABLE V

Summary of Results Obtained on Samples Made with Samarium from Several Vendors.
Nominal Blend Composition was 37% Sm, 63% Co

Sample	Treatment (hr, °C)	B_s (kG)	B_r (kG)	H_c (kOe)	H_{ci} (kOe)	$(BH)_{max}$ (MGOe)	d (g/cm^3)	H_d (B/H = - 1/2) (Oe)
GP461 A	1, 1110	10.1	9.0	-6.6	-8.8	18.3	7.85	-5400
GP462 A	2, 1110	9.9	8.9	-6.2	-12.6	17.8	7.93	-5000
GP449 B	1, 1110	9.8	8.8	-5.9	-11.5	18.1	7.95	-5200
GP450 B	2, 1110	9.9	8.8	-5.9	-11.8	18.1	7.94	-5000
GP499 B	1, 1110	9.7	8.5	-6.1	-14.2	16.3	7.83	-5200
GP500 B	1, 1110	9.8	8.6	-6.2	-13.8	18.3	7.85	-5200
GP339 C	0.5, 1110	9.6	8.0	-7.5	-17.2	15.2	7.56	-5200
GP340 C	0.5, 1110	9.6	8.2	-6.9	-16.7	16.0	7.62	-5200
GP453 E*	1, 1110	9.7	8.7	-6.6	-15.8	18.2	8.02	-5300
GP454 E*	2, 1110	9.7	8.7	-6.7	-15.9	18.1	8.01	-5250
GP473 D	1, 1110	9.6	8.6	-5.4	-10.9	15.9	7.93	-4700
GP474 D	2, 1110	9.7	8.6	-5.3	-10.8	17.2	7.90	-4700
GP487 D†	2, 1110	10.3	9.0	-6.5	-14.9	18.2	7.8	-5200
GP488 D†	2, 1110	10.3	9.1	-6.8	-15.7	19.5	7.8	-5500

*Made from 99.8% pure samarium.

†Blend composition modified to 63.5% Co.

TABLE VI

Properties of Some Magnets Made from RD Powder
(A) As a base metal powder:
(B) As a source of Co and Sm in the melting process; Half of the Sm was provided from RD powder

Sample	Nominal Composition Co-Sm (%)	Treatment (hr, °C)	B_s (kG)	B_r (kG)	H_c (kOe)	H_{cl} (kOe)	$(BH)_{max}$ (MGOe)	d (g/cm^3)	P	A	H_d (B/H = - 1/2) (Oe)
(A)		RD Powder Used Directly									
GP 287	62-38	1, 1100	7.8	6.4	-6.3	-36.3	10.2	7.76	.91	0.90	-4300
GP 288	62-38	0.5, 1100	7.8	6.3	-6.2	-35.0	9.5	7.65	.90	.90	-4200
GP 300	70-30	0.5, 1125	9.7	4.9	-2.6	- 5.0	3.5	6.69	.78	.66	--
GP 301	63.5-36.5	0.5, 1125	7.8	6.0	-4.8	-15.5	6.9	7.8	.91	.85	-3350
GP 302	64.5-35.5	0.5, 1125	7.4	5.5	-4.9	-25.0	6.8	7.6	.88	.85	-3300
(B)		RD Powder Used in Melting Process									
GP 457	62.5-37.5	1, 1110	9.9	8.9	-5.3	- 9.9	14.1	8.0	.93	.97	
GP 458	62.5-37.5	2, 1110	9.8	8.9	-5.3	-10.5	14.3	8.0	.93	.97	
GP 459	62.5-37.5	1, 1115	10.1	9.3	-4.6	- 5.6	15.0	8.1	.94	.97	

use in a melting process or directly as Co-Sm base metal powder. Both approaches have been tried. The results are summarized in Table VI.

First consider the case where the RD powder was used directly as the base metal powder, Part A in Table VI. The magnetic properties are for the most part lower than those reported in Table V (Part 1). The exception is the extremely high values of H_{ci} for samples GP287 and GP288, about twice the H_{ci} values measured for the magnets made in Part 1. The value of 36,300 Oe is one of the highest values ever reported. This high resistance to demagnetization for these samples is interesting, but unfortunately the lower saturation (7800 gauss) which these samples possess, results in low B:H properties.

Another method for using the RD powder is to supply samarium for melting stock in the powder-from-ingot process. This was tried by using pressed RD powder to provide 1/2 of the samarium in a Co_5Sm ingot (the supply of RD powder was limited). The pressed powder (80% packing) did not melt readily in the induction furnace, but an ingot was obtained which was then processed into powder, and magnets by the standard process. The results are given in Part B of Table VI. The properties are slightly lower than those reported in Table V, where 99.9% samarium was used for the melting process. However, the values are high enough to justify optimism for the ultimate success of a process based on using RD powder as melting stock.

The conclusion to be made from these studies is that the powder-from-ingot process using bulk samarium should be used in Phase III. The processes using RD powder are not as advanced, and additional study and evaluation are needed to optimize the use of RD powder for making Co-Sm magnets.

Task 2--Melting and Casting (M.G. Benz)

An evaluation to determine a process suitable for large scale (5 to 100 lb) alloy melting has been made. Aspects of the various methods that have been evaluated include: type of melting process, type of atmosphere, type of crucible and mold, and melting procedures.

Much of our earlier work with small scale (100 gram) melts was accomplished by melting in an argon atmosphere, tungsten electrode, cold hearth (water-cooled copper) arc melting furnace. With this method, weighed quantities of cobalt and samarium are placed on the cold hearth. The inert argon atmosphere is introduced. An arc is struck between the electrode and the metal, causing all the cobalt and samarium to melt except that in immediate contact with the water-cooled copper hearth. The resulting ingot is cooled, turned over, and remelted. This remelt procedure is repeated several times in order to homogenize the ingot. This is a convenient method for the preparation of small melts, but cannot be readily scaled up for larger melts.

Larger scale arc melting is possible, however, with consumable electrode arc-melting procedures. With this method, weighed quantities of cobalt and samarium (prefereably powder) are mixed and pressed into long cylindrical electrodes. These electrodes are introduced into the arc melting furnace such that the arc melts the tip off the electrode as it is continuously advanced towards the solidifying ingot contained in a water-cooled copper mold. As a practical matter, electrode preparation from pure metals, electrode homogeneity, and resultant ingot homogeneity are somewhat difficult to control for complex systems such as cobalt-samarium. For this reason, consumable electrode arc melting was not used to prepare melts from pure metals for this program. On the other hand, this consumable electrode arc melting should be ideal as a remelt operation for RD powder, as preparation of homogeneous electrodes would only require a simple powder pressing operation.

Induction melting had also been used for our earlier small scale (400 gram) melts and seems more ideally suited for scale-up to large scale operations. With this method, cobalt is melted in the furnace. The atmosphere is vacuum. The crucible is aluminum oxide. When the cobalt is molten, the atmosphere is changed to argon, samarium is added to the melt, stirring is allowed to proceed for several minutes, and then the entire melt is chill cast into copper molds. Subsequent melts can be made with the same crucible without cooling the furnace, if the furnace is equipped with appropriate feed hoppers and multiple molds.

This process has been used successfully for 5 lb melts and is suited for scale up to much larger melts.

Sample melts were prepared by arc melting and induction melting. The arc-melted heats were prepared with the tungsten electrode, cold hearth, argon atmosphere furnace. The induction-melted heats were prepared in the vacuum/argon atmosphere furnace. These heats were chill cast into a copper mold.

Raw materials and the cast cobalt-samarium were sampled for chemical analysis. A list of the analytical results is presented in Table VII. A slight aluminum pickup is noted for the induction-melted heats. This does not appear to cause any difficulties.

Samples from the above heats were crushed and milled to powder. Standard test bars were prepared for comparison of magnetic properties. The general results for these samples were much lower than desired (Table VIII). Insufficient attention had been paid to alignment, composition control, and precise control of sintering temperature. These difficulties were corrected in later studies and high-performance samples were fabricated (see Supplementary Study 1).

TABLE VII

Chemical Analysis of Heats Prepared by Arc Melting and Induction Melting

Melting Method	Melt No.	Co % (nominal)	Co % (analysis)	Oxygen (ppm)	Al (%)	Cu (%)	[illegible]	Ni (%)
Arc	MH 520-2	66.2	66.3	640	0.006	0.004	0.01[illegible]	0.25
Arc	MH 520-3	66.2	66.3	620	--	--	--	--
Arc	MH 520-4	66.2	66.3	580	--	--	--	--
Arc	MH 520-5	66.2	66.2	700	--	--	--	--
Arc	MH 520-6	40	41.0	--	.006	.004	.006	.16
Induction	3884	66.2	66.2	260	0.10	.002	.016	.26
Induction	3883	40	40.3	--	.06	.002	.012	.17
Raw Material: Co		--	--	--	.008	.005	.019	.35
Raw Material: Sm		--	--	--	.006	.003	.006	.002

TABLE VIII

Comparison of Co-Sm Samples Made by Arc Melting and Induction Melting

Melting Method	Sample No.	Sintering Treatment (hr, °C)	B_s (kG)	B_r (kG)	H_c (kOe)	$(BH)_{max}$ (MGOe)	H_d at B/H = - 1/2 (kOe)	Density (g/cm^3)
Arc	MH520 A	1/2, 1115	8.57	6.68	-5.8	10.2	-4.2	7.38
	B	1/2, 1130	9.21	7.79	-3.5	10.0	-3.4	8.06
	C	1/2, 1110	8.77	6.99	-5.5	11.0	-4.2	7.49
	D	1/2, 1110	8.41	6.93	-4.7	9.7	-3.8	7.85
Induction	3884 A	1/2, 1115	8.93	6.95	-6.2	11.3	-4.4	7.28
	B	1/2, 1130	9.10	7.63	-5.3	12.0	-4.3	7.62
	C	1/2, 1110	9.04	7.25	-6.4	12.2	-4.6	7.38
	D	1/2, 1110	9.05	7.45	-5.9	13.0	-4.7	7.52

The above considerations and studies have led to the conclusion that induction melting will be utilized for preparation of the larger scale cobalt-samarium melts for the remainder of this program.

Task 3--Crushing (M.G. Benz)

Cast ingots of cobalt-samarium must be crushed to a size range that makes good feed stock for subsequent milling to powder. The particle size objective for crushing is a size which passes through a 35 mesh screen (420 micron spacing).

Cast ingots of cobalt-samarium are easily crushed as evidenced by the fact that a mortar and pestle were used for the earlier laboratory scale studies.

Studies have been performed using a jaw crusher and double disk pulverizer in order to determine the effectiveness of using such equipment for larger scale operations.

The jaw crusher used is a 3 1/4-inch by 4 1/2-inch machine with a rated capacity of several hundred pounds per hour. It is equipped with an enclosed dust cover. Studies have shown that a nitrogen cover gas is necessary to prevent sparking. This is particularly true for full-speed operation with the samarium-rich compositions. The output from this machine is generally minus 1/8 inch in particle size.

A double disk pulverizer is used to further reduce the particle size. This is a smaller machine rated at 50 lb or so per hour. It is also equipped with a nitrogen cover gas for spark suppression. The output from this machine is generally minus 35 mesh in particle size and is ideally suited for input to the subsequent milling operation.

Although both these operations employ hardened steel working surfaces, no measurable contamination was detected using normal chemical analysis techniques.

As these two machines performed satisfactorily, they are considered acceptable and will be utilized for the preparation of cobalt-samarium powder.

Task 4--Milling and Classifying (C.E. VanBuren and M.G. Benz)

The 35-mesh powder produced by crushing has to be further reduced in size to yield a finer powder for use in magnet fabrication. Several techniques have been evaluated in order to select the best method for milling and classifying the powder. These techniques include ball milling, vibratory milling, fluid energy milling, and classifying.

Ball Milling Studies

The ball milling studies were carried out with a 0.33 gal ribbed stainless steel mill. For the grinding media, a mix of 1/4-inch-diameter and 1/2-inch-diameter hardened steel balls was employed. This mix consisted of 700 grams of the 1/4-inch balls and 500 grams of the 1/2-inch balls. A powder charge of 100 grams and sufficient liquid to cover the balls was placed in the mill for each test.

The milling variables which were studied consisted of the size of the feed material, the milling time, and the liquid suspending medium (including one test dry). The feed materials used consisted of two lots, a -65 and a -35 + 65 mesh power. The milling times included 2, 4, 24, and 96 hours with a mill speed of 60 rpm. Isopropyl alcohol, methyl alcohol, and water were evaluated as liquid mediums for milling.

The time study revealed that the -65 mesh materials could be reduced to a powder with an average particle diameter of 7.15 microns in two hours of ball milling with isopropyl alcohol as the liquid medium. Further size reductions were realized with milling times up to 24 hours, while longer milling times, up to 96 hours, yielded only very minor changes, as shown in Figure 2

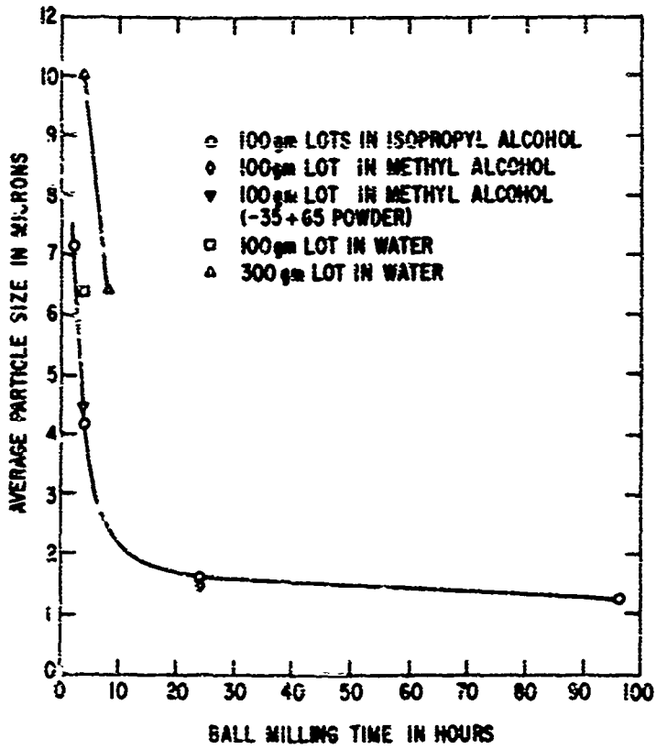

Figure 2 Average particle diameter of Co-Sm powder versus ball milling time under various conditions.

The use of methyl alcohol as the liquid medium resulted in the same average particle size as obtained with the isopropyl alcohol for a given milling time. Water as a liquid medium, however, was not as efficient. For a given milling time the average particle size realized was 50% higher than that obtained with alcohol. The desired size of 7 microns could be realized, however, with approximately 3 hours of milling in water as opposed to 2 hours for alcohol.

Although most of the tests were run on the -65 mesh material, a lot of -35 + 65 mesh material was also tested. This coarser material behaved the same as the finer feed material, yielding essentially the same average particle diameter for a given milling time. A lot of -10 mesh material was also run but the results were not conclusive. However, all indications were that it did not reduce easily in size by milling.

The attempt to ball mill the -10 mesh powder dry proved to be unsuccessful in that the material caked up in the corners of the mill. This caking problem limited the size reduction that could occur and made it difficult to discharge the mill.

The scanning electron micrographs in Fig. 3 indicate that the ball milled particles have a platelike shape and a wide range of sizes. It is also noted that the different liquid milling media studied result in the same particle shape characteristics.

The oxygen content of the ball milled Co-Sm powder is shown in Table IX. The increase in oxygen content with increasing milling time is due to the more active surfaces produced with the smaller diameter particles obtained with the longer milling times. Methyl alcohol tends to yield a slightly higher oxygen content than isopropyl alcohol for a given milling time. Water appears to be slightly better than alcohol with regard to oxygen contamination.

Vibratory Milling Studies

The grinding process of vibratory milling was studied with a laboratory size mill. A 110 cc steel jar with 242 grams of 0.143-inch-diameter tungsten carbide balls was used. For each test a charge of 30 grams of the -35 + 65 mesh cobalt samarium powder was placed in the jar and it was then filled with isopropyl alcohol.

The main variable for this process study was the milling time which ranged from 1/2 to 4 minutes. A test was performed with water as the liquid medium and the effects of feed material size were checked.

The vibratory milling studies have revealed that a powder with an average particle diameter of 7 microns can be realized in just two minutes of milling in isopropyl alcohol. In Fig. 4 it is shown that the average

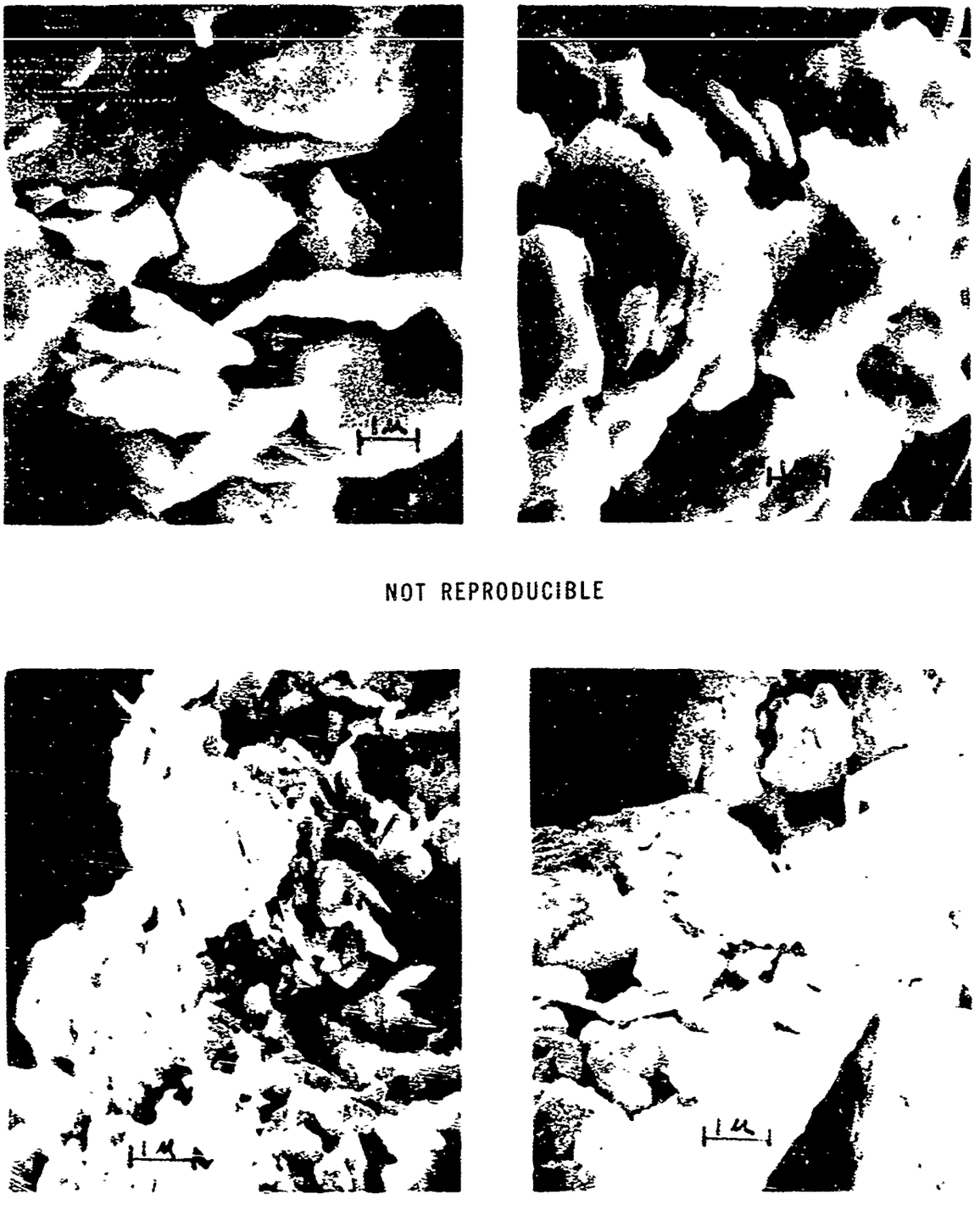

Figure 3 Scanning electron micrographs of ball milled Co-Sm. (a) 2 hours of milling; (b) 4 hours of milling; (c) 24 hours of milling; (d) 4 hours of milling. a, b, and c in isopropyl alcohol, d in water. 1000X

TABLE IX

Oxygen Content in Co-Sm Powder Ball Milled Under Varying Conditions

Sample	Liquid Media[a]	Milling Time (hr)	Oxygen (wt %)
3884-1(before milling)	--	--	0.026
3884-1a7	A	2	0.59
3884-1a6	A	4	0.92
3884-1a8	B	4	0.79
3884-1a4	A	24	3.91
3884-1a5	C	24	4.50
3884-1a3	A	96	7.07
3884-1a10[b]	B	8	0.72

Note (a)--A = isopropyl alcohol; B = water; C = methyl alcohol.

Note (b)--300-gram mill charge, rather than 100 grams.

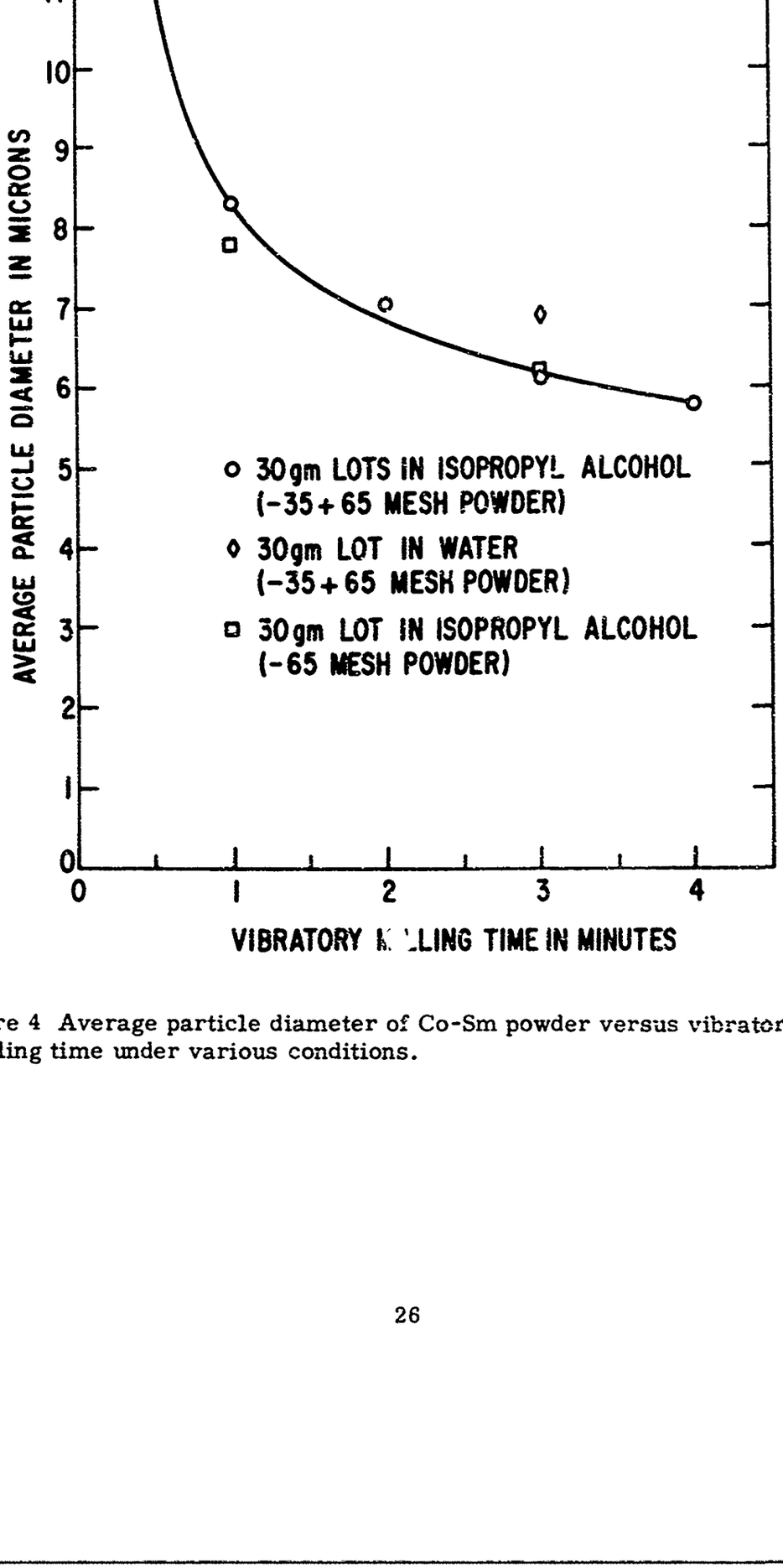

Figure 4 Average particle diameter of Co-Sm powder versus vibratory milling time under various conditions.

particle size of this material can be varied from 11.2 to 5.6 microns over the milling time range of 0.5 to 4.0 minutes.

The average particle size for a particular grinding time is increased slightly when water is used in place of alcohol as the liquid medium. The difference, which amounts to less than 1 micron for the 3 minute milling period, is not as signficant with this process as it was with ball milling.

The use of a finer feed material in the mill for the 1-minute milling time resulted in a smaller diameter powder than the coarser feed material. However, the 3-minute milling period yields the same size material with both feeds. The scanning electron micrographs of Fig. 5 show the large range of particle sizes present and the random shapes. There are some platelike particles present, but they are not as prevalent with this process as they were with the ball milling process.

The oxygen content of the vibratory milled powder is in the nominal 5000 ppm range. The 3-minute milling time with isopropyl alcohol yielded a value of 5200 ppm, while water for the same milling time yielded 5700 ppm. The finer (-65 mesh) feed material gave 5600 ppm of oxygen after 3 minutes of milling in isopropyl alcohol.

Fluid Energy (Jet) Milling Studies

Powder in the size range of 10 microns and less has been readily produced by a fluid energy mill. This mill both grinds and classifies the material. The mill works in the following manner. Coarse powder is entrained in two opposing high-velocity streams of gaseous nitrogen. As these gas streams meet, collision of the coarse particles with each other creates a grinding action which grinds the powder down in size. The mill is equipped with a centrifugal classifier which separates out particles of the desired size and returns the oversize particles to the grind section of the mill for further grinding. The nitrogen gas can be collected, recompressed, and recycled back through the mill on a closed loop basis. The existing pilot scale mill is rated at a capacity of approximately 2 pounds per hour.

The fluid energy mill is capable of accepting material as coarse as -10 mesh and readily grinds it to less than 10 microns. The use of a finer starting material, for instance, -35 mesh, yields the same product but in less time.

A set of operating conditions has been established for the fluid energy mill which consistently yield material with an average particle diameter of approximately 7 microns as determined with a permeability method particle analyzer. A scanning electron micrograph of this powder is shown in Fig. 6. Note that the shape of the particles is somewhat more equiaxed than that observed for powder produced by ball or vibratory milling.

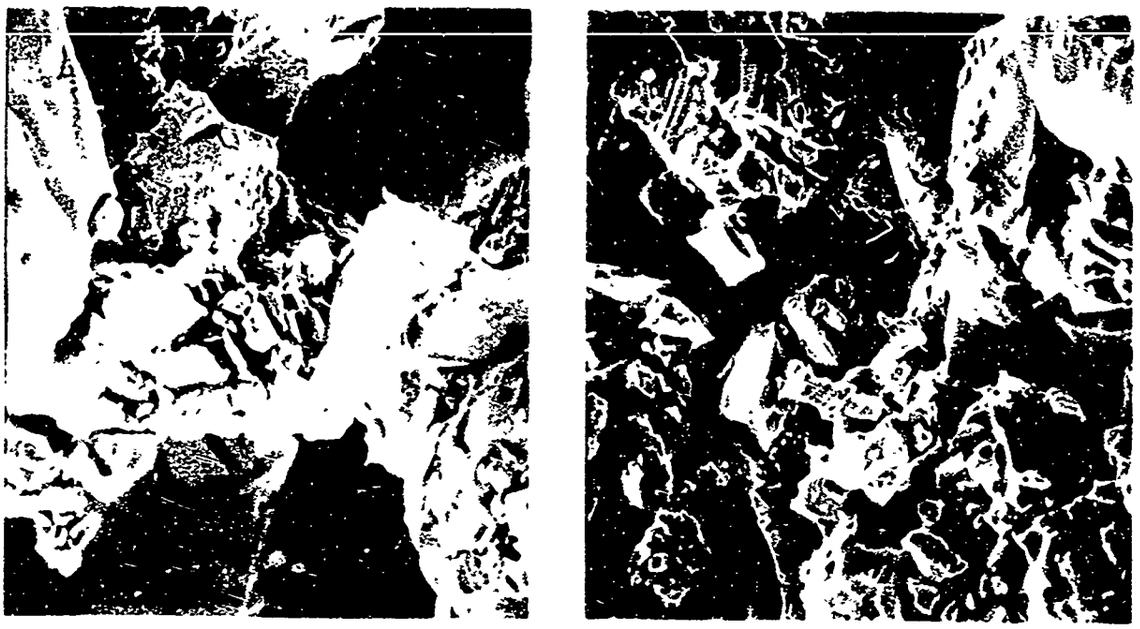

(a) (b)

(c)

Figure 5 Scanning electron micrographs of vibratory milled Co-Sm: (a) 1 minute of milling; (b) 3 minutes of milling, both in isopropyl alcohol; (c) 3 minutes of milling water. 100X

Figure 6 Scanning electron micrograph of fluid energy milled Co-Sm (Lot 3943)
1000X

The oxygen level for powders produced in this manner is shown in Table X. The small diameter of these particles makes them very surface active. This accounts for the increase in oxygen content as the powder size is reduced from 35 mesh to below 10 microns. The observed oxygen level has not caused any problem with respect to fabrication of magnets. It should be noted that the oxygen level observed for the powder is approximately the same as that observed for finished sintered magnet. Little or no oxygen is picked up during sintering.

Classification

As indicated, the fluid energy mill serves as its own classifier. In addition to this, magnetic sieving in the presence of an alternating magnetic field has also been utilized to classify the powder. This is a very time-consuming process and has offered little or no additional control of the average particle size. It will not be used for processing during the balance of this program.

Magnetic Properties

Standard test bars were made from powders prepared by the three milling processes. The results of measurements on these samples are summarized in Table XI. As can be seen, samples made from powders prepared by ball milling and vibratory milling did not achieve the same high performance level as those made from powders prepared by fluid energy milling. This was due to three factors: (1) the shape of the ball and vibratory milled powders was more platelike and hence the powder was more difficult to align (measurements on ease of alignment are included in the subsection on Task 7); (2) higher oxygen levels; and (3) less previous experience with handling ball and vibratory milled powders, as most of the studies prior to this program were based on the use of fluid energy milled powders.

Based on the above, fluid energy milling will be utilized for the balance of this program. The other milling processes do work, but have not been carried to the point where they could be selected at this time.

Task 5--Powder Storage (M.G. Benz)

Cobalt-samarium in fine powder form is somewhat reactive when exposed to the oxygen and moisture in air. To determine whether or not prolonged exposure to air would have a degrading effect on magnet properties, and in order to study possible powder storage methods, five powder storage conditions have been evaluated. These conditions are: (1) open container exposed to air (average relative humidity approximately 40%); (2) closed container filled with air and maintained at 100% relative humidity; (3) closed container filled with air and maintained near 0% relative humidity with desiccant; (4) open container exposed to air at 150°C; and (5)

TABLE X

Oxygen in Co-Sm Powder Prepared with a Fluid Energy Mill

Condition	Lot No.	Wt % Sm (Nominal)	Wt % O_2 (Measured)*
Coarse Powder			
20 mesh	3884-1	34	0.026
	MH520-2	34	.064
	-3	34	.062
	-4	34	.058
	-5	34	.070
	3883-1	60	.104
	MH520-6	60	.242
Fluid Energy			
Milled Powder	3884-1	34	.317
5u to 10u	MH520-2 through 5	34	.302
	3883-1	60	.739
	PV647B	60	.488
	PV647B(2)	60	.861
Sintered Bar	From 3884-1	37	.4
	From MH520	37	.35

* Oxygen measured by vacuum fusion analysis.

TABLE XI

Summary of Results for Task 4--Milling and Classifying

Type of Mill	Milling Time	Liquid Media[a]	Wt % Oxygen	Sample[b] Weight Before Alignment (grams)	Sintering Temp (°C)	Sintering Time (hr)	Sample	B_s (kG)	B_r (kG)	H_c (kOe)	H_k (kOe)	H_{ci} (kOe)	$(BH)_{max}$ (MGOe)	Density (g/cm³)	F	A	H_d at B/H = -1/2 (kOe)
Ball	2 hr	A	0.59	11	1100	1/2	3884-1A7	7.25	4.93	-4.5	-2.6	-11.0	5.3	7.10	0.84	0.81	-2.9
Ball	4 hr	A	0.82	11	1100	1/2	3884-1A6	7.95	5.08	-4.4	-2.4	-26.5	7.5	7.52	0.83	0.86	-3.3
Ball	6 hr	A	0.79	11	1100	1/2	3884-1A8	8.12	5.14	-3.3	-1.5	- 8.8	5.5	7.36	0.86	0.83	-2.8
Ball	8 hr	B	0.71	6	1110	1	CVB-1	8.38	7.81	-4.5	-2.0	- 7.4	11.0	7.56	0.88	0.95	-3.9
Ball	8 hr	B	0.72	7	1110	1	CVB-2	8.35	7.44	-4.0	-2.0	- 7.6	9.6	7.23	0.84	0.95	-3.8
Ball	8 hr	B	0.72	8.5	1110	1	CVB-3	9.51	7.72	-4.4	-2.0	- 7.4	10.2	7.50	0.87	0.95	-3.8
Ball	8 hr	B	0.72	11	1110	1	CVB-4	8.38	6.45	-4.2	-1.4	- 8.2	7.3	7.43	0.86	0.89	-3.3
Ball	8 hr	B	0.72	11	1100	1/2	3884-1A10	8.13	6.04	-4.2	-1.8	-10.1	6.7	7.32	0.85	0.87	-3.2
Ball	24 hr	A	5.91	11	1100	1/2	3884-1A4	9.40	5.5	-3.0	-1.5	- 3.0	5.2	7.01	0.92	0.91	-2.6
Ball	96 hr	A	7.07	6.6	1100	1/2	3884-1A3	10.0	<1.0	- -	- -	- -	- -	7.5	0.87	- -	- -
Vibratory	1 min	A	- -	11	1110	1	3884-1A11	7.29	6.23	-4.3	-2.8	- 7.8	8.2	7.67	0.89	0.80	-3.6
Vibratory	1 min	A	- -	11	1110	1	3884-1B3	8.38	6.86	-3.7	-1.3	- 5.2	9.0	7.91	0.92	0.89	-3.2
Vibratory	3 min	A	0.52	9	1110	1	3884-1B5	8.85	7.65	-5.5	-3.6	-11.3	13.0	7.98	0.93	0.93	-4.5
Vibratory	3 min	A	0.56	21	1110	1	3884-1B12	7.79	6.36	-5.2	-4.0	-15.7	9.2	8.12	0.94	0.87	-3.9
Vibratory	3 min	A	- -	11	1110	1	3884-1B6	8.16	6.78	-5.3	-4.0	-26.2	10.0	8.19	0.94	0.93	-4.0
Vibratory	3 min	B	0.57	11	1110	1	3884-1B7	8.26	6.55	-5.3	-4.1	-12.3	10.1	7.87	0.89	0.82	-4.0
Fluid Energy		- -	0.3[c]	11	1110	1	T-9-5-1	9.84	8.84	-7.3	-6.7	-15.8	18.1	7.81	0.91	0.97	-5.5
Fluid Energy		- -	0.3[c]	11	1110	1	T-9-5-2	9.74	8.53	-7.3	-7.0	-15.8	17.7	7.78	0.91	0.97	-5.5

Note (a). A = Isopropyl Alcohol; B = water.

(b). Sample weight at a fixed volume. Eleven grams is equivalent to approximately 3.5 g/cm³.

(c). This is the value measured for typical fluid energy milled samples. It is used as an estimate for these samples.

container filled with argon and maintained near 0% relative humidity with a desiccant. A fresh lot of powder was prepared for this study. Test bar samples were made to characterize the fresh powder. The balance of the powder was divided and stored for one month under the five conditions listed above. Two test samples were made from the powder stored under each condition. Data for these samples are summarized in Table XII. As can be seen, storage under conditions of excessive heat (Condition 4) and excessive moisture (Condition 3) are to be avoided.

Task 6--Mixing Additives (D. L. Martin)

The basic liquid-phase sintering process requires mixing of a base metal powder of nominal Co_5Sm composition with a sintering additive of nominal 60 wt % samarium, 40 wt % cobalt composition to form a 37 to 38 wt % samarium mixture.

The objective of Task 6 studies was to determine a satisfactory method of mixing the two powders to form a homogeneous mixture suitable for being sintered into magnets.

A dry mixing process was preferred to simplify the process, and to avoid contamination of the powder with hydrocarbons, water, etc. A rotating P-K twin shell blender was tried and found to be satisfactory.

A nominal 35 wt % samarium base metal and a nominal 60 wt % samarium sintering additive were used for the study. These were prepared from ingots by jaw crushing and fluid energy milling as described in Tasks 2, 3, and 4.

Chemical analysis was the main basis for evaluating the effectiveness of the mixing. A number of samples were analyzed to provide sufficient data for a statistical analysis.

The plan was to mix about 5 pounds of dry powder together in the P-K twin blender and to check for homogeneity after 10, 100, 1000, and 2000 revolutions of the blender. The analytical sample taken at each stage consisted of nine spot samples taken at random from the mixed powder in the blender. The results are summarized in Table XIII.

The original charge consisted of 1888 grams of base metal and 192 grams of additive. Using the mean values for cobalt reported in Table XIII for these two powders the mean composition of the blended composition was 62.93 wt % Co. The mean cobalt after 1000 revolutions of the blender was 63.0±% Co. Thus, it appears that 1000 revolutions is sufficient to insure uniform mixing of the powder. The best uniformity, as indicated by the standard deviation was obtained after 2000 revolutions.

TABLE XII

Summary of Results for Task 5--Powder Storage

	Powder Storage Condition (Stored for 1 month)	Sample[a]	B_s (kG)	B_r (kG)	H_{cB} (kOe)	H_k (kOe)	H_{cJ} (kOe)	$(BH)_{max}$ (MGOe)	Density (gr/cm³)	P	A	H_d at B/H = -1/2 (kOe)
1.	Air - Open	T-5-5-1	9.84	8.84	-7.3	-8.7	-18.8	18.1	7.81	0.91	0.97	-5.5
	Air - Open	T-5-5-3	9.74	8.53	-7.3	-7.0	-15.8	17.3	7.76	0.92	0.97	-5.8
2.	Air - Closed - Dry	T-5-2-1	9.78	8.60	-7.3	-6.4	-15.3	18.0	7.82	0.91	0.97	-5.5
	Air - Closed - Dry	T-5-2-2	9.84	8.68	-7.3	-6.7	-15.5	18.9	7.83	0.91	0.97	-5.6
3.	Air - Closed - Wet	T-5-3-1	9.43	7.30	-2.4	-1.4	- 2.6	7.4	7.08	0.82	0.93	-2.9
	Air - Closed - Wet	T-5-3-2	9.60	7.45	-2.3	-0.7	- 2.3	5.5	7.08	0.92	0.95	-2.1
4.	Air - Open - 150°C	T-5-4-1	9.03	1.95	-0.3	-0.3	- 0.3	<1.0	6.73	0.78	--	--
	Air - Open - 150°C	T-5-4-2	10.0	1.82	-0.3	-0.3	- 0.3	<1.0	6.74	0.78	--	--
5.	Argon - Closed - Dry	T-5-1-1	9.77	8.57	-7.1	-6.4	-16.3	17.9	7.85	0.91	0.96	-5.4
	Argon - Closed - Dry	T-5-1-2	9.84	8.66	-7.1	-6.2	-14.7	18.0	7.83	0.91	0.97	-5.3
	Fresh Powder - As Prepared	T-5-11	9.83	8.68	-7.3	-6.8	-15.9	18.0	7.85	0.91	0.97	-5.5
	Fresh Powder - As Prepared	T-5-12	9.86	8.80	-7.4	-6.4	-16.0	17.2	7.77	0.90	0.97	-5.4

Note (a) Samples sintered for 1 hour at 1110°C.

TABLE XIII

Summary of Analytical Results for Blending Study

	No. Tests	Wt % Co Mean	S Standard Deviation	95% Conf. Range Low (% Co)	High (% Co)
Base Metal	5	65.33	0.41	64.53	66.13
Additive	8	39.39	.27	38.86	39.92
After P-K Blending Number of Revolutions					
10	4	63.13	.26	62.62	63.64
100	5	63.12	.35	62.44	63.80
1000	9	63.04	.27	62.52	63.56
2000	7	62.96	.22	62.54	63.38

Powder did collect on the side of the blender and, therefore, in using the P-K blender to mix the powders it seems advisable to stop several times during the mixing process to remove material sticking to the side of the container.

The best proof of the success of the blending operation are the results reported for blended powder after 2000 revolutions in Supplementary Study 1--Multi-task Interaction Study, where only 2 out of 16 samples failed to meet the goal of -5000 Oe for H_d at $B/H = -1/2$. The failure of those two samples to meet the goal is more likely to be related to the sintering treatment or alignment than to the powder homogeneity.

The conclusion of this study is that dry mixing of the powders in a P-K blender is an acceptable process step for making high-energy product, high coercive force Co-Sm magnets.

Task 7--Magnetizing and Aligning Powder (R. P. Laforce and D. L. Martin)

Magnetic alignment of the powder particles so that their preferred magnetization directions are parallel is one of the critical processing steps in the production of high-quality magnets. The basic magnetic properties cannot be high without a high degree of alignment. Likewise, it is also true that a high degree of alignment alone is not sufficient, the packing and resistance to demagnetization must also be high in order to obtain the peak properties.

Studies made before the start of this program have shown that packing the blended Co-Sm powder in a rubber tube and aligning in a magnetic field of 50,000 to 100,000 Oe was a good way to obtain a high degree of alignment. The procedure for making the standard test bar (Table III) was based on these earlier studies. In Task 7 Studies a closer look has been taken at the alignment process with the objective of improving it.

Alignment is defined as ratio of the remanent magnetization at zero field to the intrinsic magnetization value at 100 kOe, $4\pi J_{100}$. That is,

$$\frac{B_r}{4\pi J_{100}} .$$

If the alignment is almost perfect the drop of magnetization will be small when the field is reduced from the saturation field to zero. To state it another way the B_r value will approach $4\pi J_{100}$ as the alignment factor approaches 1.

The basic technique we have used is to first align the powder particles in a magnetic field, change the volume to lock the particles in position and then transfer the container holding the aligned powder to a hydrostatic press where a pressure of 100,000 psi was applied. Basically, the problem of

alignment is to contain the powder particles loosely enough so they can rotate freely when the aligning field is applied. Then the volume is changed by evacuating the tube or by end compression with a plunger to lock the aligned particles until the sample is hydrostatically pressed.

Alignment studies were typically done on samples 0.300 inch in diameter by 1.0 inch long. Much of the work focused on the question of how dense the prealignment packing could be while still obtaining satisfactory alignment for a given field level. In this connection, one experiment consisted of packing three tubes to different prealignment densities and measuring the alignment factor at each level as the magnetizing field was increased. In this case, the alignment factor was defined as the remanent magnetization divided by the intrinsic magnetization at the aligning field, or 4πI at the usual field of 100 kOe. The results are shown in Fig. 7. It can be seen that 100% alignment was readily achieved when the packing density was 3 g/cm³ or less, but at higher densities the alignment suffered considerably. The small discontinuity in the 4.5 g/cm³ curve occurred when the tube was accidentally jarred while in the magnetic field.

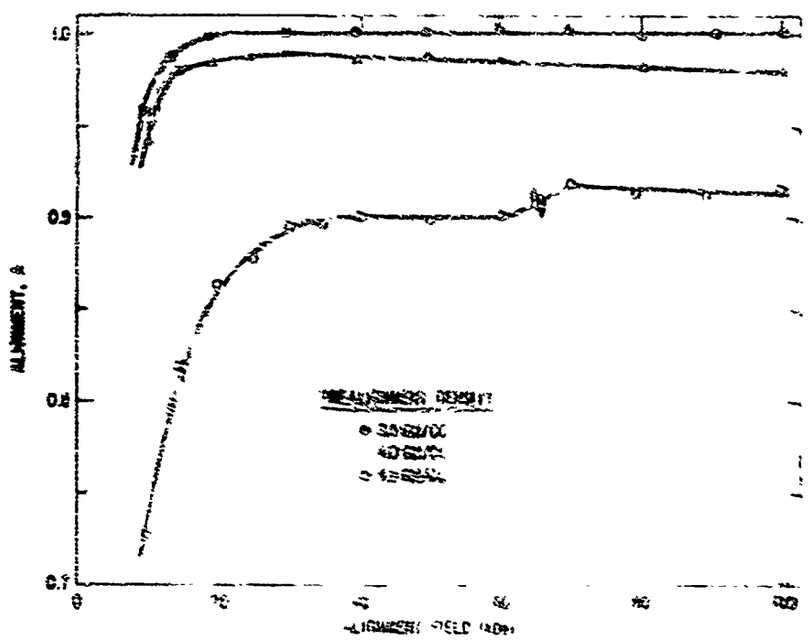

Figure 7 Effect of prealignment packing on alignment of jet energy milled Co-Sm powder. The alignment factor is $4\pi I_r/4\pi I_a$ where $4\pi I_a$ corresponds to the aligning field.

Another series of experiments was undertaken to determine the magnitude of field required to obtain a high degree of alignment (i.e., about 0.95) when the prealignment packing was about 50% of full density. The results are given in Figs. 8, 9, and 10 and show that an alignment field of about 60 kOe or more is needed to achieve peak properties. Note that even low alignment fields significantly improve all properties except H_{ci}.

The high H_{ci} obtained for a random, unaligned sample is explained by the fact that the force opposing the magnetization of the particle is proportional to the cosine of the angle between the axis of easy magnetization of the crystal and the applied field. Take note that a high H_{ci} does not necessarily mean high B-H properties.

The standard test procedure calls for vibration of the sample during alignment in the superconducting solenoid. This has been normal practice, however, it was reasonable to ask whether vibration (from an air hammer fastened to the rod holding the sample) helps to improve alignment. Results given in Table XIV show that the value of alignment was increased slightly by vibration from 0.950 to 0.954. The unit B-H properties are higher for the vibrated samples (Item 3 in the table), but since the packing is slightly higher the improvement cannot be related entirely to vibration.

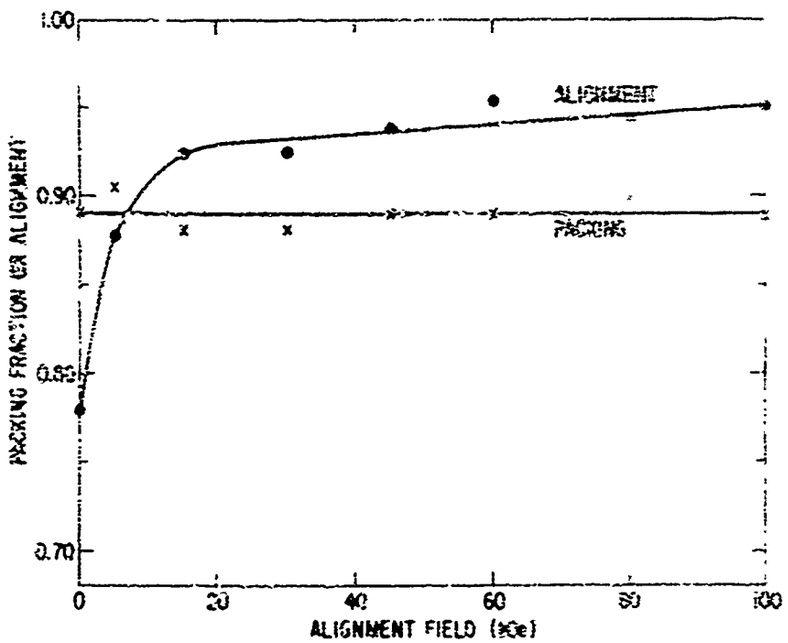

Figure 8 Alignment factor and packing fraction for sintered bars versus alignment field.

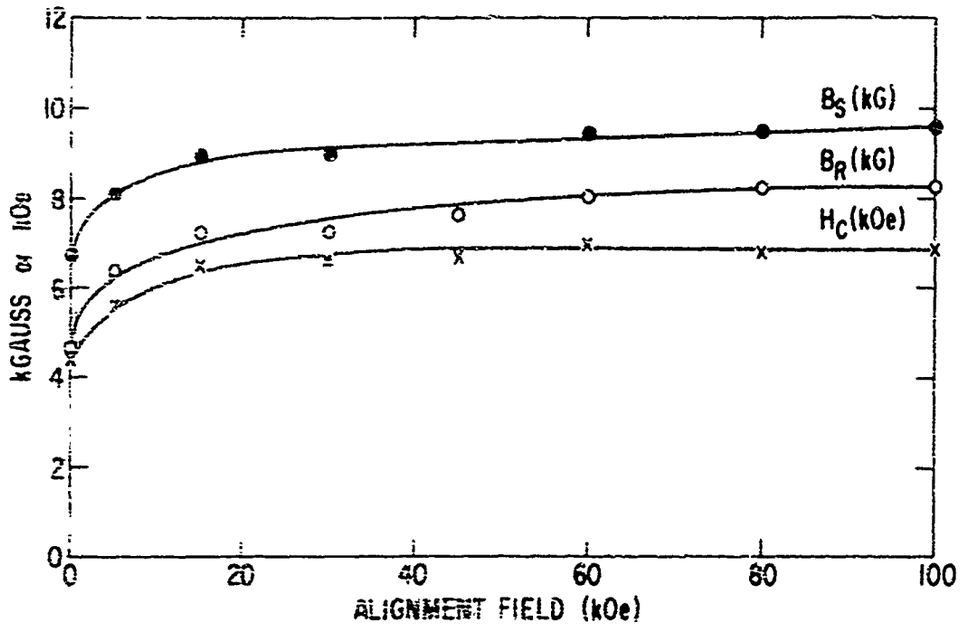

Figure 9 B_S, B_r, and H_C for sintered bars versus alignment field.

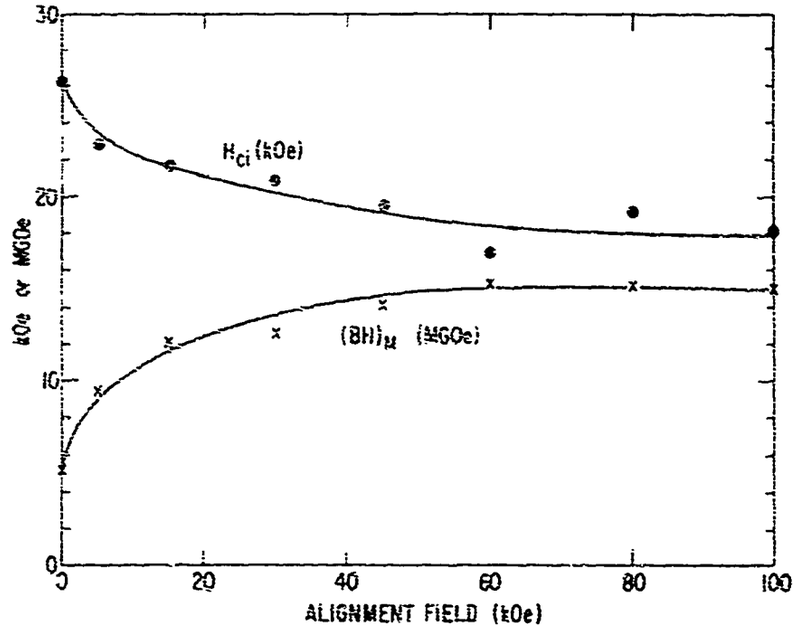

Figure 10 H_{ci} and $(BH)_{max}$ for sintered bars versus alignment field.

TABLE XIV

Effect of Vibration and Shock During Alignment on the Properties of Sintered Magnets

Condition	B_s (kG)	B_r (kG)	H_c (kOe)	H_{ci} (kOe)	$(BH)_{max}$ (MGOe)	Density (g/cm^3)	P	A	H_d at B/H = -1/2 (kOe)
#1 Not Aligned	6.45	4.47	-4.1	-35.5	4.5	7.79	0.91	0.765	-2.80 (1 sample)
#2 Not Vibrated	9.04	7.54	-6.6	-17.7	13.6	7.55	0.88	0.950	-4.85 (2 sample avg)
#3 Vibrated	9.59	8.08	-6.8	-16.5	15.4	7.60	0.89	0.954	-5.07 (6 sample avg)
#4 Vib. + Shock	9.72	8.21	-6.9	-16.5	16.3	7.58	0.88	0.958	-5.15 (2 sample avg)
#5 Vib. + Shock + Die Press	9.98	8.62	-6.8	-13.6	17.8	7.68	0.89	0.968	-5.30 (2 sample avg)

The discontinuity in the 4.5 g/cm^3 curve in Fig. 7 which occurred when the sample was accidentally jarred in the magnetic field suggested that the frequency of vibration might be important. In particular it was thought that an impact or shock might be more effective. This turned out to be the case. During alignment the sample holder was hit sharply with a hammer in an attempt to momentarily free the particles and allow them to rotate and move into better alignment with the magnetic field. The results in Table XIV (item 4) show an improvement in B:H properties, as well as a slight improvement in the alignment factor.

The last item in Table XIV gives the results for a new alignment technique which replaced the first version of the standard test bar procedure described in Table IV. In the first version of the procedure, the rubber tube is evacuated after alignment to freeze the particles in position until the sample was hydrostatically pressed at 200,000 psi. The new method eliminates the need for evacuation. The method ultimately worked out was to pack the powder loosely in a thin-walled rubber tube supported on the outside by a nonmagnetic, metal tube. Two nonmagnetic plungers were inserted in opposite ends so they were free to slide smoothly inside the rubber. The assembled tube was then placed in an axially oriented magnetic field (typically 60,000 Oe). The tube assembly was then vibrated or shocked by giving it sharp blows with a hammer. The two plungers were then pushed toward each other, thus compacting the powder and "locking in" the alignment. The tube assembly was then removed from the field. Since there were small holes in the metal tube around the rubber sleeve, hydraulic fluid could pass through and the entire tube assembly could be hydropressed as a unit, resulting in minimum distrubance to the powder.

The results achieved by this method (item 5) are the highest shown in Table XIV and represent a significant improvement over the standard test bar procedure (item 3). It can be seen that although there was only a subtle change in alignment from the second condition to the last (less than 2%), H_d changed over 9% and $(BH)_{max}$ improved 31% . Measuring the properties of a magnet in the final sintered condition is a much more satisfactory method of determining the effect of process variables.

Up to this point the studies have been made on powder prepared by fluid energy milling. Ball milling has also been studied (Task 4). The effect of prealignment packing and magnitude of the magnetic field on the alignment of ball milled powder were determined in a manner similar to that used to obtain the data plotted in Fig. 11. The ball milled powder does not align as well as the jet milled powder (Fig. 7). This result is probably associated with the platelets formed by ball milling.

An attempt was made to determine whether premagnetizing the powder before packing it into the tubes for alignment would improve the final magnetic properties in any way. Several samples were prepared in this fashion

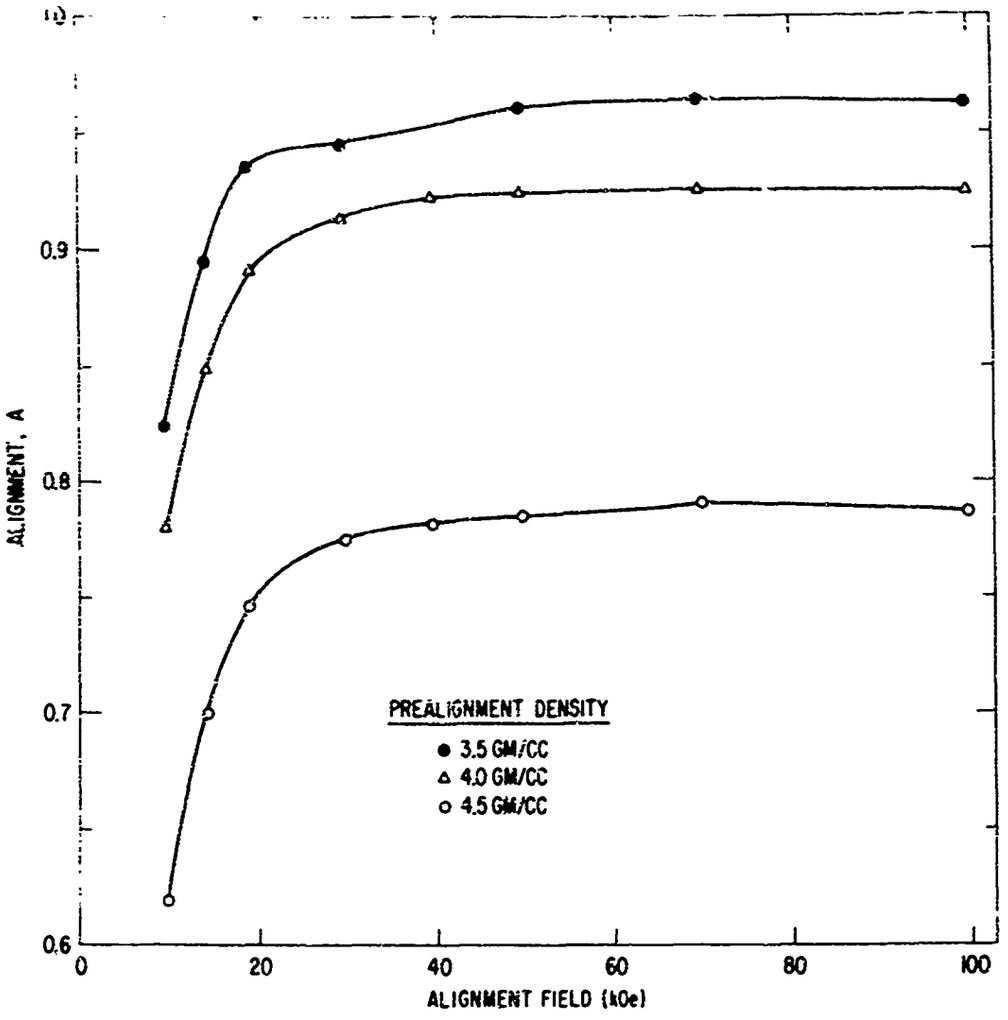

Figure 11 Effect of prealignment packing on alignment of ball-milled Co-Sm powder. The alignment factor is defined as $B_r/4\pi J_a$, where $4\pi J_a$ corresponds to the aligning field.

and were aligned at 60 kOe. There was no noticeable change in properties. Experience seems to indicate that premagnetizing the powder would only improve the magnetic properties when the alignment field was fairly weak (less than 10 kOe).

To summarize, the studies on alignment have shown that slight improvements of alignment can result in significant increases of permanent magnet properties such as the energy product. The jet milled powder aligns better than the ball milled powder. An alignment field in excess of 20 kOe is needed

for loosely packed powder, and in excess of 50 kOe for aligning powder with a packing of 50%.

Task 8--Pressing--Part I(F.G. Jones)

Initial densification of the cobalt-samarium magnets is achieved by means of hydrostatic pressing. This step follows alignment and increases the density of the magnet material to approximately 80% of that for a fully dense body.

Test bar specimens were prepared and evaluated in an effort to elucidate the relationships between pressing pressure, sintering temperature, and sintering time. The specific responses which have been evaluated are:

1. Green density (as-pressed)
2. Influence of green density on handling
3. Sintered density
4. Magnetic properties

All specimens were prepared from the same lot of powder (#3916) obtained from Task 1 studies. Pressing pressures studied were 100, 150, and 200 kpsi. Pressed specimens were then sintered at selected temperatures in the range from 1075° to 1125°C for times ranging from 30 to 1020 minutes. Relative densities of most specimens were determined before and after sintering. The magnetic properties of all specimens were measured after sintering.

The influence of pressing pressure on green density and handling ability is shown in Table XV. The qualitative comments concerning handling are based on cylindrical grinding of specimens to obtain green density data. This is the same type of grinding as might be used in manufacture of TWT magnets. Clearly, magnets pressed at 100 kpsi are difficult to handle in subsequent presintering processing. On the other hand, the increased strength of magnets pressed at 200 kpsi makes presintering machining possible; however, lighter cuts must be taken to avoid overheating and ignition.

The relative densities after sintering as well as selected magnetic properties are shown in Tables XVI, XVII, and XVIII.

Three factors affect the choice of pressing pressure:

1. Need to achieve sufficient density to promote long-time stability.
2. Need to reproducibly achieve a relatively high value of H_d.
3. Availability of suitable pressing equipment.

TABLE XV

Relative Densities and Handling Characteristics of As-pressed Specimens

Pressing Pressure (kpsi)	No. of Specimens	Mean Relative Density (%)	Handling Ability
100	12	72.0	Fragile. Ground only with great care to avoid fracture. Powders easily
150	5	76.0	Can be ground with care. Slight amount of dusting during handling
200	5	79.2	Can be ground. No apparent tendency to dusting during handling

TABLE XVI

Selected Properties of Specimens Pressed at 100 kpsi and Sintered as Indicated

Specimen	Sinter Temp (°C)	Sinter Time (min)	Packing Green (%)	Packing Sintered (%)	$(BH)_{max}$ (MGOe)	H_d at B/H = -1/2 (kOe)
AF-21	1075	126	--	78.6	7.3	-3.60
AF-22	1075	360	--	79.1	10.2	-4.25
AF-23	1075	960	--	80.5	10.7	-4.20
AF-18	1095	120	--	82.6	9.9	-4.20
AF-19	1095	360	--	83.1	8.4	-3.85
AF-20	1095	1020	--	84.2	11.2	-4.25
AF-1	1110	30	71.8	81.4	10.9	-4.45
AF-2	1110	120	72.2	90.4	13.3	-4.50
AF-14	1115	90	72.2	89.2	15.0	-4.80
AF-15	1115	90	71.7	87.4	13.7	-4.50
AF-3	1120	30	71.6	87.6	15.0	-4.80
AF-4	1120	120	72.3	95.0	13.7	-4.30

TABLE XVII

Selected Properties of Specimens Pressed at 150 kpsi and Sintered as Indicated

Specimen	Sinter Temp (°C)	Sinter Time (min)	Packing Green (%)	Packing Sintered (%)	$(BH)_{max}$ (MGOe)	H_d at B/H = - 1/2 (kOe)
AF-10	1105	90	76.1	86.7	14.8	-5.00
AF-12	1115	30	76.3	88.6	14.8	-5.00
AF-9	1115	90	75.8	91.5	15.2	-4.80
AF-13	1115	90	75.3	90.7	14.1	-4.70
AF-11	1125	90	76.3	95.2	14.1	-4.25

TABLE XVIII

Selected Properties of Specimens Pressed at 200 kpsi and Sintered as Indicated

Specimen	Sinter Temp (°C)	Sinter Time (min)	Packing Green (%)	Packing Sintered (%)	$(BH)_{max}$ (MGOe)	H_d at B/H = - 1/2 (kOe)
AF-5	1110	30	79.3	88.4	13.5	-4.85
AF-6	1110	120	78.7	93.2	16.8	-5.20
AF-16	1115	90	79.0	93.4	15.4	-4.80
AF-7	1120	30	79.6	93.1	15.4	-4.75
AF-8	1120	120	79.3	96.7	10.2	-3.50

Examination of the data shows that the first two criteria are best met by pressing at 200 kpsi. This choice of pressure, however, may not be the best from the point of view of overall economics of the process, and in some cases it may be best to utilize lower cost 100 kpsi pressures.

In addition to pressure-sintering relationships, studies have been focused on learning how to make hollow cylinders of sufficient size to allow manufacture of one-inch diameter TWT rings. Three approaches to tooling design have been taken. One set of tooling (Hollow Core) was fabricated according to the general design shown in Fig. 12. The mandrel is left in during filling and magnetic alignment, but removed prior to final hydrostatic pressing. Thus, pressure during pressing is applied to both the outside diameter and the inside diameter of the tube compact.

The second set of tooling is shown schematically in Fig. 13. In this arrangement the powder is compacted onto the mandrel which is subsequently removed.

Magnetically nonaligned pressings were made in both sets of tooling at a press pressure of 100 kpsi. Size and surface finish were acceptable, but final density was below that thought necessary for stability.

Magnetically aligned pressings were made at a press pressure of 200 kpsi. As expected, the subsequently sintered billets had higher density than those pressed at 100 kpsi.

The third approach which we studied involved creating the hole in a solid sintered cylinder by electro-discharge machining. In addition to poorer concentricity of the inside diameter and outside diameter this approach drastically reduces the yield of material in finished magnets.

The second approach outlined seems preferred and will be utilized with press pressures of 200 kpsi for fabrication of the cobalt-samarium magnets.

Task 8--Pressing--Part II (M.G. Benz)

In addition to studies of hydrostatic pressing of previously magnetically aligned powder, simultaneous alignment and pressing in semiautomatic die pressing equipment was briefly studied. The die body was a nonmagnetic molybdenum alloy. The punches were hardened tool steel. A tantalum carbide core pin was used. Powder was loosely loaded into the die cavity, the field was then increased to approximately 15 kOe, and the punches were advanced to apply the pressure.

Several rings were formed in this way. A photograph of one is shown in Fig. 14. The magnetic properties of such a ring, measured after sintering, are listed in Table XIX. For comparison the properties that would have been

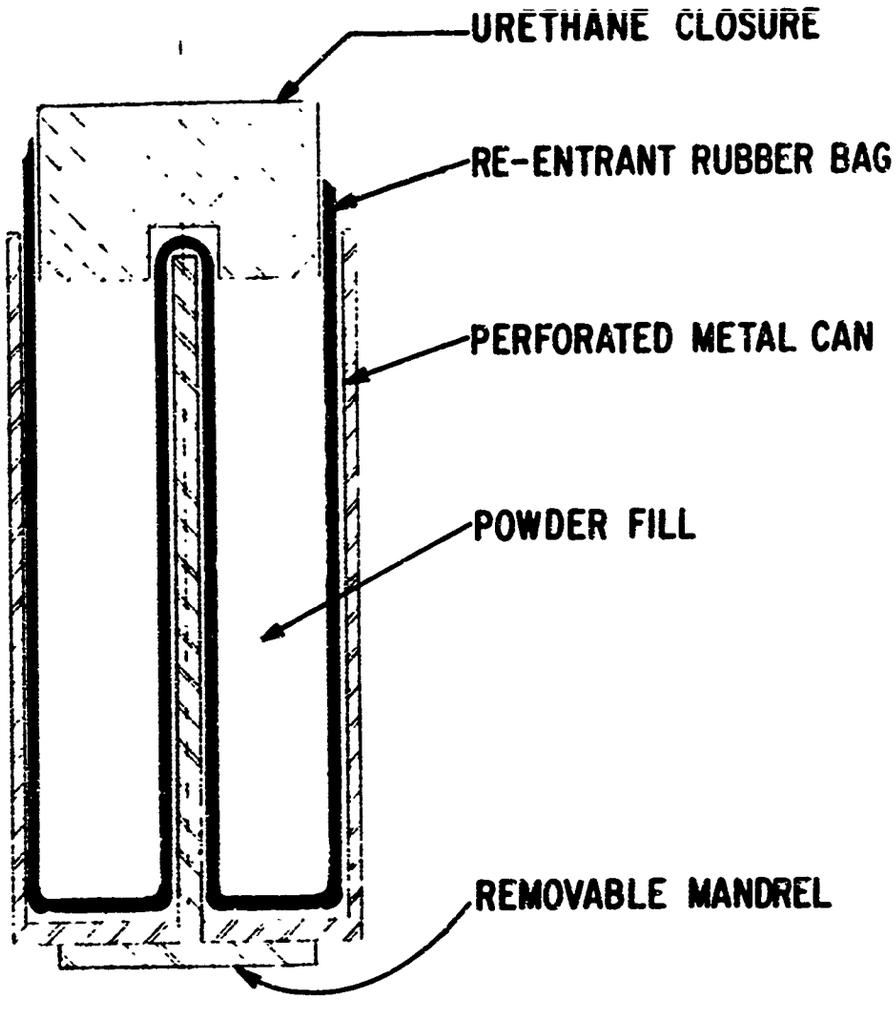

Figure 12 Schematic diagram of "hollow core" tooling. (Mandrel is removed during pressing.)

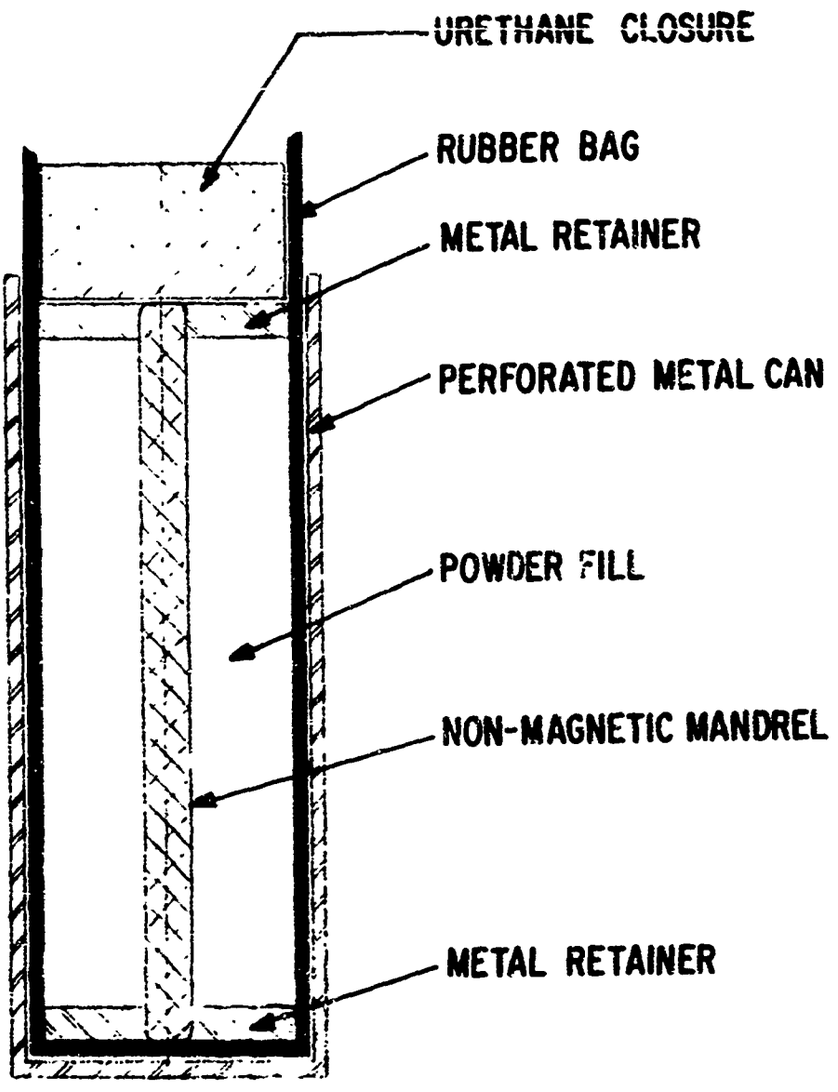

Figure 13 Schematic diagram of mandrel tooling. (Mandrel is left in during pressing.)

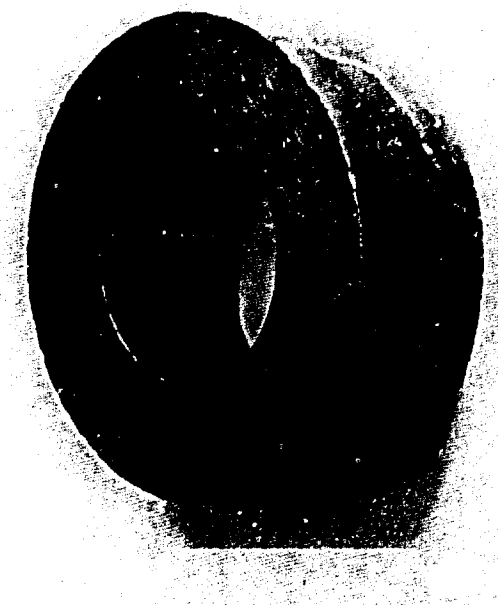

Fig. 14 Ring prepared by die pressing and sintering. Size: 0.475 inch ID by 0.917 inch OD by 0.302 inch thick. Maximum energy product 12 MGOe. Sample T-8-D-3.

TABLE XIX

Magnetic Properties for a Die Pressed Ring and for a High-Field Aligned Plus Hydrostatic Pressed Ring

	Die Pressed Ring[a]	High-Field Align plus Hydrostatic Pressed Ring[b]
Magnetization[c], $4\pi J$, kG	6.90	8.10
Demagnetizing Factor[d]	0.457	0.457
B/H Load Line[d]	-1.186	-1.186
Induction, B, kG	3.75	4.40
Field, H, kOe	-3.16	-3.70
Maximum Energy Product, $(BH)_{max}$, MGOe	12	16
Alignment Factor, A[e]	0.82	0.93

(a) Sample No. T-8-D-3; 0.475 in. I.D. × 0.917 in. O.D. × 0.302 in. thick. Density = 7.64 g/cm³. Packing = 0.89.

(b) Expected properties based on measurements from samples of slightly different dimensions.

(c) Magnetization measured with a torque magnetometer.

(d) Calculated using Eversheds Polar Radiation model (Ref. 6 in Section II).

(e) The alignment factor for the die pressed ring is calculated. It is that value which would account for the lower maximum energy product.

achieved utilizing the high field alignment plus hydrostatic pressing approach are also listed. The die pressing approach always gave lower magnetic results, primarily because the alignment factor was much lower with this approach. Therefore, as extremely high-performance rings are the goal of this program, work on die pressing was not continued.

Task 9--Sintering (M.G. Benz)

Final densification of the cobalt-samarium magnets is achieved by means of sintering. This step follows pressing and increases the density of the magnet material to approximately 90% of that for a fully dense body. A relative density in excess of approximately 87% is necessary to achieve the closed-pore structure desired for elimination of the loss of magnetic properties during long time exposure to air at elevated temperatures which is normally observed for open pore structures (see Supplementary Study 2). A photomicrograph showing this closed-pore structure is shown in Fig. 15.

The studies for this task have centered on: (1) furnace requirements, (2) atmosphere requirements, (3) time and temperature requirements, and (4) container materials. Test bar samples were prepared from a well characterized lot of powder. These samples were sintered in four different

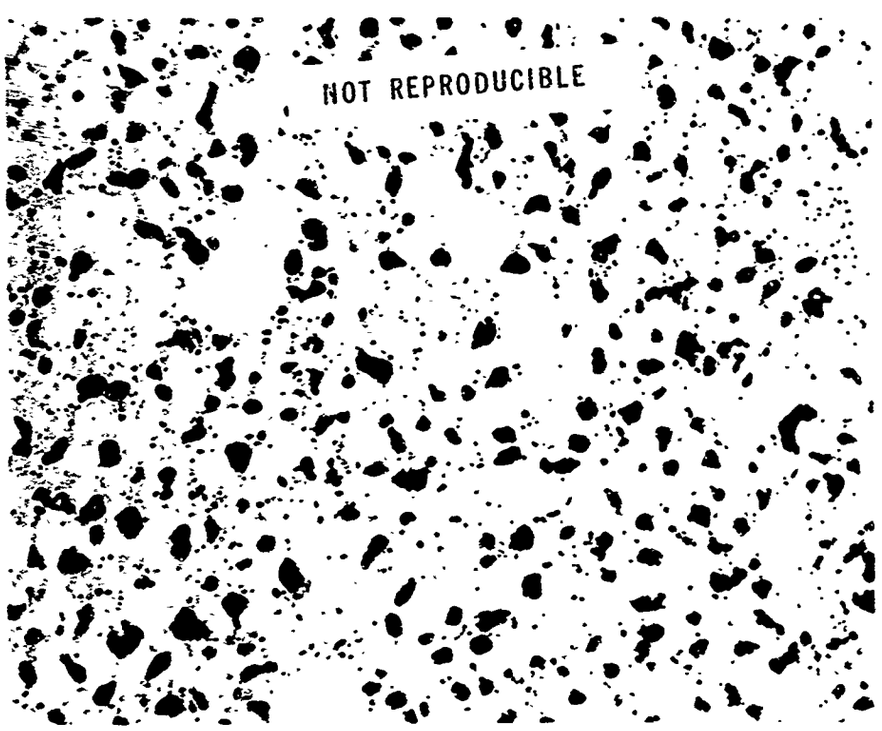

Figure 15 Photomicrograph of sintered Co-Sm showing closed pore structure. 1000X

furnaces under three different atmospheres for a variety of times and temperatures, using several types of containers and container materials. Test results from these samples are summarized in Table XX.

1. Furnace requirements. The furnaces used for this study were located in four different locations and operated by different operators. Furnaces B and M are vertical tube furnaces operated under laboratory conditions. Furnaces J and N are horizontal tube furnaces operated under pilot line and service operation conditions. Complete equivalence was observed for samples prepared in these furnaces. The small differences in results can be attributed to differences in temperature calibration of the units under consideration.

2. Atmosphere requirements. The atmospheres used for this study were argon, hydrogen, and nitrogen. Of the samples sintered under these atmospheres, only those sintered under argon achieved the expected relative density and full magnetic properties. With argon, no significant increase in oxygen level was detected during sintering. Vacuum fusion analysis was used for this determination. The samples prepared under dry hydrogen or nitrogen were not acceptable and in some cases showed a marked swelling and a spallation type of disintegration several days after the sintering. In previous studies, helium has been used interchangeably with argon; thus one of these two inert gases seems preferred for the sintering atmosphere. Vacuum was not used for these studies as it is quite oxidizing to samarium unless it is extremely good and gettered for oxygen. Such an atmosphere was not readily available.

3. Time and temperature requirements. A plot of relative density versus time at several temperatures is shown in Fig. 16. Maximum coercivity and maximum energy product are not necessarily achieved at maximum density. Careful examination H_c, H_d at $B/H = -1/2$ and $(BH)_{max}$ versus time and temperature as listed in Table XX indicate that careful attention to control of temperature and also time is necessary in order to achieve the desired result. In this program, emphasis is placed on the H_d at $B/H = -1/2$ as this will be the condition under which the magnets will operate in the device being evaluated.

4. Container types and container materials. The container types investigated were fabricated from niobium or tantalum. These included an open container, a closed container formed by nesting together open containers with one inverted, a closed container with a zirconium foil getter placed between the nested containers, and a closed container with a samarium getter inside. The results listed in Table XX indicate that either of the closed container systems with a getter is satisfactory.

Iron and molybdenum can be satisfactorily substituted for the niobium and tantalum. Sample T-9-26 was prepared this way and gave satisfactory

TABLE XX

Summary of Results for Task 9--Sintering

STUDY	FURNACE	ATMOSPHERE	TEMP (°C)	TIME (hr)	CONTAINER[a]	SAMPLE	B_s (kG)	B_r (kG)	H_c (kOe)	H_k (kOe)	H_{ci} (kOe)	$(BH)_{max}$ (MGOe)	DENSITY (g/cm^3)	P	A	H_d at B/H = 1/2 (kOe)
Furnace Requirements	B	Argon	1110	1	C	T-9-11	9.83	8.68	-7.3	-6.6	-15.9	16.0	7.85	0.91	0.97	-5.5
	B	Argon	1110	1	C	T-9-12	9.86	8.90	-7.4	-6.4	-16.0	17.8	7.77	0.90	0.97	-5.4
	M	Argon	1110	1	C	T-9-18	9.73	8.25	-6.8	-5.5	-16.8	16.0	7.60	0.88	0.96	-5.1
	M	Argon	1110	1	C	T-9-19	9.76	8.35	-7.4	-7.7	-18.2	16.8	7.64	0.89	0.96	-5.4
	I	Argon	1110	1	C	T-9-1	9.99	8.54	-7.2	-6.7	-14.0	17.2	7.63	0.89	0.96	-5.4
	J	Argon	1110	1	C	T-9-30	9.87	8.51	-7.4	-6.7	-14.5	17.0	7.67	0.89	0.97	-5.5
	N	Argon	1110	1	C	T-9-17	9.78	8.24	-6.3	-4.8	-12.7	15.9	7.52	0.88	0.96	-4.9
	N	Argon	1110	1	C	T-9-20	9.68	7.96	-7.1	-8.0	-17.1	15.8	7.36	0.86	0.96	-5.2
Atmospheres Other than Argon	N	Nitrogen	1110	1	O	T-9-8	-- -	Did not measure, sample fell apart after sintering								
	N	Nitrogen	1110	1	C-1	T-9-27	----	0.6	--	--	--	--	6.48	-	(sample fell apart after 2 days)	
	N	Hydrogen	1110	1	O	T-9-9	----	Did not measure; sample fell apart after sintering								
Temperature and Time	B	Argon	1090	1	C	T-9-13	9.78	7.87	-6.7	-6.3	-14.8	14.9	7.19	0.86	0.96	-5.0
	B	Argon	1090	2	C	T-9-14	9.80	7.84	-6.2	-5.0	-13.1	14.8	7.23	0.86	0.97	-4.8
	B	Argon	1090	4	C	T-9-15	9.96	8.20	-5.8	-4.6	-11.2	15.5	7.29	0.85	0.97	-4.7
	B	Argon	1090	16	C	T-9-16	9.97	8.54	-6.5	-5.0	-13.3	17.5	7.57	0.88	0.97	-5.1
	B	Argon	1100	1	C	T-9-1	9.81	8.23	-7.0	-7.0	-15.4	16.9	7.46	0.87	0.97	-5.4
	B	Argon	1100	1	C	T-9-2	9.78	8.16	-7.5	-8.0	-15.2	16.8	7.46	0.87	0.97	-5.4
	B	Argon	1100	2	C	T-9-28	9.76	8.19	-7.4	-7.4	-16.8	16.7	7.51	0.87	0.96	-5.3
	K	Argon	1100	4	C	T-9-29	9.90	8.55	-7.9	-6.6	-17.8	17.7	7.70	0.90	0.97	-5.5
	B	Argon	1110	1/2	C	GP 436	9.52	8.08	-7.1	-6.8	-10.8	16.0	7.54	0.88	0.97	-5.3
	B	Argon	1110	1/2	C	1963-33L	9.42	8.03	-7.5	-7.8	-13.4	16.1	7.49	0.87	0.96	-5.2
	B	Argon	1110	1	C	GP 429A	9.49	8.48	-7.1	-6.5	-14.2	18.1	7.81	0.92	0.97	-5.5
	B	Argon	1110	1	C	GP 436	9.55	8.48	-7.3	-6.8	-15.8	18.0	7.89	0.92	0.97	-5.7
	B	Argon	1110	2	C	GP 429B	9.59	8.52	-6.6	-5.4	-12.6	18.4	8.10	0.95	0.98	-5.3
	B	Argon	1110	2	C	GP 437	9.57	8.84	-6.6	-5.6	-14.0	18.0	8.20	0.95	0.97	-5.3
	B	Argon	1150	1/4	C	T-9-25	10.05	9.23	-4.2	-3.2	- 4.5	17.1	8.07	0.9-	0.98	-4.1
Container Types and Materials	B	Argon	1110	1	O	T-9-21	9.84	7.87	-6.4	-3.6	-17.2	13.5	7.18	0.84	0.96	-4.6
	B	Argon	1110	1	C-2	T-9-22	9.85	8.10	-6.1	-4.1	-15.2	14.2	7.32	0.85	0.97	-4.6
	B	Argon	1110	1	C	T-9-23	9.75	8.46	-7.3	-7.0	-15.3	17.6	7.72	0.90	0.97	-5.5
	B	Argon	1110	1	C-3	T-9-24	9.69	8.46	-7.2	-6.7	-17.9	17.4	7.79	0.91	0.96	-5.4
	B	Argon	1110	1	C-1	T-9-26	9.86	8.38	-7.3	-6.3	-12.4	16.0	7.59	0.88	0.97	-5.2

Note (a)

Code	Container Type
O	Open container fabricated from niobium or tantalum.
C	Nested open containers fabricated from niobium or tantalum with zirconium foil interlayer.
C-1	Nested open containers fabricated from iron with zirconium foil interlayer. Sample wrapped in molybdenum foil.
C-2	As for C but without zirconium foil interlayer.
C-3	As for C but with samarium getter inside containers.

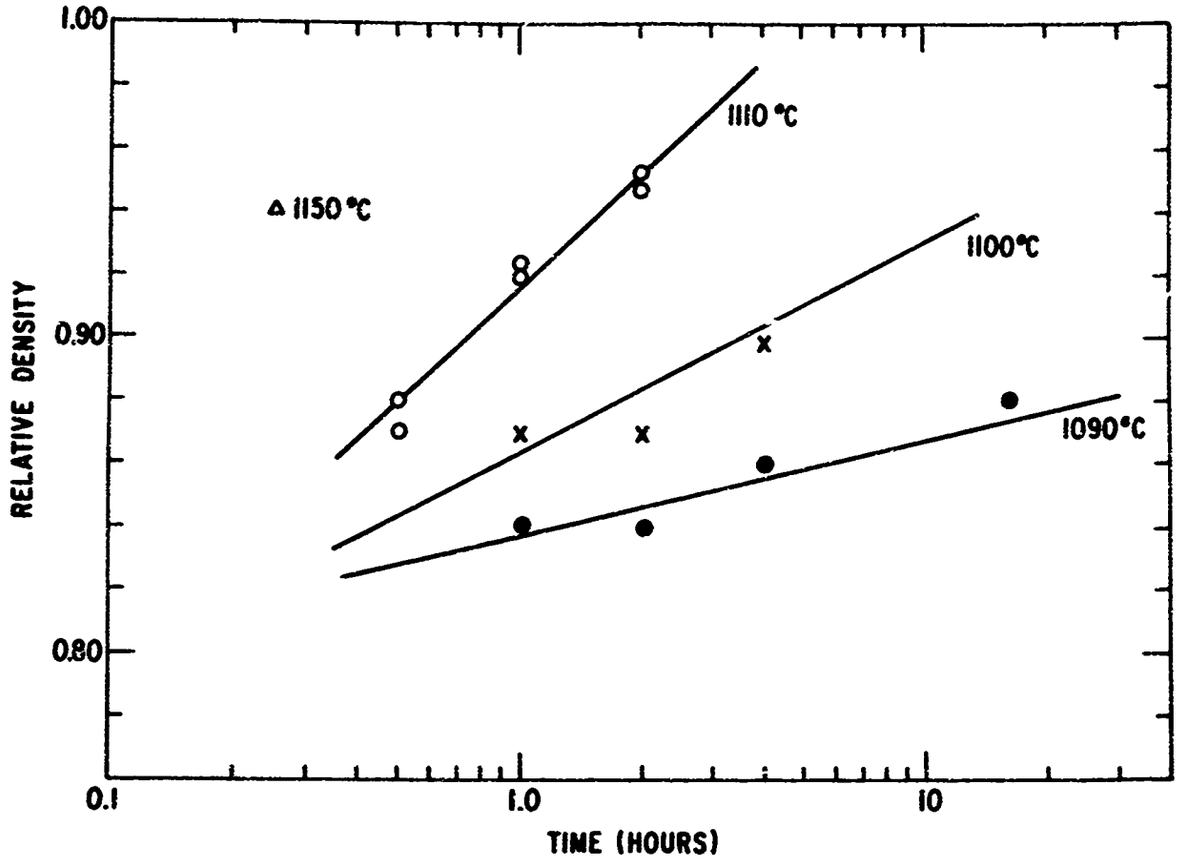

Figure 16 Relative density after sintering versus time and temperature. Relative density in the as pressed condition before sintering was 0.8.

results. The molybdenum was in contact with the sample. This in turn was inside of the iron container.

Task 10--Shaping--Part I (F. G. Jones)

Final shaping of the cobalt-samarium magnets is achieved by means of grinding and slicing after sintering. Prior to sintering, the inside diameter is established by use of a mandrel during pressing. The outside diameter is

established by dry grinding the outside diameter with coarse silicon carbide belts. Dimensions are chosen to allow for shrinkage during sintering.

After sintering, honing is used to size the inside diameter of the cylinder, and cylindrical grinding is used to size the outside diameter and to establish final concentricity. The cylinders are then sliced into rings and the rings are sliced in half for half-rings.

Solid bars and bars with center holes were prepared and used for surface grinding trials.

Tables XXI through XXV show the results of surface grinding trials using various typical wheels. The only successful grinding was accomplished with a very soft aluminum oxide wheel at metal removal rates below 0.015 cubic inches per minute.

Centerless grinding tests were carried out using a similarly soft aluminum oxide wheel (2A-601-L6-VL). All attempts to through-feed solid bars resulted in severely chipped parts. Plunge grinding could be carried out,

TABLE XXI

Al_2O_3 Type I Wheel 7" x 3/4" x 1 1/4"--32A60H8VBE

Test No.	Wheel Speed (sfpm)	Cross-feed (in)	Table Speed (fpm)	Down-feed (in)	RMS	Comments
1	5500	0.050	50	0.0005	27-32	Chipping almost nil
2	4000	.050	50	.001		Severe chipping
3	5500	.020	20	.001	18-25	No chipping
4	5500	.020	20	.002	27-32	No chipping
5	5500	.020	20	.003	34-41	Chipped on sides
6	5500	.050	50	.001	10-20	Some chipping
			Plunge Grinding			
7	5500		10	.0005	20-23	No chipping
8	5500		10	.001	22-24	No chipping
9	5500		50	.001	28-34	No chipping

TABLE XXII

Borazon Type II B1A1 Wheel 5" x 3/16" x 1 1/4" (60-80 Borazon RB#11)

Test No.	Wheel Speed (sfpm)	Cross-feed (in)	Table Speed (fpm)	Down-feed (in)	RMS	Comments
1	5500	0.050	50	0.001	110-130	Chipping nil
2	5500	.050	50	.002		Very severe chipping and large cracks
3	5500	.020	20	.002	35-47	Chipping nil
4	5500	.020	20	.003	60-75	Slight chipping
5	5500	.050	50	.0005	90-120	No chipping

TABLE XXIII

Diamond D1A1 Wheel 5" x 3/16" x 1 1/4" (60/80 RVG - RB#2)

Test No.	Wheel Speed (sfpm)	Cross-feed (in)	Table Speed (fpm)	Down-feed (in)	RMS	Comments
1	5500	0.020	20	0.0005	72-80	Slight chipping around entire workpiece
2	5500	.020	20	.002	70-85	Chipping around entire workpiece
3	5500	.050	50	.001	70-80	Severe chipping apparently from crossfeed pressure of wheel

TABLE XXIV

Al_2O_3 Type I Wheel 7" x 3/4" x 1 1/4"--32A60K5VBE

Test No.	Wheel Speed (sfpm)	Cross-feed (in)	Table Speed (fpm)	Down-feed (in)	RMS	Comments
1	5500	0.050	50	0.0005	22-29	Noticeable chipping
2	5500	.020	20	.002	33-39	Slight chipping

TABLE XXV

Silicon Carbide Type I Wheel 7" x 3/4" x 1 1/4"--39C100-J8VK

Test No.	Wheel Speed (sfpm)	Cross-feed (in)	Table Speed (fpm)	Down-feed (in)	RMS	Comments
1	5500	0.050	50	0.0005	12-17	Severe chipping. Lost ~40% of area
2	5500	.020	20	.002	20-30	Severe chipping. ~15% of area broken away

however, and metal removal rates of 0.2 cubic inches per minute with a 45 rms finish were attained.

Bars with center holes were used for trials of ID grinding, slicing of rings, and dicing of half-rings. Precision grinding of ID was accomplished using very high speed grinders and aluminum oxide abrasive. Honing is also effective for ID shaping if the amount of metal removal required is small.

Slicing of rings and dicing to half-rings is carried out using semiconductor techniques. The finish-ground hollow cylinder is mounted on a porcelain block using a high melting point wax. This is then mounted in the universal vise of a precision slicing machine and carefully aligned relative to the diamond cutting wheel. The cylinder is first diced lengthwise, then rotated 90 degrees and sliced into the appropriate number of half-rings. Gang slicing is also possible. Nearly chip-free cuts have been achieved using a 220 grit diamond wheel operating at 9000 sfm.

A limited study of lapping of ring magnets was carried out. Using a 14 micron compound, metal removal rate was 0.04 mil per minute.

Task 10--Shaping--Part II (W. A. Reed)

As most of the work outlined in the previous subsection was carried out at the General Electric Magnetic Materials Business Section (Edmore, Michigan), an alternate approach to shaping suitable for the machines available at the Research and Development Center was required. This approach is outlined in the following. It is the procedure that was used for the first shipment of full-size sample magnets in Phase III. Photographs of these operations are presented in Figs. 17 through 20.

Operation 1--Hone bore 0.330-inch diameter:

Hold part in hand on rotating hone

Sunnen Hone, A10 adaptor K10A57 stone

Sunnen Honing oil or kerosene

Average time per piece--8 minutes.

Operation 2--Grind OD 1.000 inch:

Mount part on stub mandrel held in chuck

Cincinnati Universal Grinder

Wheel 37C180-15B 14-inch diameter x 1-inch 6000 sfpm

Coolant Trim-Sol

Rotate part at 150 rpm, traverse speed 25 fpm,
infeed 0.0005-inch on diameter for each reversal of table

Average time 12 minutes.

Figure 17 Operation 1, inside diameter of a sintered bar sized by honing.

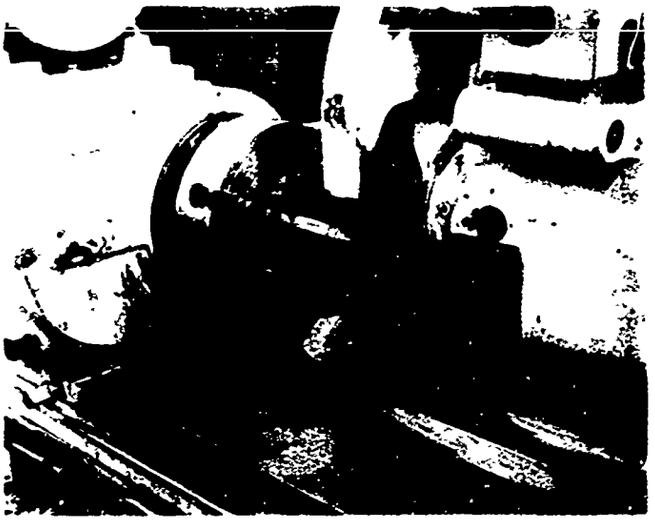

Figure 18 Operation 2, outside diameter of a sintered bar shaped by grinding.

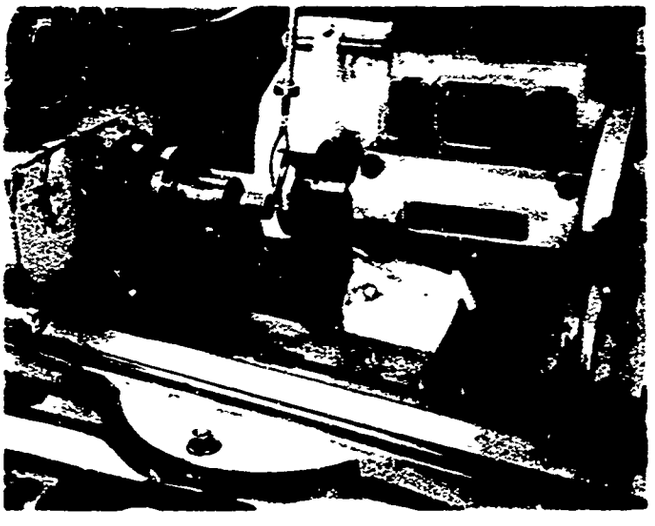

Figure 19 Operation 3, slices cut from the bar to form rings.

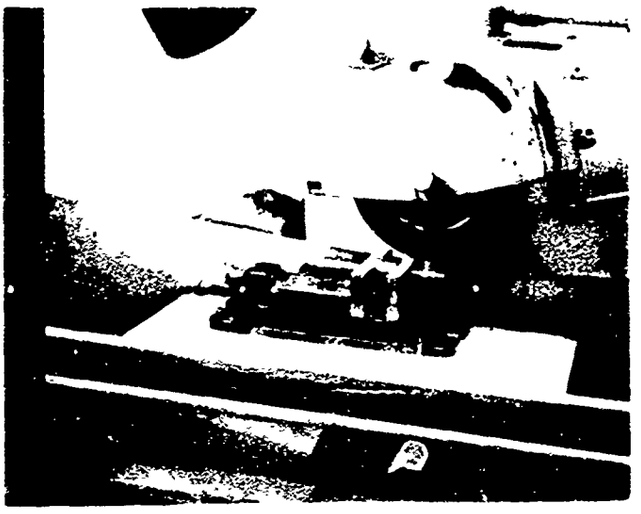

Figure 20 Operation 4, rings cut in half to form finished half-rings.

Operation 3--Cut slices from bar to form rings

Mount part on glass mandrel 0.328-inch diameter using glycol-thialate to secure part to mandrel

Mount mandrel in collet on Brown & Sharp #13 grinder

Wheel D180-L100M 1/16 Bay State Abrasive Products

Rotate part at 128 rpm; wheel speed 6000 sfpm

Plunge feed at 0.050-inch per minute manually

Average time 6 minutes per cut.

Operation 4--Cut rings into half rings:

Mount parts 10 at a time in special vise jaws which locate parts relative to removable mandrel

Do-all surface grinder Model 618-7

Wheel C120-JRA Allison Co. 7-inch diameter x 0.032 inch

Oscillate table at 50 fpm traverse speed

Downfeed manually 0.001 inch each table reversal

Approximate time 12 minutes. Wheel speed 6000 sfpm.

Task 11-Magnetization (D. L. Martin and R. J. Parker)

Our objective was to find a satisfactory method of magnetizing the TWT ring magnets. Two methods were evaluated: d-c magnetization in a superconducting solenoid and pulse magnetization.

Short samples with an L/D of 0.18 to 0.38 were measured. The pieces were demagnetized by heating to 1100°C for 15 minutes. The pieces were then magnetized in a peak field of 25 kOe, and the open-circuit magnetization was measured in a torque magnetometer in a field of ±100 Oe. The peak torque was measured for 360° rotation of the sample, and the magnetization, $4\pi J$, calculated from the relation

$$4\pi J = \frac{4\pi T}{HV \sin\theta}$$

where T is the average peak torque in dyne-cm,

H is the applied field in Oe,

V is the volume in cm^3, and sin θ is 1.

The results for several samples are listed in Table XXVI. The magnetization values are slightly higher (6% was highest increase) after being magnetized in a peak field of 100 kOe over a peak field of 25 kOe. Samples H, E, and F were initially pulse magnetized in a 25 kOe field. Again, additional magnetization at higher fields resulted in only a slight increase of the $4\pi J$ value. This experiment suggests that peak magnetizing field of 25 to 40 kOe might be adequate for magnetizing the rings.

An additional experiment was carried out on a 1.4-inch-long test bar. The sample was magnetized in increasing fields of 12, 30, 60, and 100 kOe. After each magnetization the B:H curve was measured. The results, tabulated in Table XXVII, show improvement at each higher field level. The coercive force, H_d at B/H = -1/2, and the $(BH)_{max}$ show the largest change. However, again the most rapid improvement occurs between 12 and 30 kOe.

Our conclusion from these studies is that a magnetizing field of 60 kOe is more than sufficient for magnetization of the TWT rings. Pulse magnetization appears to be a satisfactory method for magnetizing; however, we did not have equipment to explore it thoroughly at high fields.

TABLE XXVI

Effect of Peak Magnetizing Field on the Open Circuit Magnetization of the Sample

Sample	Peak Field (kOe) 25	40	80	100	% Increase for 100 kOe Magnetizing Field	L/D
	$4\pi J$, Gauss					
AF 17-B	6220	6320	6590	6580	5.8	0.181
AF 17-D	6940	7010	7040	7060	1.7	.38
AF 17-H	6610*	--	6700	6750	2.1	.18
AF 17-F	7110*	--	7120	7120	--	.38
AF 17-E	6770*	--	7020	7050	4	.38

*Samples magnetized in a pulse 25 kOe field.

TABLE XXVII

Effect of Peak Magnetizing Field on B:H Curve Data

Peak H (kOe)	B_r (Gauss)	H_c (Oe)	H_d (B/H = - 1/2) (Oe)	$(BH)_{max}$ (MGOe)
12.3	7500	-6350	-4700	13.4
30	7600	-7000	-5050	14.8
60	7600	-7200	-5050	14.8
100	7750	-7500	-5150	15.0

Task 12--Shipping--Part I (R. J. Parker)

We have studied the alternative of supplying unmagnetized magnets as opposed to supplying fully magnetized magnets. Due to the reversibility of the demagnetization curve of Co_5Sm magnets, it is possible to transfer a magnetized magnet into the magnetic circuit conditions of the TWT stack and obtain nearly full magnetic induction. For this program each magnet must be magnetized and measured. In view of this, it appears logical to package and ship the magnetized magnet rather than to demagnetize it and have the problem of remagnetization at the tube manufacturer's plant. As noted in the previous subsection, magnetization can only be achieved with extremely high magnetizing fields. It is not feasible for each tube manufacturer to maintain such field capability. At this time we favor supplying a fully magnetized and measured magnet ready for the TWT magnetic circuit.

The principal requirements of the packaging arrangement are that the magnetized magnet be protected from breakage and chipping and that a large number of magnets be so arranged that the leakage field is not objectionable to the carrier (a Federal specification exists). In Fig. 21, one possible arrangement is shown which we feel might be satisfactory. Basically the magnets are confined in a nonmagnetic packaging substance in which pockets are formed. A flat cover plate completes the confinement. At the bottom of the package, a magnetic steel plate is attached to the packaging substance. The spacing (B) is chosen so that an appreciable force of attraction exists. With this configuration the magnet should be held firmly and also a local magnetic circuit should be formed which localizes the leakage field and should make such a package acceptable from a leakage field standpoint. Actual experience in handling full size, full strength TWT half rings indicates that there is danger in breaking the half rings if one's finger should slip in removing these high energy magnets, however. The impact forces can be very large as the magnet accelerates and contacts a magnet edge.

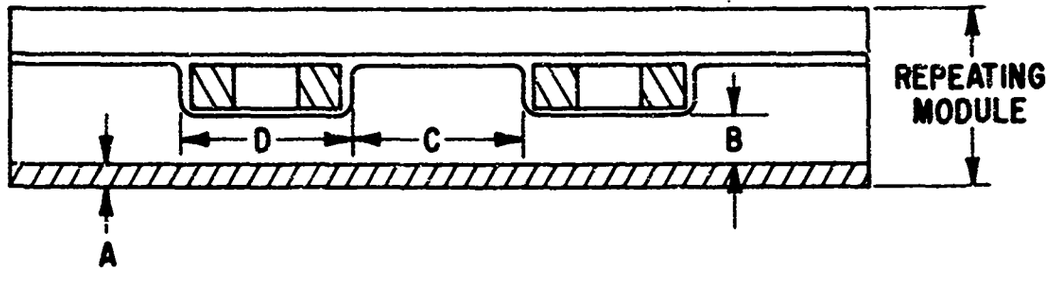

Figure 21 Packaging arrangement. D = outside diameter of magnet; C = spacing; B = distance to steel plate; and A = thickness of steel plate.

In handling magnets in the laboratory we have found that a small plastic box with a hinged top which snaps to close is a very effective and safe container and seems preferred for shipping. The magnet is placed on the bottom of the box and foam packing material is placed over it. Snapping the box shut compresses the foam and loads the magnet so that it will not slide to the side of the box if the box is dropped. We have measured the radiation field from several arrangements of half magnets in order to determine how the plastic boxes should be arranged in a packing carton for minimum radiation fields. In Fig. 22(a), readings of 0.02 to 0.08 gauss were obtained at a distance of one foot as the number of magnets was increased from 1 to 4. In Fig. 22(b) this arrangement produced approximately the same readings. In Fig. 22(c) we reversed the polarity so that a closed magnetic circuit was formed. Under these conditions the field reading was reduced to an estimated 0.005 gauss. We plan to place 84 plastic boxes in a standard shipping carton measuring 12 x 8 x 4 inches by arranging them as shown in Fig. 23.

Scaling up our modular radiation experiment the radiation (G) from the large array should be $G = A\ B/D^2$

Where A = The number of local circuits formed.

B = The gauss level per circuit at one foot.

D = The distance from the package in feet.

MIL-S-4473C is written around the allowable fields from large magnetron assemblies. It specifies the field level 7 feet from the container shall be less than 0.005 gauss.

Using our proposed package:

$$G = 21\ (0.005)\ (1/7)^2 = 0.002 \text{ gauss.}$$

Our general experience in shipping magnetized material is that carriers will accept magnetized material of about any level as long as the package is plainly marked "magnetized." Our complete package could be inserted in soft steel shielding material which would reduce the field level close to the package but not at a distance of several feet. We believe that in the interest of simplicity and to avoid the possibility of having a magnet accidentally attracted to the shielding material it is desirable to have a packaging system free from ferromagnetic components.

Task 12--Shipping--Part II (M.G. Benz)

Magnetized magnets shipped during Phase I and the early part of Phase III have been packaged with materials at hand in the following manner: (1) Each magnet is placed in a separate small cardboard box. (2) A nickel

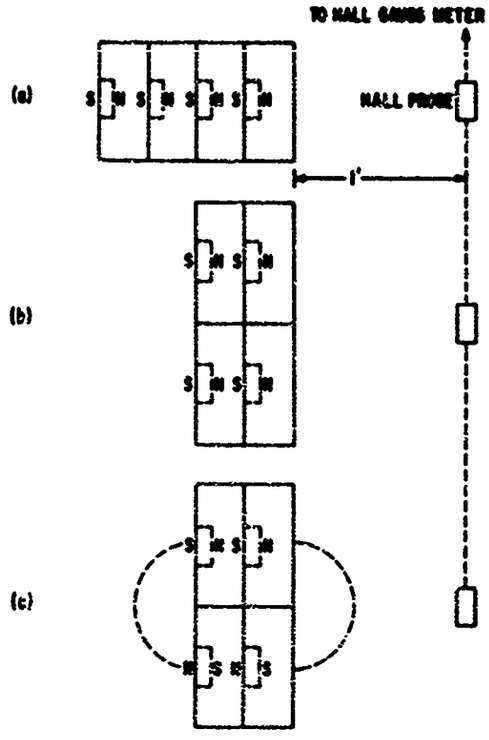

Figure 22 Schematic view of measurement of radiation field.

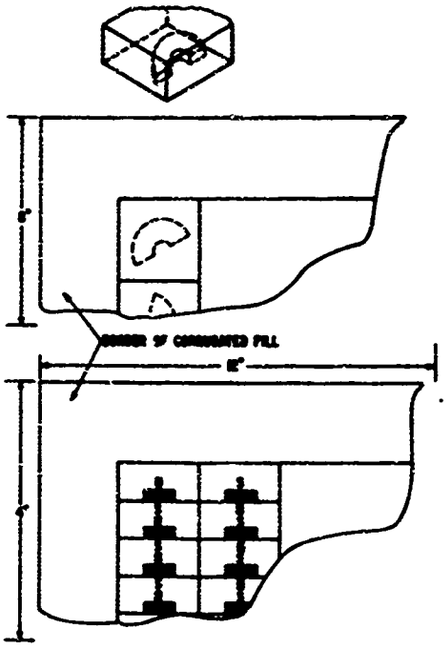

Figure 23 Packaging arrangement. View of half-ring magnet in a plastic box and partial views of plastic boxes packaged 84 per shipping carton.

keeper plate is placed on the outside of the bottom of the box. Magnetic forces hold the nickel plate onto the outside of the box and hold the magnet down inside the box. (3) Stacks of eight or so small boxes are wrapped in a paper wrapper, like a stack of coins. (4) Multiple stacks are packed into a metal container (1 gallon paint can) and arranged such that the fields tend to cancel. Foam padding is used to surround the stacks. (5) The metal container is packed in the center of a larger cardboard box so that the field level at the surface of the outer container is minimal.

Supplementary Study 1--Multi-task Interaction Study (M.G. Benz)

During the first several months of Phase I, some difficulties were noted in studies for several of the individual tasks. Therefore, it seemed appropriate to conduct a multi-task study in which all phases of powder and sample preparation were under close observation and control. Powder was prepared in the manner outlined under Tasks 1 through 5. It was blended as indicated in Task 6. The analytical chemistry results for this study are reported in Task 6. Samples were packed and aligned by several different methods, then pressed at 200 kpsi, shaped, sintered, and tested. The results are summarized in Table XXVIII. From these data it can be seen that alignment method and sintering time stand out as key factors for high performance.

Supplementary Study 2--150°C Aging Study (M.G. Benz)

In previous studies, it had been demonstrated that a sintered closed pore structure eliminates the nonrecoverable loss of magnetic properties during long time exposure to air at elevated temperatures, which is normally observed for open-pore pressed powder structures. In order to re-examine this observation, three samples were prepared, measured, exposed to air at 150°C for 1050 hours, and remeasured. The results of these measurements are summarized in Table XXIX. As can be seen, the more fully dense samples showed little or no change. These had a closed-pore structure. The less dense sample had an open-pore structure and showed considerable degradation.

Supplementary Study 3--Temperature Coefficient Study:
Reversible and Irreversible Losses--Part I (R.J. Parker)

In order to obtain data on the temperature stability of Co_5Sm under load conditions present in a TWT tube, the following measurements program was executed. One 1/2-inch-diameter bar (AF-17) was cut into short cylinders so that B/H values of approximately -0.4 and -1.0 were obtained. This bar of approximately 2 inches in length had samples 17A and 17B cut from one end, sample 17E cut from its center region, and samples 17H and 17I cut from the opposite end. A torque magnetometer was used to measure the change in magnetization. Samples were attached to the magnetometer sample holder which was located in a field established by Helmholtz coils. After saturation

TABLE XXVIII

Comparison of Co-Sm Samples--Multi-task Interaction Study

Sample No.	Packing and Alignment Method	Sintering Treatment	B_g (kG)	B_r (kG)	H_c (kOe)	$(BH)_{max}$ (MGOe)	H_d at $B/H=-1/2$ (kOe)	Density (g/cm^3)
GP431	A	1/2 hr, 1110°C	9.60	8.29	-6.70	17.0	-5.30	7.49
GP434	B	1/2 hr, 1110°C	9.52	8.08	-7.10	16.0	-5.35	7.54
GP435	C	1/2 hr, 1110°C	9.17	7.68	-7.10	14.2	-5.00	7.54
3943-32B	D	1/2 hr, 1110°C	9.10	7.78	-7.10	14.8	-5.10	7.57
3943-39L	E	1/2 hr, 1110°C	8.98	7.49	-7.00	14.0	-4.80	7.54
3943-33L	F	1/2 hr, 1110°C	9.42	8.03	-7.50	16.1	-5.20	7.49
GP432	A	1 hr, 1110°C	9.73	8.80	-7.20	19.3	-5.70	7.84
GP429A	B	1 hr, 1110°C	9.49	8.48	-7.10	18.1	-5.50	7.91
GP436	C	1 hr, 1110°C	9.55	8.48	-7.30	19.0	-5.70	7.89
3943-33B	D	1 hr, 1110°C	9.25	8.20	-7.20	16.2	-5.30	7.91
3943-36L	E	1 hr, 1110°C	8.74	7.52	-6.70	14.0	-4.80	7.93
GP433	A	2 hr, 1110°C	9.89	9.27	-6.60	20.5	-5.50	8.15
GP429B	B	2 hr, 1110°C	9.59	8.92	-6.60	18.4	-5.30	8.19
GP437	C	2 hr, 1110°C	9.57	8.84	-6.60	19.0	-5.30	8.20
3943-35B	D	2 hr, 1110°C	9.52	8.85	-7.00	18.5	-5.50	8.19
3943-37L	E	2 hr, 1110°C	9.20	8.50	-6.80	17.8	-5.30	8.24

TABLE XXIX

Summary of Results for Supplementary Study 2--150°C Aging Study
(Samples were Measured in the As-Sintered Condition and after Aging 1145 Hours at 150°C in Air)

SAMPLE CONDITION	PORE STRUCTURE	SAMPLE	B_s (kG)	B_r (kG)	H_c (kOe)	H_k (kOe)	H_{ci} (kOe)	$(BH)_{max}$ (MGOe)	Density (g/cm^3)	P	A	H_d at B/H = -1 (kOe)
As-sintered	Closed	GP 336	8.53	7.89	-6.7	-6.0	-17.6	14.8	7.69	0.89	0.94	-5.0
Aged	Closed	GP 336	9.33	7.89	-6.4	-4.9	-16.3	14.4	7.71	0.90	0.94	-4.9
As-sintered	Closed	GP 337	9.61	8.16	-6.9	-5.2	-16.1	15.6	7.64	0.89	0.96	-5.1
Aged	Closed	GP 337	9.65	8.26	-5.9	-3.7	-12.4	13.8	7.72	0.90	0.95	-4.5
As-sintered	Open	GP 342	9.58	7.75	-7.2	-7.8	-19.9	14.8	7.29	0.85	0.95	-5.1
Aged	Open	GP 342	9.72	7.50	-2.4	-0.7	- 2.7	5.2	7.34	0.85	0.91	-2.2

at 60,000 Oe the maximum torque was averaged for each sample in a constant field set at ±100 Oe. Low-temperature points (-196°C) were obtained by submerging sample in liquid nitrogen. The high-temperature points were obtained by submerging samples in heated silicone oil. The low-temperature data were determined first, and then without remagnetization the high-temperature data were obtained. Since the torque is proportional to the intrinsic magnetization of the sample, the output of the magnetometer transducer converted to dyne-cm per oersted is all that is required to calculate irreversible loss and reversible temperature coefficient. Table XXX displays the actual torque values obtained and the calculated loss and coefficients for all five samples. Since the results indicated negligible loss after low-temperature exposure, room-temperature readings were omitted on three of the five samples before proceeding with the high-temperature data.

The results confirm previous work on long rods with respect to reversible temperature coefficient in the +23° to 150°C range. This coefficient appears to be quite insensitive to load line and is approximately twice as large as that experienced with Alnico magnets with which the TWT industry has a lot of experience. The coefficient below room temperature appears to be a much lower value.

The irreversible loss after low-temperature exposure is essentially nonexistent. However, after 150°C exposure, it is rather high and the table indicates it is quite sensitive to the B/H level. Previous work with long rods (B/H = -22) disclosed an irreversible loss of only 0.1% after exposure to 175°C. With the low values of B/H, the magnet is in a strong self-imposed demagnetization field, and this field environment is a critical factor in the new energy balance at high-temperature exposure.

We have also built an additional apparatus which is convenient and accurate for determining irreversible and reversible losses. The basic elements of this equipment are illustrated in Fig. 24. Briefly, high-temperature insulated wire is used in three search coils that can be removed together from a room-temperature reference specimen, a hot specimen, and a cold specimen. By connecting coils in electrical opposition and by use of 10-turn helipots for balancing, a null can be obtained between all at room temperature. As the temperature is raised or lowered the IDVM reads the differential with respect to the stabilized room-temperature reference. We appear to have good repeatability in spite of less than optimum bearing surfaces on the rods holding the coils.

We have observed somewhat high values of irreversible loss for some Co_5Sm specimens (B/H = -1/2 at + 150°C). We have looked at two levels of a-c knockdown in an attempt to remove this irreversible loss without temperature cycling. The results obtained are shown in Fig. 25. On one Co_5Sm specimen (B/H = -1/2 at + 150°C), 98% of the irreversibility was removed with a 10% knockdown from saturation. This preliminary look at using field

TABLE XXX

Summary of Reversible and Irreversible Losses

		17A	17B	17E	17H	17I
Diameter (in)		0.535	0.529	0.529	0.532	0.527
Length (in)		.195	.095	.200	.095	.204
B/H		-.958	-.421	-1.00	-.416	-1.03
Torque (dyne-cm per Oe)	at +23°C	411.9	188.9	411.8	189.6	436.6
	at -196°C	444.6	198.2	433.4	194.9	463.6
	at +23°C		188.1			435.3
	at +150°C	344.1	154.6	351.6	149.4	375.4
	at +23°C	363.6	162.9	371.3	159.8	393.3
% Irreversible change in magnetization at +23°C after exposure to:	-196°C		+.042			+.030
" "	+150°C	-11.8*	-13.3	-9.8*	-15.8*	-9.6
Reversible temp. coef. --% magnetization change per °C over range +23° to 196°C		+.0368	+.023	+.024	+.013	+.028
Reversible temp. coef. --% magnetization change per °C over range +23° to +150°C		-.0425	-.040	-.0425	-.049	-.036

*Low-temperature irreversibility assumed to be zero on these three samples.

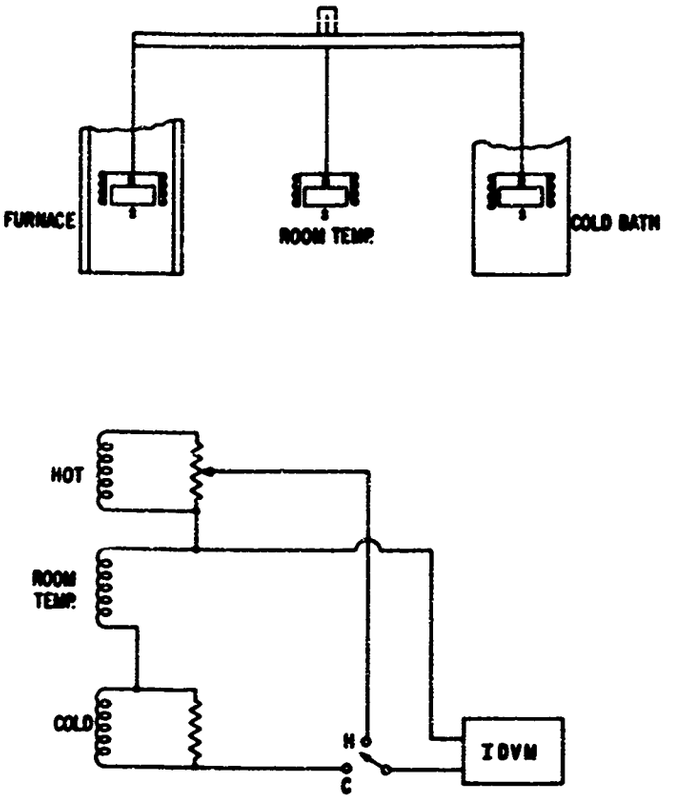

Figure 24 Schematic view of apparatus for measuring temperature losses.

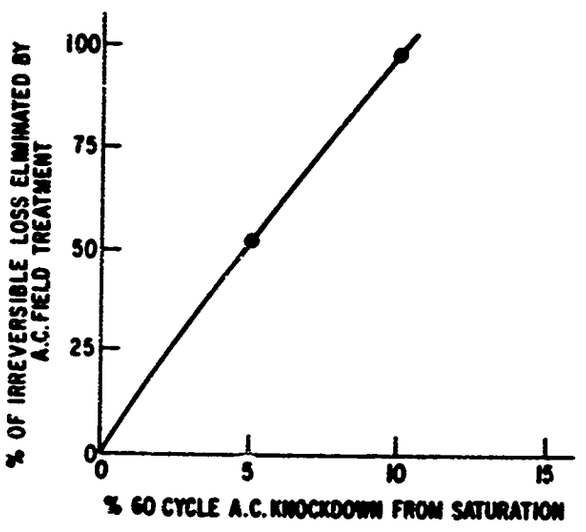

Figure 25 Irreversible loss removed by a-c knockdown of magnetization.

energy instead of thermal energy input to remove irreversibility is encouraging and may ultimately allow stabilization and calibration to be combined in tube manufacturing.

Supplementary Study 3--Temperature Coefficient Study: Reversible and Irreversible Losses--Part II (M.G. Benz)

Additional irreversible temperature loss samples were studied in order to more fully document this effect. The samples were thin disks and were heated in an open-circuit configuration. The results are summarized in Table XXXI. A correlation between relative density after sintering and irreversible losses at 250°C is noted. The reduced loss for the higher relative density samples is probably due to the fact that these samples are more nearly homogeneous in composition.

It should be noted that these samples were heated in the open-circuit configuration. Under such loading, larger demagnetizing forces occur at the edges than for closed-circuit loading at the same load line. By this hypothesis, reduced losses should be observed for closed-circuit configurations. By the same hypothesis, larger losses should be observed for half-rings in the open-circuit configuration as there is more edge area than for disks. However, in closed-circuit loading the losses should be reduced to the same value as for disks in closed-circuit loading.

It also should be noted that these irreversible losses are completely recoverable by remagnetization of the body. They are not to be confused with the loss of magnetic properties (nonrecoverable) that happens to porous structures on long time exposures to air at elevated temperatures. (See Supplementary Study 2 for a discussion of nonrecoverable losses.)

Supplementary Study 4--Electrical and Mechanical Properties (M.G. Benz)

Three sintered bar samples were ground to specimens 0.163 inch in diameter by 1 1/4 inches long. The resistivity was measured with the four-probe potentiometric technique. The three samples varied in relative density from 0.88 to 0.95. The average resistivity for these samples normalized to a relative density of 0.90 was 53×10^{-6} ohm-cm.

The center sections of these samples were polished with fine diamond polishing compound. The fracture load for 0.625 span bend tests showed a flexural strength in excess of 20,000 psi. The samples were not magnetized during these tests.

The results of the electrical and mechanical properties, including hardness, are summarized in Table XXXII.

TABLE XXXI

Irreversible Temperature Losses for Thin Disk Samples Magnetized Axially

Sample	Relative Density[a]	Sintering Time (hr)	Temp (°C)	L/D	B/H[b]	Irreversible Loss at 23°C After Exposure to: (%) 150°C	200°C	250°C
3943-36L	0.92	1	1110	0.205	-0.49	9.2	16.7	26.3
735-A6A	.92	1	1110	.229	- .55	16.9	27.9	35.4
T-9-1	.87	1	1100	.192	- .45	12.8	50.9	81.6
3943-39L	.88	1/2	1110	.245	- .60	7.2	33.8	84.8

(a) Full density = 8.6 g/cm^3.

(b) B/H calculated using Evershed's Polar Radiation Model (Ref. 6 in Section II).

TABLE XXXII

Electrical and Mechanical Properties for Sintered Cobalt-Samarium

Sample	Relative Density[a]	Resistivity (10^{-6} ohm-cm)	Flexural Strength (kpsi)	Hardness, Vickers DPH
3943-32B	0.88	58	20.3	380
3943-33B	.92	51	23.1	499
3943-35B	.95	48	23.0	568

(a) Full density = 8.6 g/cm^3.

Supplementary Study 5--Preparation and Evaluation of Sample (1/2 Scale) TWT Magnets: Part I--Preparation (M. G. Benz and A. C. Rockwood)

Five bars were prepared according to procedures outlined in Tasks 1 through 9. The outside diameter of these bars was 0.625 ± 0.006 inch.

Disks were sliced from these bars using a rotating chuck cylindrical grinder. The thickness of the disks was 0.135 ± 0.001 inch.

Holes, 0.349 inch in diameter, were drilled in these disks using an electro-discharge machine. The resulting rings were smoothed on a lap, then set up on a surface grinder and sliced in half using a 1/32-inch alumina wheel.

The resulting magnets were visually inspected, magnetized at 100 kOe, tested in a torque magnetometer for uniformity and shipped to the Electron Dynamics Division of Hughes Aircraft for evaluation. Table XXXIII summarizes the results of the above tests.

Supplementary Study 5--Preparation and Evaluation of Sample (1/2 Scale) TWT Magnets: Part II--Evaluation (Electron Dynamics Division, Hughes Aircraft Company) [see Note (a)]

Magnets were received for preliminary evaluation. The outer diameter of the pole pieces was reduced to accommodate the corresponding magnet diameter (0.625 inch).

The accompanying graph, Fig. 26, shows how the axial magnetic field varies with position through the stack at room temperature. The stack contains eleven (11) magnets and twelve (12) pole pieces. The variation of peak fields from magnet to magnet is due in part to end effects which tend to

Note (a) Taken from progress reports submitted by A. M. Orta of Hughes Aircraft Company in partial fulfillment of subcontract.

TABLE XXXIII

Phase I--TWT Magnets

	First Half				Second Half		
	Ring No.	Thickness (in)	Relative[1] Magnetization	Surface Cond.	Thickness (in)	Relative[1] Magnetization	Surface Cond.
64881	1	0.1352	1.015	Good	0.1352	1.003	Outside Chip
	2	.1357	.985	OD Chip	.1357	1.001	OD Face Chip
	3	.1354	.977	Good	---	---	Good
	4	.1351	.943	Good	---	---	Good
	5	.1353	1.077	Good	.1352	1.061	Good
	6	.1353	1.099	Good	---	---	Good
	7	.1360	.946	Corner Chip	.1355	.944	Corner Chip
64882	1	.1355	.983	Good	---	---	Good
	2	.1357	.982	Good	---	---	Good
	3	.1345	1.028	Good	---	---	Good
	4	.1360	.997	Good	---	---	Good
	5	.1358	1.087	Good	.1357	1.073	Good
	6	.1351	1.008	Good	---	---	Good
64883	1	.1354	.965	Good	---	---	Good
	2	.1346	.937	Good	.1347	.943	Good
	3	.1350	.964	Good	---	---	OD Chip
	4	.1345	.945	Good	---	---	Corner Chip
	5	.1348	1.057	Good	---	---	Corner Chip
	6	.1354	.923	Good	.1354	.919	Good
	7	.1347	.998	Good	---	---	Good
64885	1	.1355	.948	Good	---	---	Good
	2	.1360	1.054	Good	---	---	Good
	3	.1354	.989	Good	---	---	Good
	4	.1342	.985	Good	.1342	1.008	Good
	5	.1350	1.051	Good	---	---	Good
	6	.1350	.985	Good	---	---	Good
	7	.1347	.969	Good	---	---	Good
64886	1	.1350	1.012	Corner Chip	---	---	Corner Chip
	2	.1351	1.001	Good	---	---	Good
	3	.1353	1.029	Good	---	---	Good
	4	.1358	1.068	Good	---	---	Good
	5	.1354	1.004	Good	---	---	Good
	6	.1350	1.001	Good	---	---	Good
	7	.1361	.909	Good	---	---	Good

(1)Magnetization (B-H) was determined with a torque magnetometer using an applied field of 100 Oe. Magnetization is proportional to torque per unit field for magnets of equal volume. Relative magnetization is defined as the magnetization divided by the average magnetization for the total lot of magnets. The average torque per unit field for the half ring magnets was 125.3 dyne-cm/Oe. The torque per unit field for a full (uncut) ring was 277.9 dyne-cm/Oe.

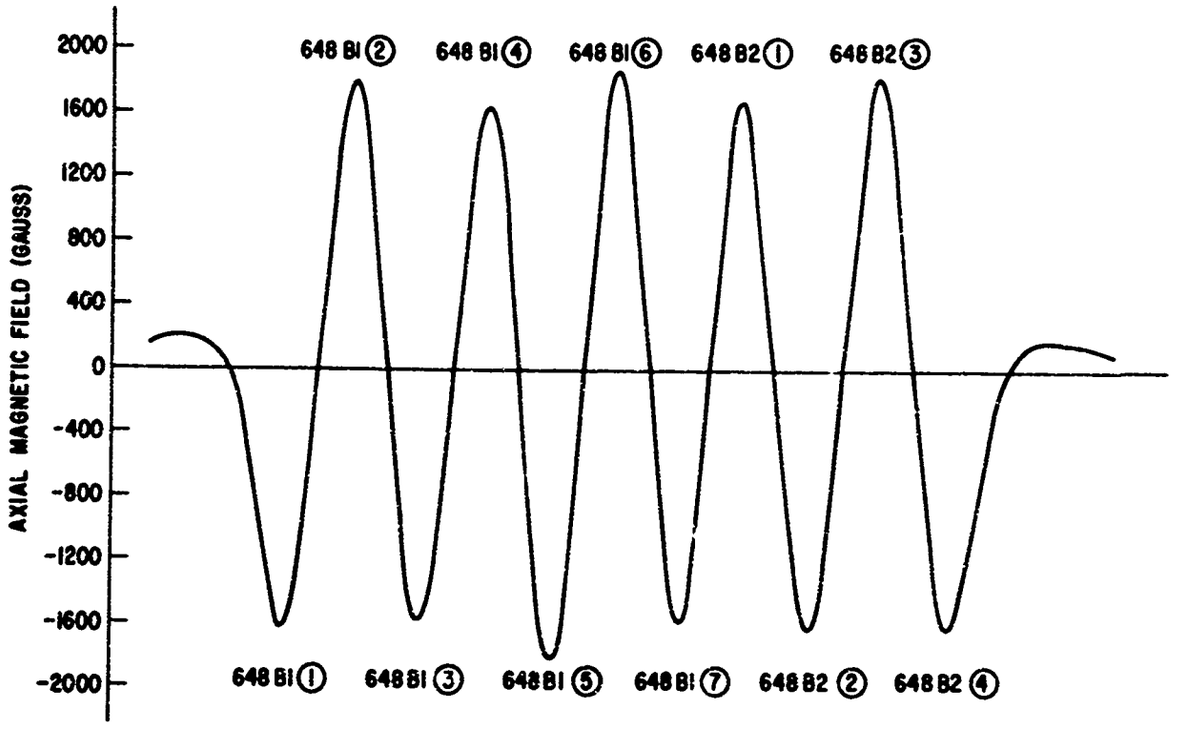

Figure 26 Axial magnetic field versus position.

propagate inward. A summary of the theoretical and measured axial fields is given below. The highest peak field measured, which occurs at the center of the stack, is essentially the same as that predicted by theory.

THEORETICAL

Load line slope = -1.21

H_d = 3500 Oe (from magnetic properties of lot PV648B)

B_{peak} = 1875 gauss

B_{pole} = 10,400 gauss max.

MEASURED

B_{peak} = 1870 gauss max.

This same magnet stack has been subjected to many temperature cycles to determine both the reversible and irreversible temperature coefficients. Since the load line of this structure is -1.21, the coefficients only apply in the vicinity of this value.

A search coil was used in conjunction with an integrating fluxmeter to provide a means of measuring the axial magnetic field of the PPM stack at elevated temperatures. The stack was cycled from 24° to 100°C in 25°C increments four different times. No measurable irreversible loss was observed after the first temperature cycle. That is, there was a complete recovery of magnetic field in cycling from 24° to 100°C and then back to 24°C after the initial loss. The stack was then cycled another four times from 24° to 175°C. Again an irreversible loss was observed on the first cycle, but complete field recovery was observed on subsequent cycles. A summary of the reversible and irreversible coefficients is given below:

TEMPERATURE COEFFICIENTS

(Load line slope = -1.21)

Reversible

0.042% per °C

Irreversible

4.4% from 24° to 100°C

7.9% from 100° to 175°C

12.3% from 24° to 175°C

Supplementary Study 6--Safety (J. M. Reynolds)

Safety practice during processing should comply with the Walsh-Healy Safety Standards Act of May 1969. Standards for cobalt and samarium oxide are as follows:

Cobalt (Dust and Fume)

The applicable standard for cobalt (dust and fume) is included in sub-part D of the Act, titled "Gases, Vapors, Fumes, Dusts and Mists."

The standard essentially includes the following:

(A) No employee shall be exposed by inhalation, ingestion; skin absorption or contact to any material or substance at a concentration above that specified in the "Threshold Limit Values (TLV)* of Airborne Contaminants for 1968" of the American Conference of Governmental Industrial Hygienists (ACGIH).

(B) In all cases, feasible engineering controls must first be determined and implemented. Methods of control in the working environment include local exhaust ventilation, general room air ventilation for dilution of the contaminant, substitution of a less toxic material, and isolation or enclosure of the process or operation. In cases where protective equipment in addition to other measures is used as the method of protecting the employee, such protection must be approved for each specific case by a competent person trained in the field of industrial hygiene.

The accepted TLV for cobalt dust and fume is 0.1 mg/m^3 as established by the ACGIH.

Samarium Oxide (Dust and Fume)

The applicable standard for samarium oxide is included in sub-part C of the Act, titled "Exposure to Airborne Radioactive Material."

The Standard essentially includes the following:

(A) No employer shall possess, use, or transport radioactive material in such a manner as to cause any employee, within a restricted area, to be exposed to airborne radioactive material in an average concentration in excess of the limits specified in Table I or Appendix B to 10 CFR Part 20. The limits in Table I are for exposure to the concentrations specified for 40 hours in any work week of 7 consecutive days.

(B) "Exposed" as used in this rule means that the individual is present in an airborne concentration. No allowance shall be made for the use of protective clothing or equipment, or particle size except as authorized by the Director, Bureau of Labor Standards.

---

*The TLV's refer to airborne concentrations of substances and represent conditions under which it is believed that nearly all workers may be repeatedly exposed, day after day, without adverse effect. They are based on the best available information from industrial experience, from experimental human and animal studies, and when possible from a combination of the three.

Samarium oxide contains approximately 13.7% Samarium-147 an alpha emitting radionuclide. The limit for Samarium-147 as specified in the above reference (A) is 7×10^{-11} μCi/ml. To convert this value in terms of mg/m^3 it is necessary to find the specific activity of Sm-147, then through dimensional analysis and percent Sm-147 content. The permissible limit is 27.2 mg/m^3 of Samarium Oxide.

This figure compares with such relatively nontoxic chemicals as---

Substance	TLV (mg/m^3)
Boron Oxide	15
Iron Oxide Fume	15
Titanium Dioxide	15
Ronnel (Food additive)	15

Comparing its specific radioactivity with other alpha emitting nuclides and calculating the specified limits in terms of (mg/m^3)---

Substance	Specific Activity (Ci/g)	Specified Limits (mg/m^3)
Plutonium-239	6.2×10^{-2}	3.2×10^{-4}
Radium-226	1.0	3.0×10^{-8}
Uranium-238	3.3×10^{-7}	0.2
Uranium-235	2.2×10^{-6}	0.2
Thorium-232	1.0×10^{-7}	0.3
Samarium-147	2.0×10^{-8}	3.7
Samarium oxide	2.7×10^{-9}	27.2

It is apparent that samarium oxide can be regarded as a low toxicity radioactive material.

With respect to radioactivity, it should be further emphasized that no detectable radiation (alpha emission) has been observed for the cobalt-samarium magnets fabricated on this program. In addition, as the magnets contain specific radioactivity equivalent to that of potassium in its natural state (0.001 microcurie/gram), they are exempt (Exemption 10 and pending Exemption 15) from the New York State Industrial Code--Rule No. 38. This code reads as follows:

> Rule No. 38, "Radiation Protection," applies to every person who, in any industry, trade, occupation, or process in the State, transfers, receives, possesses, or uses any radiation source. The general requirement of the rule is that no person shall transfer, receive, possess, or use any agreement material unless he is duly licensed to do so pursuant to the Rule.

The specific exemptions to the Rule under Section 38-3 are:

Exemption 10. Radioactive material, other than agreement material containing a specific radioactivity that does not exceed that of potassium occurring in its natural state (0.001 microcurie/gram).

Exemption 15 (pending). Rare earth metals and compounds, mixtures, and products containing not more than 0.25 percent by weight thorium, uranium, or any combination of these. This Exemption does not apply to the manufacture or importation of any of these products.

Selection of Microwave Device (Electron Dynamics Division Hughes Aircraft Company) [See note (a)]

The traveling wave tube to be used in the evaluation of the cobalt-samarium magnets shall be Hughes 641H. The performance characteristics of this tube as currently fabricated are:

Output power	61 dbm min
Frequency	4.0 to 8.0 GH_z
Duty cycle	10%
Gain	25 db
Size	2 5/8 by 14 1/2 inches
Weight	8 3/4 lb
Cooling	Dielectric oil

The 10% duty cycle is the maximum level that this tube has achieved with its present focusing structure. The tube has not been subjected to the requirements of MIL-E-5400 Class II at this high duty cycle.

Magnet Characterization (M. G. Benz)

The typical properties of the cobalt-samarium magnets to be produced on this program are listed in Table XXXIV. The specific dimensions of the magnets are included in Figs. 27 and 28. Eighty (80) standard circuit magnets (SP61367) and four (4) match magnets will be required for each tube. The match magnets are required at the input and output of the tube to allow access to the r-f couplers. Magnets fabricated to the above performance characteristics and dimensions should produce a B(peak) of 2760 gauss in the 641H period permanent magnet structure.

Note (a) Taken from monthly progress reports submitted by A. M. Orta of Hughes Aircraft Company in partial fulfillment of subcontract.

TABLE XXXIV

Typical Properties of Cobalt-Samarium Magnets[a]

Residual Induction, B_r	8200 Gauss
Induction Coercive Force, H_c	-6500 Oe
Intrinsic Coercive Force, H_{ci}	Greater than -12,000 Oe
Energy Product, $(BH)_{max}$	15×10^6 Gauss-Oe
Reversible Temp Coefficient (Average from -196° to +150°C)	-0.04% per °C
Irreversible Temp Change at 23°C after exposure to	
-196°C	+.04%
+150°C	-10%
(Sample B/H = -1)	
Magnet Life (Sample B/H = -1)	Less than 5% variation over 1000 hr at 120°C
Density	7.7 g/cm^3
Resistivity	50×10^{-6} ohm-cm
Flexural Strength (polished specimen)	20 kpsi
Fracture Mode	Brittle
Impact Strength	Capable of withstanding normal shipping, assembly, handling, and operation of TWT tubes consistent with MIL-5400 class II environmental requirements
Hardness, Vickers DPH	500

Note (a). This list of properties was prepared by the Research and Development Center, General Electric Company, Schenectady, New York, at the completion of Phase I--Analysis (June 15, 1970) of USAF Contract No. F33615-70-C-1098, "Manufacturing Methods and Technology for Processing Cobalt-Samarium Magnets," initiated under Project No. 612-9A.

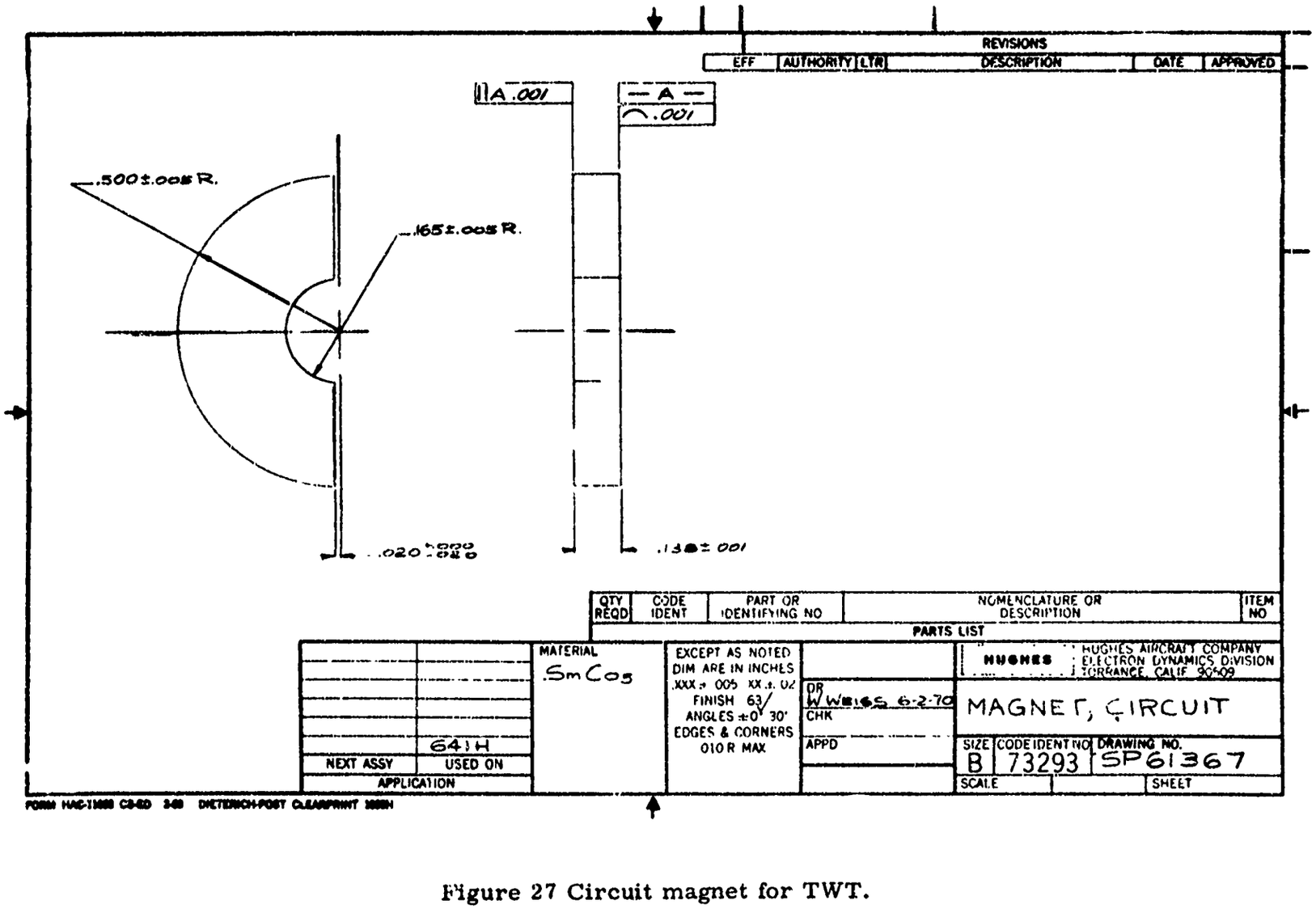

Figure 27 Circuit magnet for TWT.

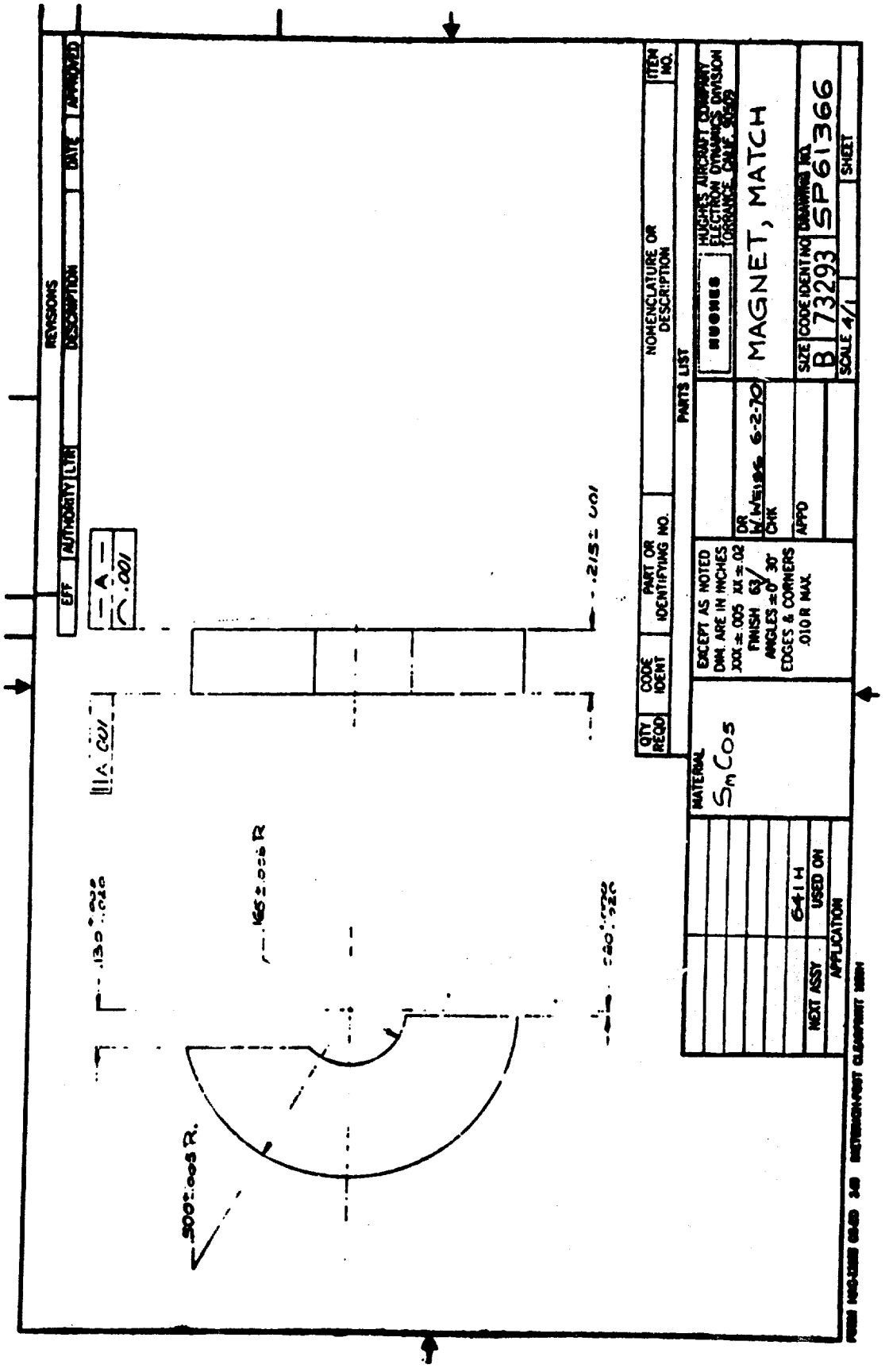

Figure 28 Match magnet for TWT.

Pre-Production Samples (M. G. Benz)

Pre-production samples were delivered at the completion of Phase I. These were characteristic of the samples utilized during Phase I to establish the technical basis for design of the TWT magnets to be fabricated during the balance of the program. The documentation submitted with these samples is included in the next section of this report.

SECTION IV

Phase I--Pre-Production Samples

These samples were prepared during Phase I--Analysis in order to establish specifications in accordance with Exhibit A, paragraph B. 1. d(2).

Submitted at the conclusion of Phase I--Analysis (June 15, 1970).

List of Samples

Sample	
A	Test Bar Sample GP432. $(BH)_{max}$ = 19.3 MGOe. H_d (at B/H = -1/2) = -5.7 kOe
B	Test Bar Sample GP429A. $(BH)_{max}$ = 18.1 MGOe. H_d (at B/H = -1/2) = -5.5 kOe
C	Test Bar Sample GP436. $(BH)_{max}$ = 19.0 MGOe. H_d (at B/H = -1/2) = -5.7 kOe
D	Test Bar Sample GP433. $(BH)_{max}$ = 20.5 MGOe. H_d (at B/H = -1/2) = -5.5 kOe
E	Test Bar Sample GP437. $(BH)_{max}$ = 19.0 MGOe. H_d (at B/H = -1/2) = -5.3 kOe
F	Reversible and Irreversible Temperature Loss Sample 3943-36L
G	Stability Sample GP336. Heated in air at 150°C for 1050 hours
H	Mechanical Properties Sample 3943-35B
I	Sample (1/2 Scale) TWT Magnet (Full Ring) No. 648 B2. From lot of half-ring samples evaluated at the Electron Dynamics Division, Hughes Aircraft Company
J	Test Ring Sample E-M-11
K	Test Ring Sample E-M-12
L	Test Half-Ring Sample E-C-11
M	Test Half-Ring Sample E-C-12

Sample Data

The enclosed samples were prepared during Phase I--Analysis.

Samples A through E are test bar samples. This type of sample was utilized as a standard test bar. Full magnetic documentation is possible for such a size and shape. A summary of magnetic properties for these samples is presented in Table XXXV.

TABLE XXXV

Summary of Magnetic Properties for Samples A Through E

	SAMPLE				
	A	B	C	D	E
Saturation Magnetization, B_s, kG	9.73	9.49	9.55	9.89	9.57
Remanent Magnetization, B_r, kG	8.80	8.48	8.48	9.27	8.92
Induction Coercive Force, H_c, kOe	-7.20	-7.10	-7.30	-6.60	-6.60
Intrinsic Coercive Force, H_{ci}, kOe	-11.8	-14.2	-15.6	-9.9	-14.0
Maximum Energy Product, $(BH)_{max}$, MGOe	19.3	18.1	19.0	20.5	19.0
H_d (at B/H = -1/2) kOe	-5.70	-5.50	-5.70	-5.50	-5.30
Density, g/cm^3	7.84	7.91	7.89	8.15	8.20
Sintering Treatment	1 hr 1110°C	1 hr 1110°C	1 hr 1110°C	2 hr 1110°C	2 hr 1110°C

An example of the demagnetization curve from which these data are taken is presented in Fig. 29.

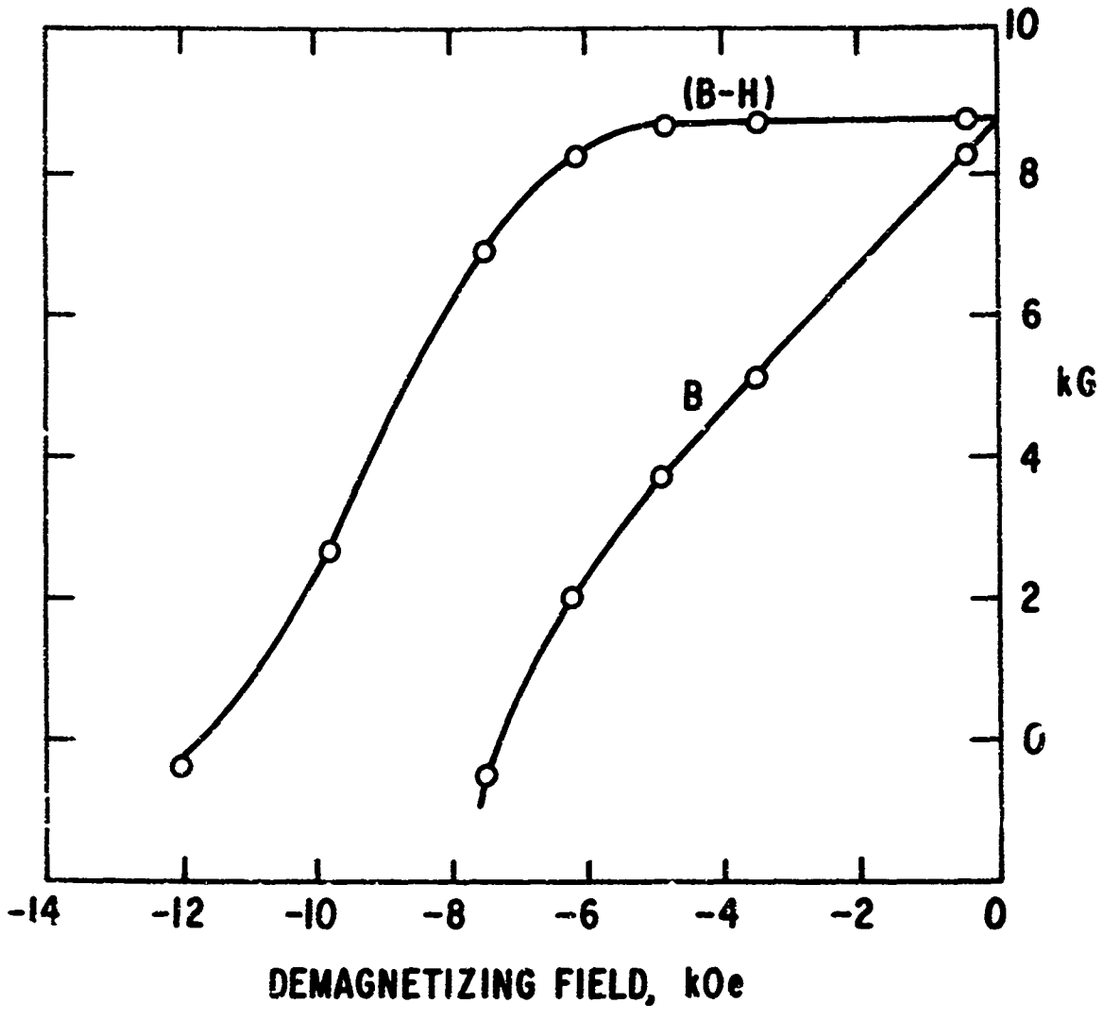

Figure 29 Demagnetizing curve for sample A.

Sample F is a reversible and irreversible temperature loss sample. This sample shows a reversible temperature loss of 0.04% per °C between 23° and 150°C; and an irreversible loss at 23°C of 9% after exposure to 150°C and 17% after exposure to 200°C.

Sample G is a stability sample. It has been heated in air at 150°C for 1050 hours. A summary of magnetic properties before and after this exposure is included in Table XXXVI.

Sample H is one-half of a mechanical properties sample. The original sample was 0.1632 inch in diameter by 1 1/4 inches long. The surface at the midsection was highly polished. The fracture load for a 0.625 span bend test was 63 lb. This is equivalent to a flexural strength of 23,000 psi. The

TABLE XXXVI

Summary of Magnetic Properties for Sample G
Before and After Exposure to Air at 150°C for 1050 Hours

	Before	After
Saturation Magnetization, B_s, kG	9.33	9.33
Remanent Magnetization, B_r, kG	7.89	7.89
Induction Coercive Force, H_c, kOe	-6.70	-6.40
Intrinsic Coercive Force, H_{ci}, kOe	-17.6	-16.3
Maximum Energy Product, $(BH)_{max}$, MGOe	14.8	14.4
H_d (at $B/H = -1/2$), kOe	-5.0	-4.9
Density, g/cm^3	7.7	7.7

other half of the sample was mounted for a hardness test. The measured hardness was Vickers, DPH = 568. The samples were not magnetized during the tests.

Sample I is a 1/2 scale TWT Magnet (Full Ring). This is from the lot of half-ring samples evaluated at the Electron Dynamics Division, Hughes Aircraft Company. A photograph of the half-ring samples is shown in Fig. 30.

Samples J and K are full-ring samples approaching the size to be fabricated during Phase III. (Note: The center holes are somewhat off-center.)

Samples L and M are close to the final geometry selected for Phase III magnets. (Note: These samples were primarily for geometric studies. These were not magnetically aligned and therefore do not have full properties.)

Figure 30 1/2 scale TWT magnets.

Typical Properties of Cobalt-Samarium Magnets[a]

Residual Induction, B_r	8200 Gauss
Induction Coercive Force, H_c	-6500 Oe
Intrinsic Coercive Force, H_{ci}	Greater than -12,000 Oe
Energy Product, $(BH)_{max}$	15×10^6 G-Oe
Reversible Temp Coefficient (Average from 196°C to +150°C)	-0.04% per °C
Irreversible Temp Change at 23°C after exposure to	
-196°C	+0.04%
+150°C	-10%
(Sample B/H = -1)	
Magnet Life (Sample B/H = -1)	Less than 5% variation over 1000 hours at 120°C
Density	7.7 g/cm^3.
Resistivity	50×10^{-6} ohm-cm
Flexural Strength (polished specimen)	20 kpsi
Fracture Mode	Brittle
Impact Strength	Capable of withstanding normal shipping, assembly, handling, and operation of TWT tubes consistent with MIL-5400 Class II environmental requirements
Hardness, Vickers DPH	500

Note (a). This list of properties was prepared by the Research and Development Center, General Electric Company, Schenectady, New York, at the completion of Phase I--Analysis (June 15, 1970) of USAF Contract No. F33615-70-C-1098, "Manufacturing Methods and Technology for Processing Cobalt-Samarium Magnets," initiated under Project No. 612-9A.

Phase III Magnet

Figure 31 gives the details of the TWT half-ring magnets to be fabricated during Phase III. When assembled into the PPM stack they should produce a $B_{(peak)}$ of 2760 gauss.

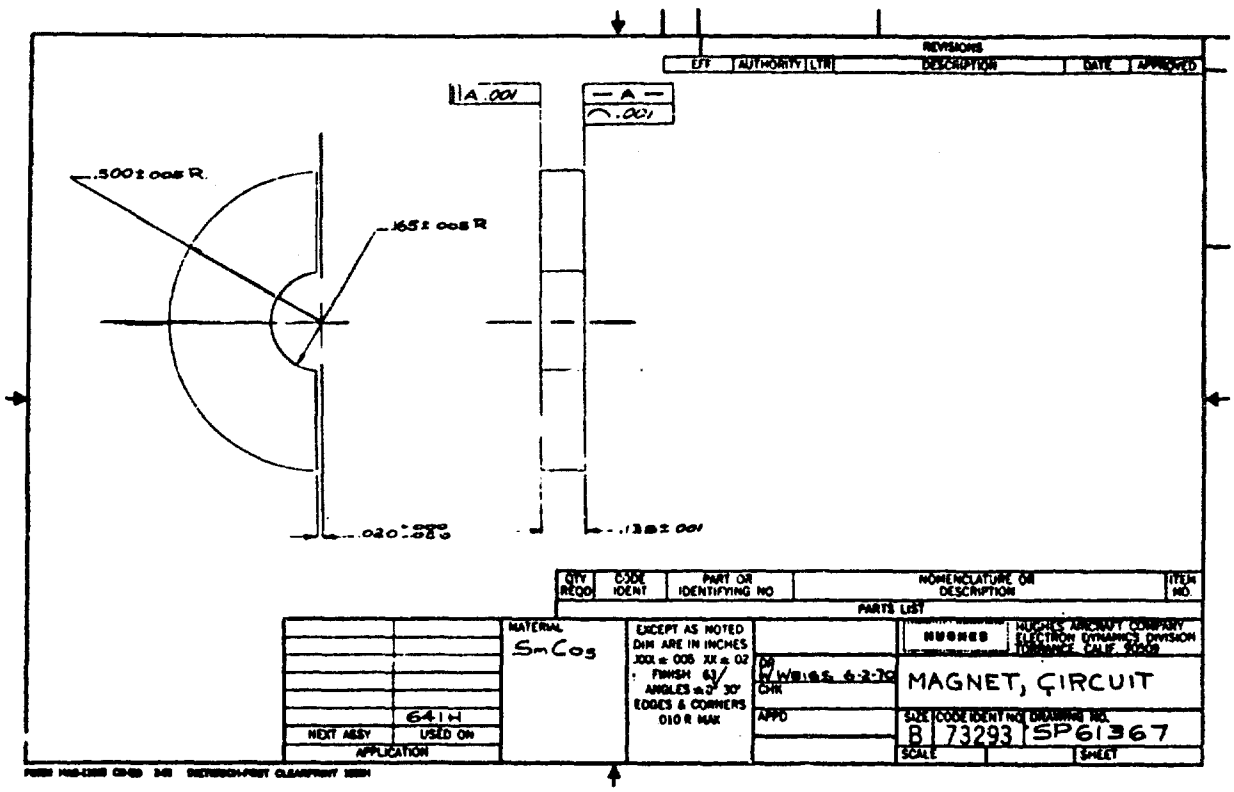

Figure 31 TWT half-ring magnet.

SECTION V

Phase II--Determination of Manufacturing Process (M. G. Benz)

As stated in Exhibit A of the contract work statement, the objective, criteria, and approach for this phase are:

- Objective - The objective of this phase is to finalize the processes and techniques that comprise the most economic and reliable manufacturing operation.

- Criteria and Approach - This determination shall be based on the information obtained in Phase I. Phase I steps will be reviewed to optimize each step.

Phase II studies have been completed. The finalized processes and techniques to be utilized are as follows:

1. Raw Materials - Purchase samarium metal and cobalt metal. Samarium purchased from any of the four different vendors evaluated during Phase I is considered acceptable.

2. Melting and Casting - Utilize vacuum/inert atmosphere induction melting. Crucibles are to be of aluminum oxide. Molds are to be of copper. Melt size is to be in the 5 to 30 lb range. Two compositions will be prepared. These will be mixed as powders during the blending step. The compositions are Co + 34 wt % Sm and Co + 60 wt % Sm.

3. Crushing - Utilize a jaw crusher and a double disk pulverizer to reduce ingots to the -35 mesh powder size. A nitrogen cover gas is to be utilized to eliminate sparking for high feed rate conditions, particularly for the samarium-rich composition.

4. Milling and Classifying - Utilize a fluid energy mill to reduce crushed powder to the 10μ size range. Nitrogen will be used as the working gas for this process. A permeability method particle size analysis will be used to measure the average particle size.

5. Powder Storage - Powders will be stored in air, but in closed containers. Desiccants will be contained within the closed containers for storage for long periods of time, particularly during the humid summer months.

6. Mixing Additives - Powders from the two compositions prepared will be weighed and blended to a composition with a samarium content, generally in the range of 37 to 38 wt %. Samples prepared from trial blends will

be utilized to determine the actual blend ratio for the final lot. Chemical analysis will also be utilized for determination of the desired blend ratio. A rotating twin-shell dry blender will be utilized for the mixing. This will be rotated 1000 to 2000 revolutions.

7. Magnetizing and Aligning Powder - The blended powder will be packed into rubber tubes to a density of 3.5 g/cm^3. This tube will also contain a core pin mandrel and centering plugs. The filled tube will be placed in a magnetic field of 60 kOe to align the powder. At this stage the centering plugs will be moved to increase the packed density to 4.5 g/cm^3, and the tube removed from the aligning field.

8. Pressing - The tube of aligned powder will be placed in a hydrostatic pressure vessel and the pressure will be increased to 200,000 psi. Subsequent to release of pressure, the pressing will be removed from the tube, and the core pin will be removed from the pressing. The sharp edges will be removed from the ends of the pressing by dry grinding.

9. Sintering - The pressing will be placed in containers and placed in a sintering furnace containing an argon or helium atmosphere for time sufficient to reach a relative density of about 90%. The temperature will be approximately 1120°C. The time will be approximately 1 hour. The sintered bar will be chamber cooled.

10. Shaping - Sintered bars will be shaped into half-rings. The inside and outside diameters will be honed and ground as required. Half-rings will be cut from these bars with slicing machine tool equipment.

11. Magnetizing the Magnets - A dc field of 60 kOe will be utilized to magnetize magnets. Torque magnetometry, and axial field plots of ppm stacks will be utilized for quality control of the resulting half-ring magnets.

12. Shipping - Individual compartments or chambers with adjacent keeper plates will be utilized to contain the magnetized magnets during shipment. These will be enclosed within a shipping container such that field levels outside the shipping container will be at acceptably low levels.

SECTION VI

Phase III (Part 1)--Pre-production Pilot Line: Powder (M. G. Benz and A. C. Rockwood)

As stated in Exhibit A of the contract work statement, the objective, criteria, and approach for this phase are:

- Objective. The objective of this phase is to establish a pilot line capable of producing 1000 magnets[(a)] per month (per 8-hour shift)

- Criteria and Approach. A production of 250 fully qualified Co_5Sm magnets[(a)] produced by production personnel shall be delivered to the Air Force Materials Laboratory to demonstrate production line performance. The performance characteristics of production line magnets shall be determined to insure compliance with the performance specification defined in Phase I. Magnet dimensions shall be suitable for incorporation into Hughes 641H traveling wave tubes. Exact size, shape, etc. shall be submitted for approval by AFML-MATE through the Procuring Contracting Officer at completion of Phase II.

In order to accomplish the above objective, Phase III (Part 1) was divided into three tasks:

1. Pilot Line Construction: Powder
2. Pilot Line Process Optimization Studies
3. Pilot Line Production: Powder

Pilot Line Construction: Powder

As determined during Phase II of this program (see Section V of this report), the pre-production pilot line for powder preparation consists of the following:

1. Raw Materials. Purchase samarium metal and cobalt metal. Samarium purchased from any of the four different vendors evaluated during Phase I is considered acceptable.

2. Melting and Casting. Utilize vacuum/inert atmosphere induction melting. Crucibles are aluminum oxide. Molds are copper. Melt size is

(a) A magnet is defined as two half-rings or one whole ring.

in the 5 to 30 lb range. Two compositions are prepared. These are mixed as powders during the blending step. The compositions are Co + 34 wt % Sm and Co + 60 wt % Sm.

3. Crushing. Utilize a jaw crusher and a double disk pulverizer to reduce ingots to the -35 mesh powder size. A nitrogen cover gas is utilized to eliminate sparking.

4. Milling and Classifying. Utilize a fluid energy mill to reduce crushed powder to the 10μ size range. Nitrogen is used as the working gas for this process. A permeability method particle size analysis is used to measure the average particle size.

5. Powder Storage. Powders are stored in air, but in closed containers. Desiccants are contained within the closed containers for storage for long periods of time.

6. Mixing Additives. Powders from the two compositions prepared are weighed and blended to a composition with a samarium content, generally in the range of 37 to 38 wt %. Samples prepared from trial blends are utilized to determine the actual mixture for the final blend. A rotating twin-shell dry blender is utilized for the mixing.

A schematic diagram of this pilot line is shown in Fig. 32. Specific items of equipment are shown in Figs. 33 through 37.

Pilot Line Optimization Studies

Effort centered on control of the various process steps in order to maximize the properties of the magnets produced from the powder.

The primary variable controlled during powder preparation was the composition of the final blend.

In order to achieve a maximum H_d (at $B/H = -1/2$) after exposure to 150°C, samples were prepared from trial blends of base metal (Co + 34 wt % Sm) and additive (Co + 60 wt % Sm). The final blend was then mixed to be equivalent to the trial blend showing the highest performance.

Pilot Line Production: Powder

Powder for the magnets used on the traveling wave tubes (see Section VIII describing Phase IV) and the pilot line production for AFML/MATE was prepared as outlined in the previous two subsections. A complete summary of the magnetic properties of trial blend samples and final blend samples for the pilot line production for AFML/MATE is given in Table XXXVII.

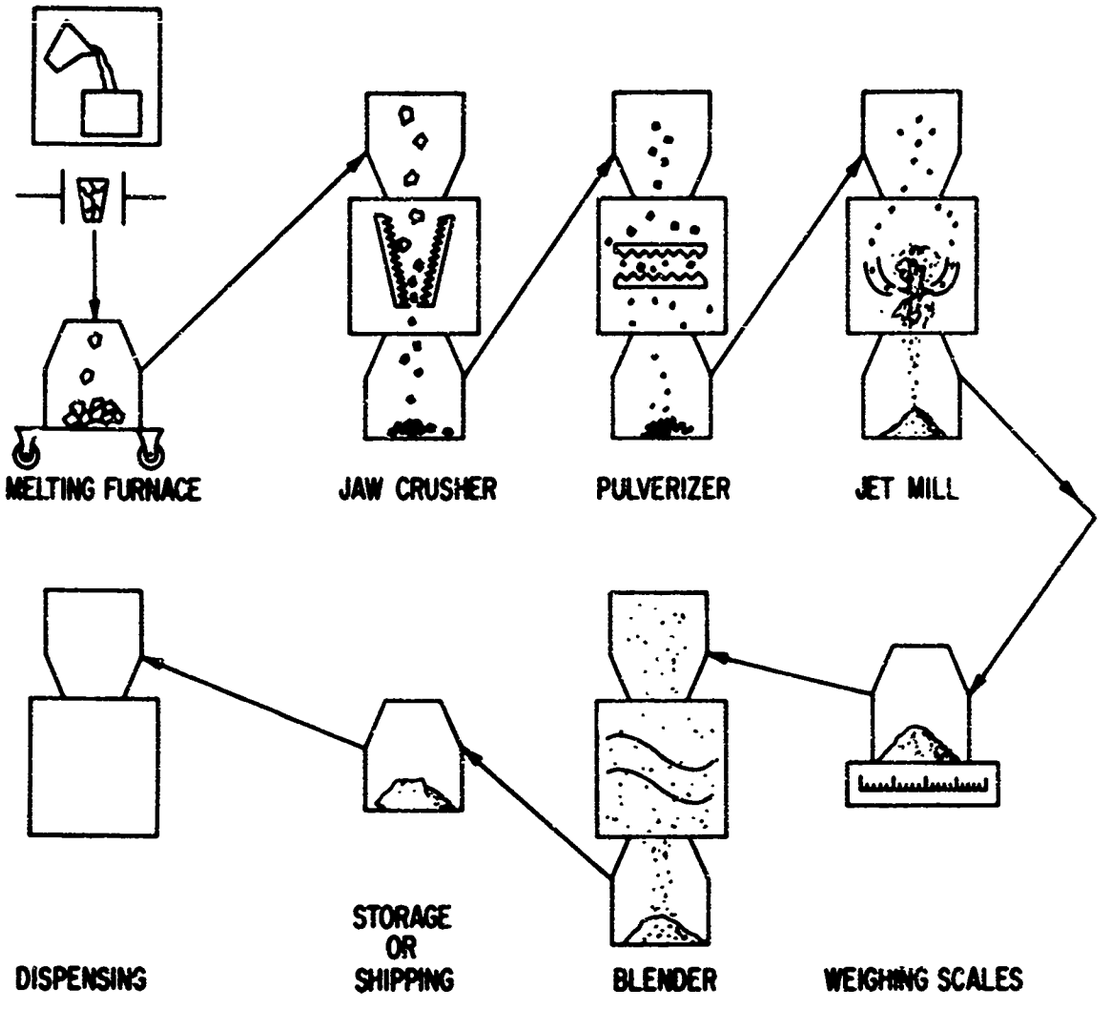

Figure 32 Schematic diagram: pre-production pilot line: powder.

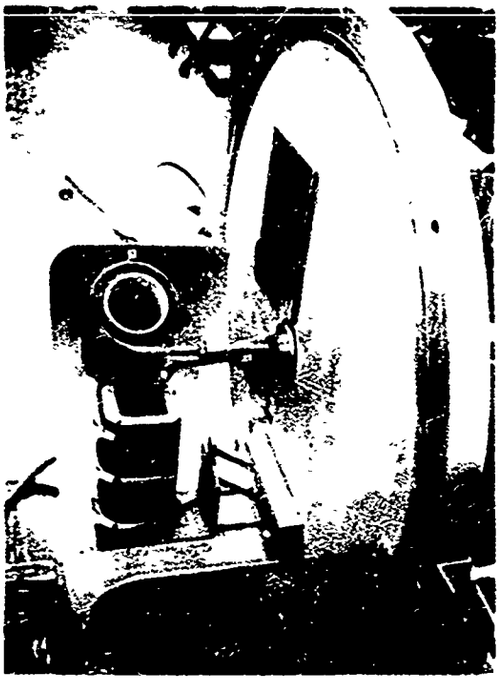

Figure 33 Vacuum/inert atmosphere induction melting furnace used for melting and casting (shell removed).

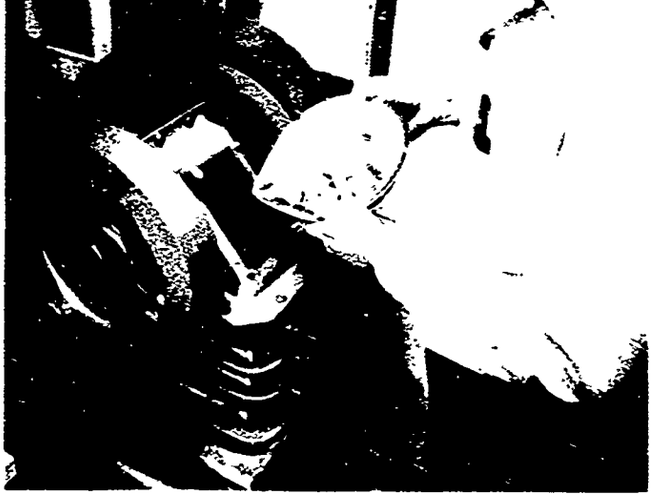

Figure 34 Jaw crusher used for crushing.

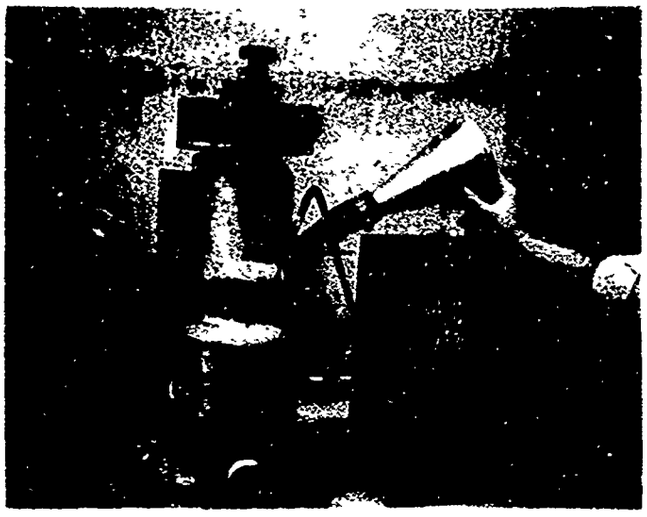

Figure 35 Pulverizer used for pulverizing.

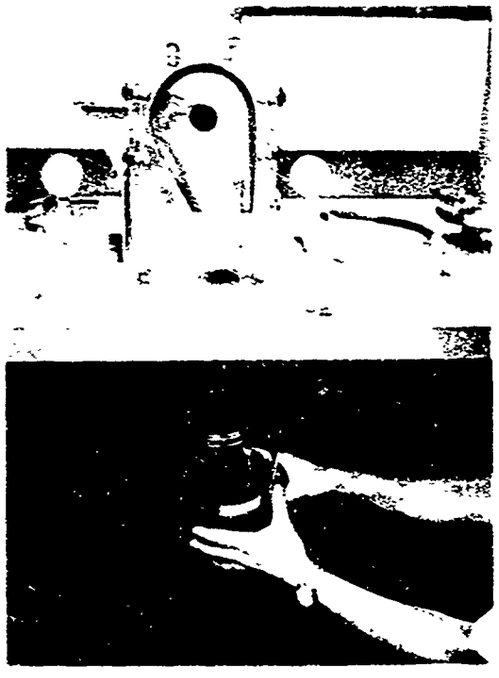

Figure 36 Fluid energy mill used for milling and classifying.

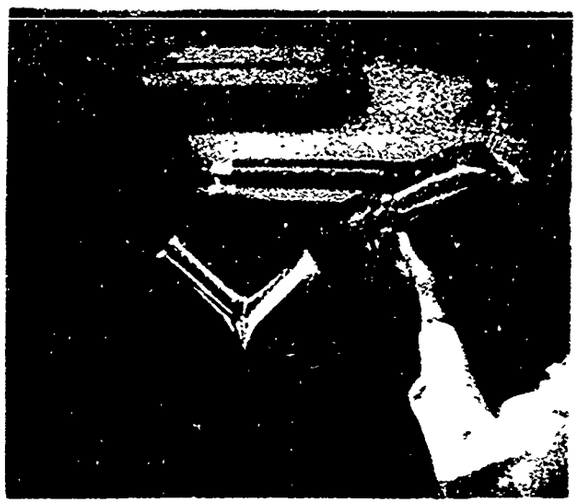

Figure 37 Twin-shell blender used for blending.

The sintering and post-sintering thermal treatments are as listed. These are discussed in more detail in Refs. 1 through 4.

REFERENCES

1. M. G. Benz and D. L. Martin, "Initial Observations: Cobalt-Mischmetal-Samarium Permanent Magnet Alloys," J. Appl. Phys. 42, 1534 (1971).

2. M. G. Benz and D. L. Martin, "Cobalt-Mischmetal-Samarium Permanent Magnet Alloys: Process and Properties," J. App. Phys. 42 (June 1971).

3. D. L. Martin and M. G. Benz, "Magnetization Changes for Cobalt-Rare Earth Permanent Magnet Alloys when Heated up to 250°C," Intermag. Conf., Denver, Colo., April 13-16, 1971.

4. D. L. Martin and M. G. Benz, "Magnetization Changes for Cobalt-Rare Earth Permanent Magnet Alloys when Heated up to 650°C," General Electric Company TIS Report No. 71-C-186, June 1971, submitted to IEEE Trans. Magnetics.

TABLE XXXVII

Magnetic Properties of Trial Blend Samples and Final Blend Samples: Pilot Line Production for AFML/MATF. Lot L-25

No.	Nominal w/o Cobalt	Treatment	$4\pi J_S$ (kGauss)	B_r (kGauss)	H_c (kOe)	H_k (kOe)	$_iH_c$ (kOe)	$(BH)_{max}$ (MGOe)	Density (g/cc)	P	A	H_d at B/H=-1/2 (kOe)	Irreversible Loss on Exposure to 150°C B/H=-1/2 (%)
Samples From Trial Blends													
AAA	63.8	1 hr 1120°C	10.0	8.4	-3.6	-2.5	- 4.6	12.8	7.4	0.86	0.975	-3.2	53.8
AA	63.6	1 hr 1120°C	9.95	8.6	-4.9	-3.7	- 7.1	15.5	7.6	.88	.981	-4.3	4.8
A	63.4	2 hr 1120°C+Age 950°C	10.0	9.23	-7.1	-5.7	-10.8	19.9	8.1	.94	.983	-5.65	12.3
A-2	63.4	1 hr 1120°C	9.86	8.94	-6.02	-4.7	- 8.45	18.1	7.9	.92	.995	-5.1	7.1
A-B	63.2	1 hr 1120°C	9.75	8.77	-6.57	-4.92	- 9.31	16.8	7.9	.92	.981	-5.2	11.6
B	63.0	2 hr 1120°C+Age 950°C	9.78	9.08	-6.1	-4.8	- 9.5	19.7	8.1	.94	.983	-5.2	34.7
C	62.8	2 hr 1120°C+Age 950°C	9.74	9.02	-5.4	-4.2	- 7.8	18.1	8.1	.94	.982	-4.9	34.1
D	62.6	2 hr 1120°C+Age 950°C	9.65	8.92	-5.4	-3.9	- 7.1	17.0	8.1	.94	.977	-4.8	35.1
E	62.2	2 hr 1120°C+Age 950°C	9.25	8.54	-4.75	-3.9	- 6.2	16.4	8.1	.94	.976	-4.3	28.5
Samples From Final Blend													
A-1-B	63.4	1 hr 1120°C+Age 950°C	9.94	8.81	-8.16	-8.73	-13.74	19.0	7.8	.90	.981	-5.75	2.8

Note (a): Irreversible losses measured for disk samples with a length to diameter ratio of 0.206 and therefore a B/H = -1/2. Samples chamber cooled rapidly from 950°C.

SECTION VII

Phase III (Part 2)--Pre-production Pilot Line: Magnets (F.G. Jones and R.J. Parker)

As stated in Exhibit A of the contract work statement, the objective, criteria, and approach for this phase are:

- Objective. The objective of this phase is to establish a pilot line capable of producing 1000 magnets[a] per month (per 8-hour shift).

- Criteria and Approach. A production of 250 fully qualified Co_5Sm magnets[a] produced by production personnel shall be delivered to the Air Force Materials Laboratory to demonstrate production line performance. The performance characteristics of production line magnets shall be determined to insure compliance with the performance specification defined in Phase I. Magnet dimensions shall be suitable for incorporation into Hughes 641H traveling wave tubes. Exact size, shape, etc. shall be submitted for approval by AFML-MATE through the Procuring Contracting Officer at completion of Phase II.

In order to accomplish the above objective, Phase III (Part 2) was divided into five tasks:

1. Pilot Line Construction: Magnets
2. Pilot Line Process Optimization Studies
3. Sample Magnets for TWT's
4. Pilot Line Production for TWT's
5. Pilot Line Production for AFML/MATE

A. Description of Pre-production Pilot Line

A pre-production pilot line for magnet fabrication has been established. The unit processes were selected in Phase II and optimized during Phase III.

Figure 38 shows schematically the sequence of operations used to make magnets. A more detailed description is given below.

(a) A magnet is defined as two half-rings or one whole ring.

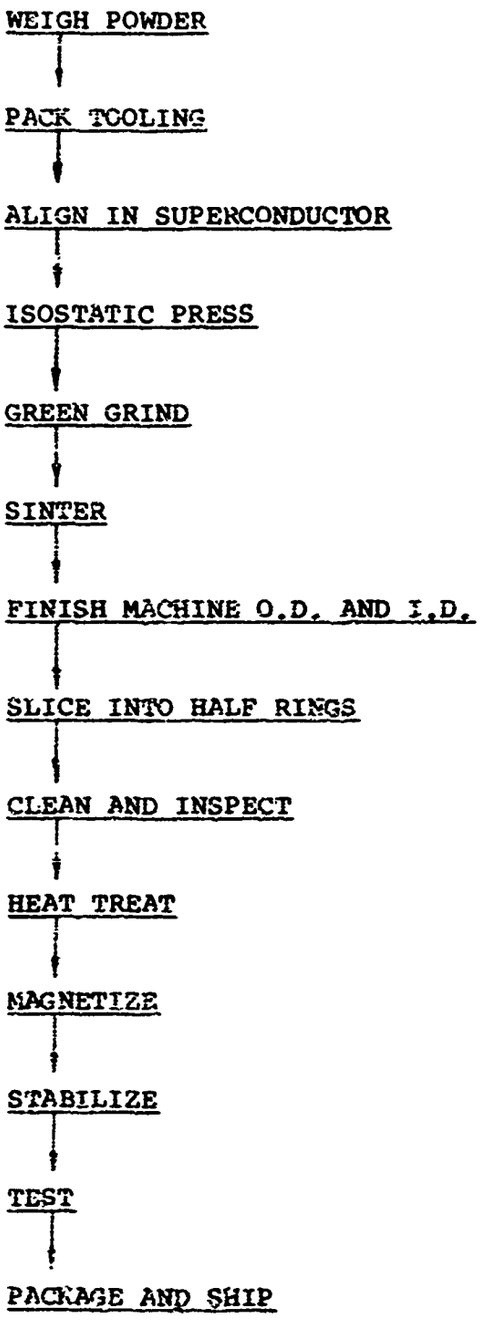

Figure 38 Schematic flow diagram of pre-production pilot line processes.

1. Weigh, Powder and Pack Tooling. Fully qualified powder (prepared as described in Section VI) is packed into a rubber tube to a density of 3.5 g/cm^3. This tube also contains a core pin mandrel and nonmagnetic centering plugs.

2. Align in Superconductor. The filled tube is placed in a magnetic field of 60 kOe to align the powder. A superconducting solenoid is used to obtain the high field value. At this stage the centering plugs are moved to increase the packed density to 4.5 g/cm^3, and then the tube is removed from the aligning field.

3. Isostatic Press. The tube of aligned powder is placed in a hydrostatic pressure vessel and the pressure is increased to 200 kpsi. After release of pressure the pressing is removed from the rubber tube and the core pin is removed from the pressing.

4. Green Grind. The outside diameter of the green pressing is reduced to the desired dimension. The ends of the pressing are squared-off and sharp edges are chamfered.

5. Sinter. The pressing is placed in a sintering furnace containing an argon or helium atmosphere for time sufficient to reach a relative density of about 90%.

6. Finish Machine. The inside and outside diameters of the sintered tube are ground as required.

7. Slice into Half-Rings. Half-rings are cut from the sintered tubes with slicing equipment.

8. Clean and Inspect. The magnets are ultrasonically cleaned and checked for physical tolerances.

9. Heat Treat. The magnets are reheated to temperatures in the range from 350° to 1125°C and cooled. This treatment is intended to increase temperature stability.

10. Magnetize. A d-c field of 30 to 60 kOe is used to magnetize the magnets.

11. Stabilize. The magnetized magnets are heated to temperatures in the range of 80° to 300°C for stabilization.

12. Test. Open circuit comparative flux density, torque magnetometry, and axial field plots of ppm stacks are utilized for quality control checks of the resulting magnets.

13. Package and Ship. Individual boxes are used to contain magnetized magnets during shipment. These are placed within a shipping container with adjacent magnets in opposition. Field levels outside the container are, thus, kept at acceptably low levels.

B. Pilot Line Production for TWT's

As a portion of Phase III, magnets were supplied to Hughes Aircraft Company, Electron Dynamics Division, for construction and evaluation of five traveling wave tubes (see Section VIII). A total of five batches of magnets were produced and shipped. These are identified by the month of shipment; viz. August, September, October, and November 1970 and January 1971.

Detailed descriptions of the specific production steps used for each batch have been given in the several quarterly reports. The discussion presented here is mainly an attempt to summarize the total effort. Major emphasis has been placed on the resultant magnetic quality aspects.

Figures 39(a) through (e) show histograms of the quality distribution for each batch. The August batch [Fig. 39(a) was made at R&DC. All magnets exceeded the Hughes requirement for quality in the freshly magnetized condition. The September [Fig. 39(b)] and October [Fig. 39(c)] batches were made partly at R&DC and partly at Edmore, Mich., but entirely by Edmore personnel. Comparison of the three histograms shows the improved consistency which was obtained with increased experience in manufacture. Not shown, however, is the fact that although the freshly magnetized properties were improved the amount of irreversible loss on subsequent heating to 150°C also increased.

This problem was attacked in the manufacture of the November batch [Fig. 39(d)]. Although the general level of properties shown for the November batch was somewhat reduced the irreversible loss was greatly reduced. For example, the open circuit loss of magnetization of a half-ring was reduced from a typical value of 30% to less than 10%. This reduction was accomplished by use of a post-sintering heat treatment at temperatures in the range from 900° to 950°C.[1-4]

The process sequence was again altered for the production of the January 1971 batch of magnets. For the first time the magnets were temperature stabilized at 150°C prior to shipment. Hence, the general level of properties, as shown in Fig. 39(e), was lower. However, those magnets would be expected to show less than 1% loss upon reheating to 150°C. Other stabilization techniques were tried, viz. a-c knockdown or d-c knockdown. Neither of these alternate approaches could be applied in production as readily as simple temperature cycling.

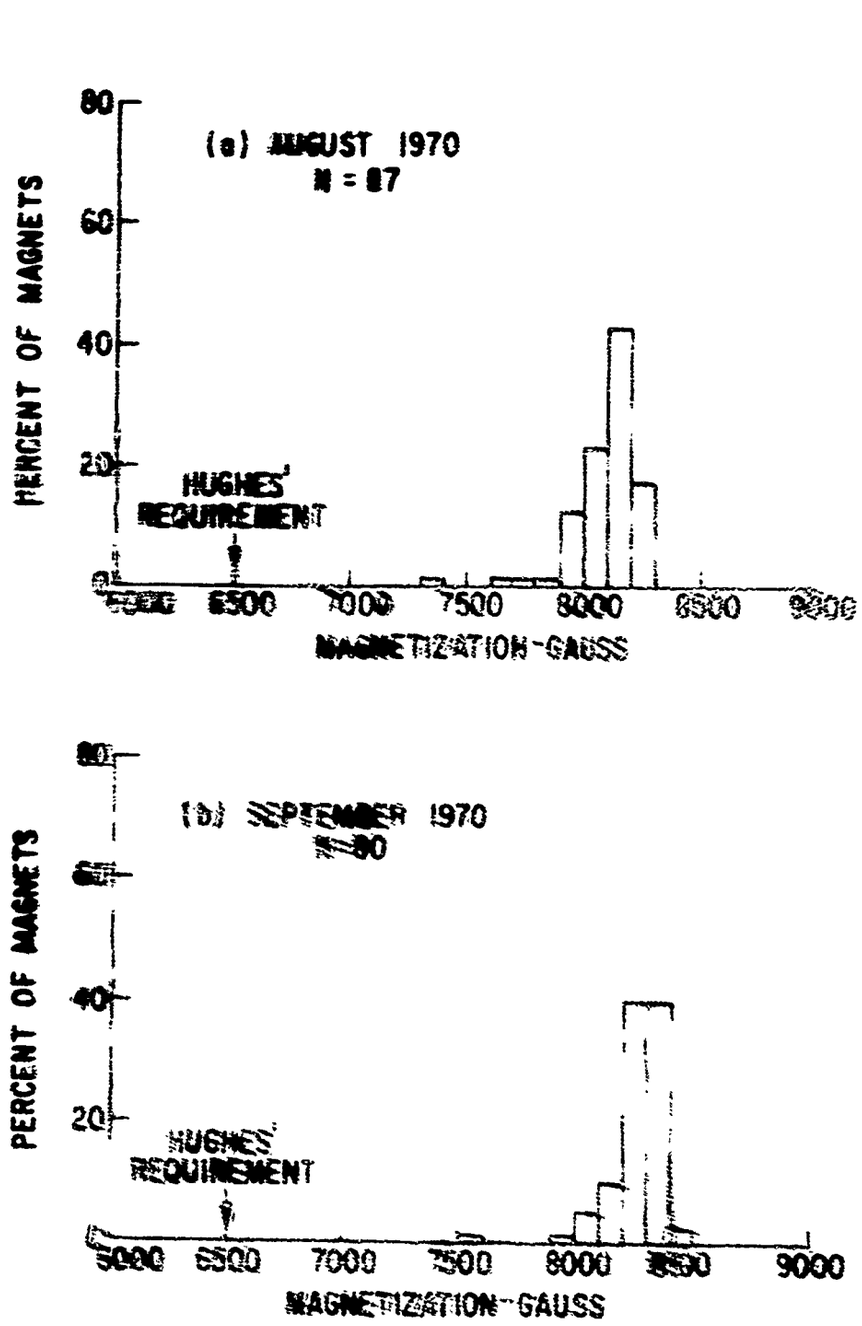

Figure 3: Histograms showing magnetic quality of half-ring magnets shipped to Hughes Aircraft Co.

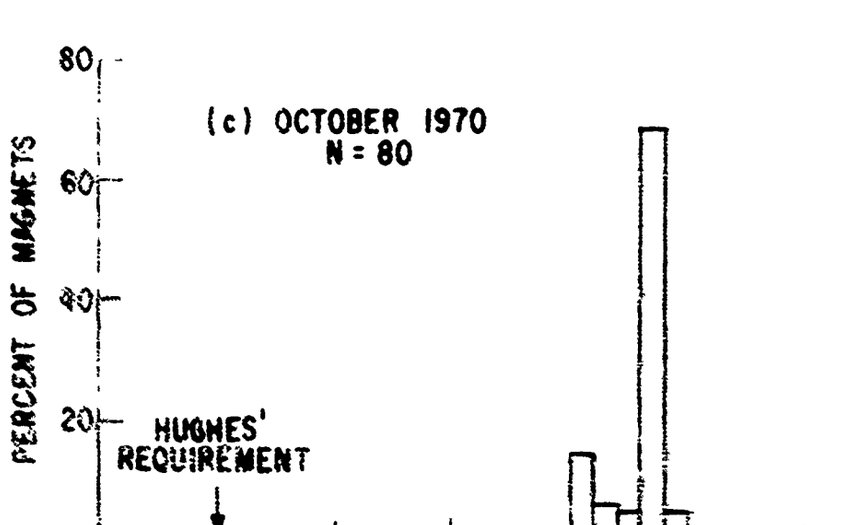

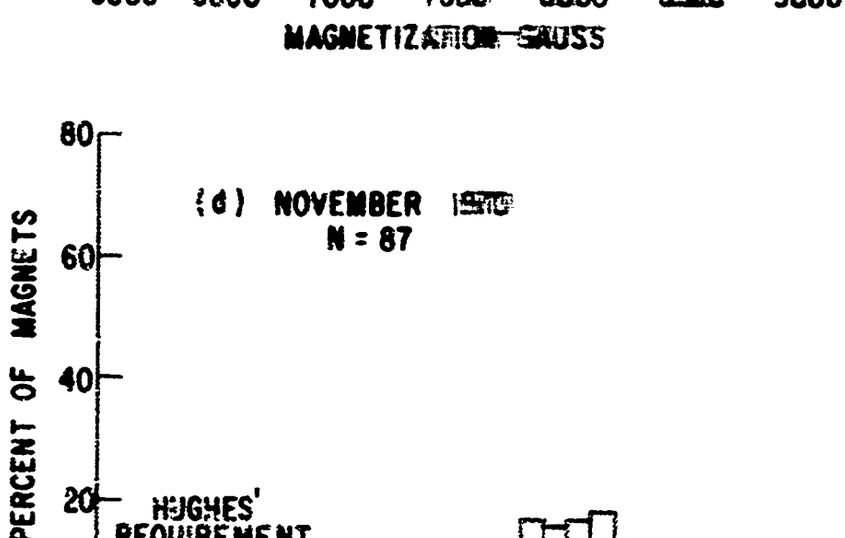

Figure 39 continued.

Figure 39 concluded.

Figure 40 is a summary of all magnets shipped to Hughes. The long tail in the distribution is misleading because of the fact that the 80 magnets shipped in January had been intentionally knocked down in properties. It is of value, however, to examine the general quality level of magnets made by our process. Note first that all magnets exceeded the Hughes design requirement for the application. Secondly, note that the median level of properties represents a magnet with an energy product equal to or greater than 16.4 MGOe. The best magnets made had energy products exceeding 18 MGOe.

C. Process Optimization Studies

During the course of work under Phase III several specific studies were carried out in an effort to optimize or simplify portions of the production process. These can best be discussed in two categories: (1) attempts to align at lower field strengths and press at lower pressures; and (2) continued study of post-sintering heat treatments.

Align/Press Studies. Attempts were made to align the powder at fields less than 60 kOe and also to press the aligned powder at 100 kpsi instead of the usual 200 kpsi. Neither approach was successful.

The results of this study are summarized in Fig. 41. In this figure we have plotted the magnetic quality of the half-ring magnets as a function of

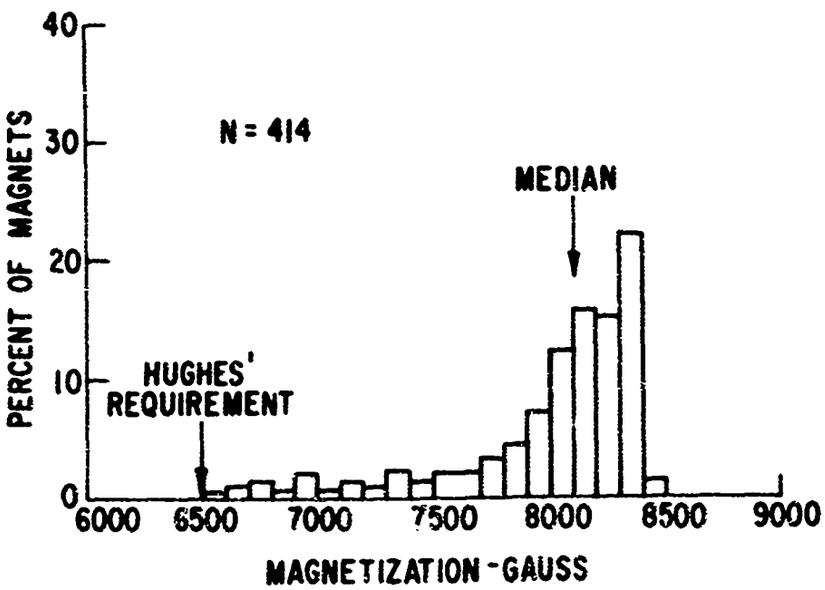

Figure 40 Summary of all magnets shipped to Hughes Aircraft Co. for construction of experimental TWT tubes.

location in the original pressing. The topmost curve is for the standard conditions of 60 kOe alignment field and 200 kpsi press pressure. Homogenity along the majority of the length of the pressing is good. The level of properties here represents material having energy products ranging from 15.5 to 18.5 MGOe.

The middle curve in the figure is for a pressing aligned at 10 kOe, but still pressed at 200 kpsi. The degradation in properties reflects decreased alignment at constant density. The properties are uniform and represent energy products in the range from 15.0 to 16.0 MGOe. After temperature stabilization this material would be marginal in quality.

The lowest curve in Fig. 41 represents the least expensive approach. The powder was aligned at 10 kOe field strength and pressed at 100 kpsi. The

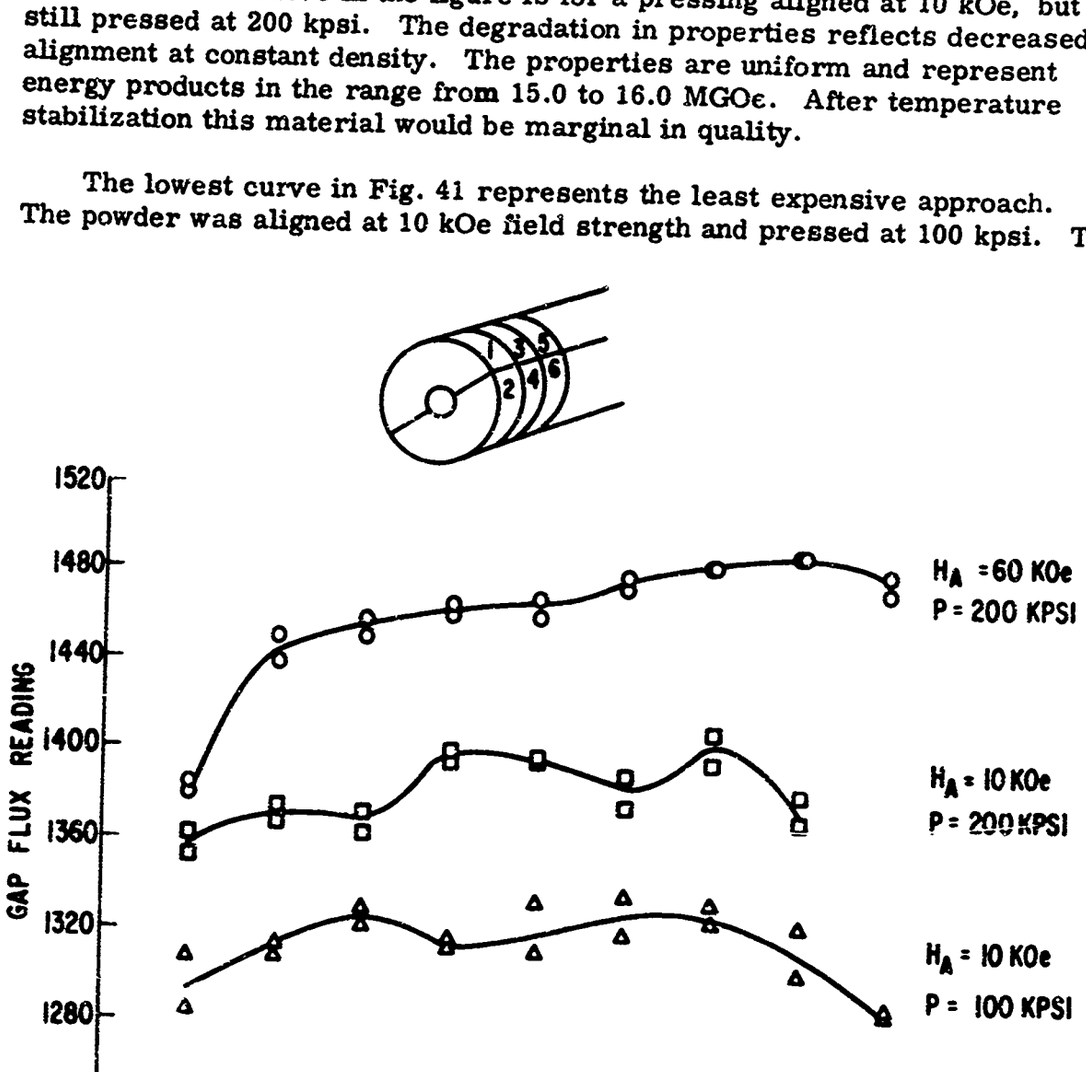

Figure 41 Effect of alignment field strength and press pressure on quality of half-ring magnets.

decreased property level is due to both a decrease in alignment and a decrease in density. The maximum energy products varied from 13.0 to 14.0 MGOe. This is below the contract requirement of 15 MGOe typical property.

The results of these studies of actual magnets confirm what had been found for test bars in Phase I. The process specifications were held at 60 kOe and 200 kpsi.

Post-Sinter Heat Treatment. Considerable effort was devoted to a study of various post-sintering heat treatments in an effort to reduce the irreversible temperature losses of magnetization of magnets. Two approaches were undertaken. First, half-ring magnets were heat treated in an effort to find the best heat treatment temperature for minimum irreversible loss. To isolate the effect of temperature these magnets were all water quenched after heat treatment.

Figure 42 shows the effect of varying heat treatment temperature on the subsequent irreversible loss at 150°C. Clearly a minimum is attained after heat treatment in the range from 900° to 1000°C. Heat treatment at temperatures both above and below this range led to higher losses. The gap flux reading after 150°C for these quenched magnets is shown in Fig. 43. As expected the best properties were associated with the minimum loss conditions. Unfortunately, none of the magnets exhibited properties up to the quality level required by this contract.

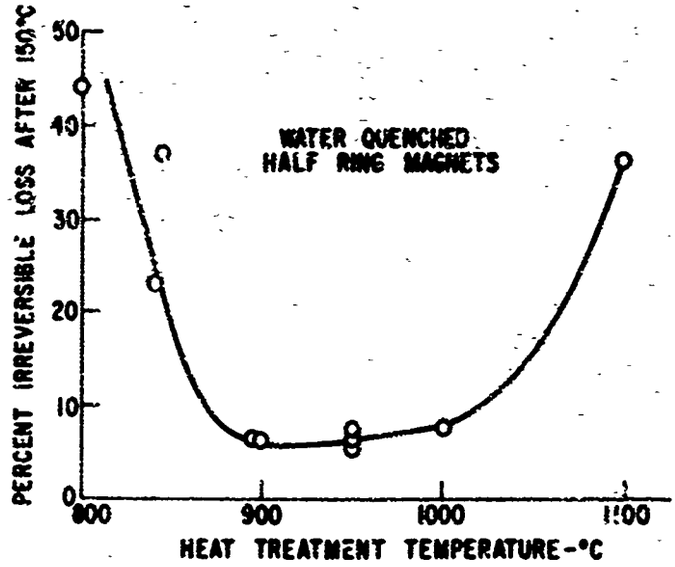

Figure 42 Effect of heat treatment temperature on subsequent irreversible loss at 150°C for water-quenched half-ring magnets.

location in the original pressing. The topmost curve is for the standard conditions of 60 kOe alignment field and 200 kpsi press pressure. Homogenity along the majority of the length of the pressing is good. The level of properties here represents material having energy products ranging from 15.5 to 18.5 MGOe.

The middle curve in the figure is for a pressing aligned at 10 kOe, but still pressed at 200 kpsi. The degradation in properties reflects decreased alignment at constant density. The properties are uniform and represent energy products in the range from 15.0 to 16.0 MGOe. After temperature stabilization this material would be marginal in quality.

The lowest curve in Fig. 41 represents the least expensive approach. The powder was aligned at 10 kOe field strength and pressed at 100 kpsi. The

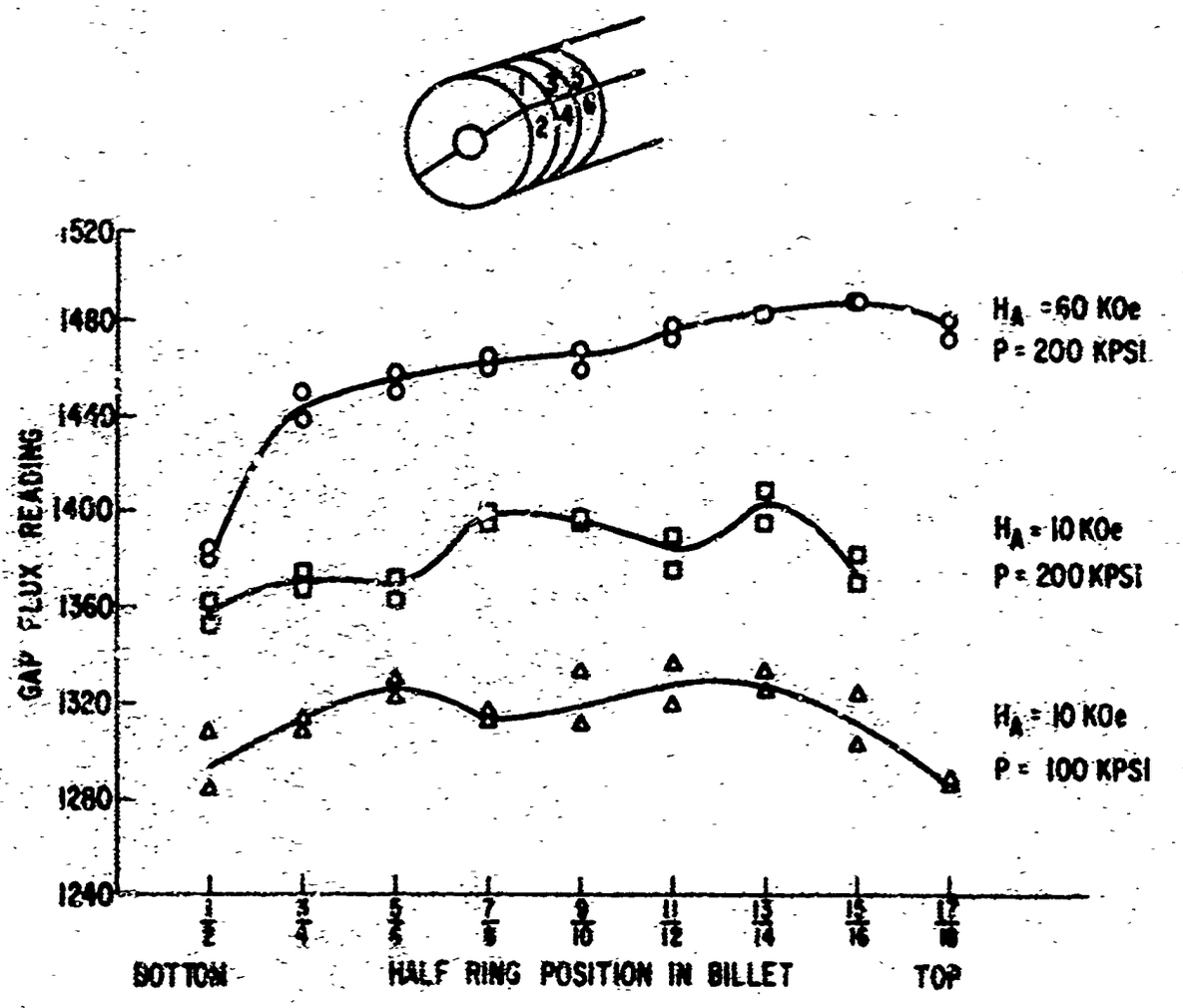

Figure 41 Effect of alignment field strength and press pressure on quality of half-ring magnets.

decreased property level is due to both a decrease in alignment and a decrease in density. The maximum energy products varied from 13.0 to 14.0 MGOe. This is below the contract requirement of 15 MGOe typical property.

The results of these studies of actual magnets confirm what had been found for test bars in Phase I. The process specifications were held at 60 kOe and 200 kpsi.

Post-Sinter Heat Treatment. Considerable effort was devoted to a study of various post-sintering heat treatments in an effort to reduce the irreversible temperature losses of magnetization of magnets. Two approaches were undertaken. First, half-ring magnets were heat treated in an effort to find the best heat treatment temperature for minimum irreversible loss. To isolate the effect of temperature these magnets were all water quenched after heat treatment.

Figure 42 shows the effect of varying heat treatment temperature on the subsequent irreversible loss at 150°C. Clearly a minimum is attained after heat treatment in the range from 900° to 1000°C. Heat treatment at temperatures both above and below this range led to higher losses. The gap flux reading after 150°C for these quenched magnets is shown in Fig. 43. As expected the best properties were associated with the minimum loss conditions. Unfortunately, none of the magnets exhibited properties up to the quality level required by this contract.

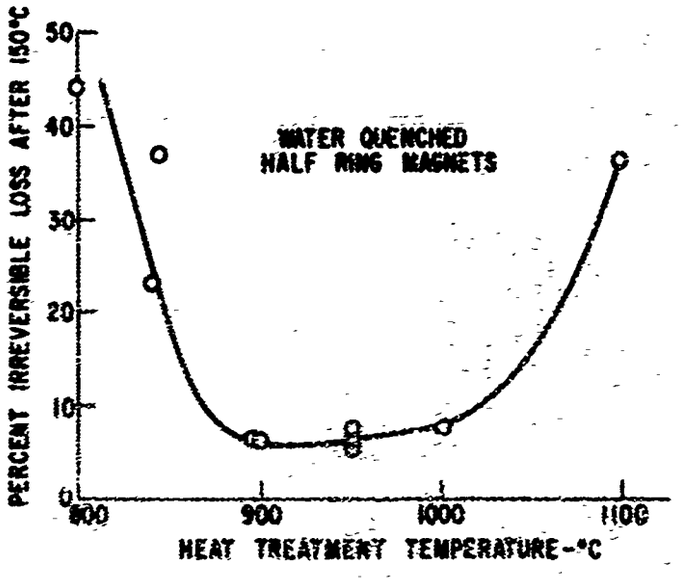

Figure 42 Effect of heat treatment temperature on subsequent irreversible loss at 150°C for water-quenched half-ring magnets.

location in the original pressing. The topmost curve is for the standard conditions of 60 kOe alignment field and 200 kpsi press pressure. Homogenity along the majority of the length of the pressing is good. The level of properties here represents material having energy products ranging from 15.5 to 18.5 MGOe.

The middle curve in the figure is for a pressing aligned at 10 kOe, but still pressed at 200 kpsi. The degradation in properties reflects decreased alignment at constant density. The properties are uniform and represent energy products in the range from 15.0 to 16.0 MGOe. After temperature stabilization this material would be marginal in quality.

The lowest curve in Fig. 41 represents the least expensive approach. The powder was aligned at 10 kOe field strength and pressed at 100 kpsi. The

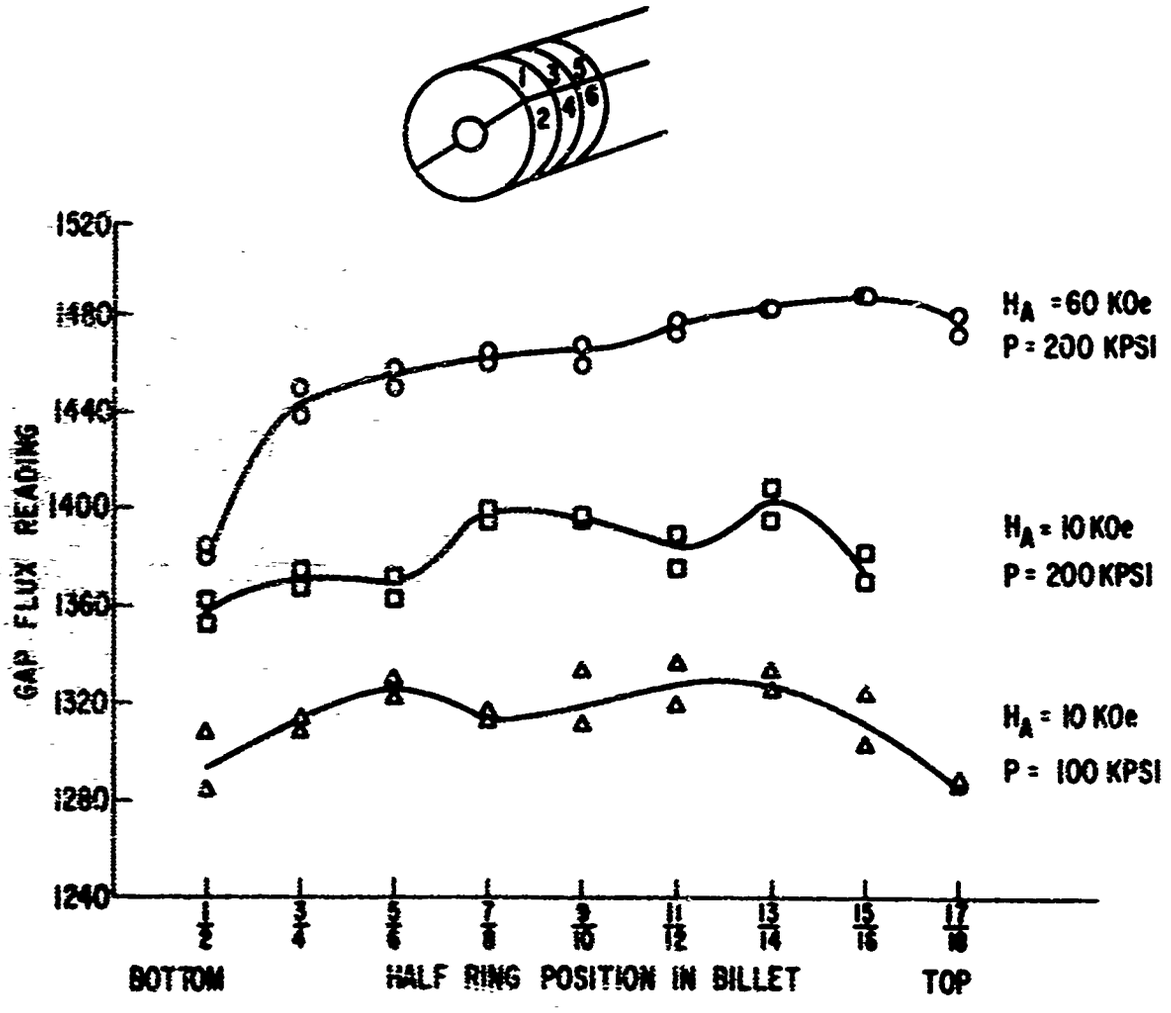

Figure 41 Effect of alignment field strength and press pressure on quality of half-ring magnets.

decreased property level is due to both a decrease in alignment and a decrease in density. The maximum energy products varied from 13.0 to 14.0 MGOe. This is below the contract requirement of 15 MGOe typical property.

The results of these studies of actual magnets confirm what had been found for test bars in Phase I. The process specifications were held at 60 kOe and 200 kpsi.

Post-Sinter Heat Treatment. Considerable effort was devoted to a study of various post-sintering heat treatments in an effort to reduce the irreversible temperature losses of magnetization of magnets. Two approaches were undertaken. First, half-ring magnets were heat treated in an effort to find the best heat treatment temperature for minimum irreversible loss. To isolate the effect of temperature these magnets were all water quenched after heat treatment.

Figure 42 shows the effect of varying heat treatment temperature on the subsequent irreversible loss at 150°C. Clearly a minimum is attained after heat treatment in the range from 900° to 1000°C. Heat treatment at temperatures both above and below this range led to higher losses. The gap flux reading after 150°C for these quenched magnets is shown in Fig. 43. As expected the best properties were associated with the minimum loss conditions. Unfortunately, none of the magnets exhibited properties up to the quality level required by this contract.

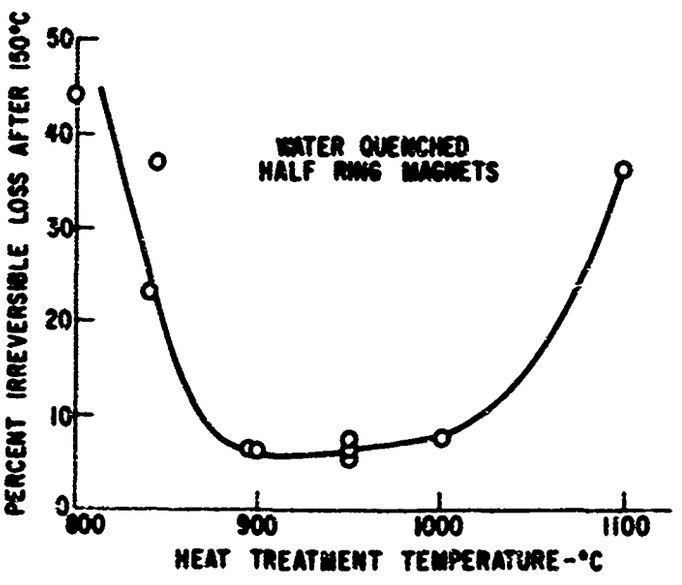

Figure 42 Effect of heat treatment temperature on subsequent irreversible loss at 150°C for water-quenched half-ring magnets.

In an effort to elucidate the causes for these lowered properties several test bar specimens were water quenched from selected temperatures and the unit magnetic properties were measured. These data are given in Table XXXVIII. The data for a specimen (AF-153-1) heated at 900°C and chamber cooled are shown for comparison. It is evident that the water quenching leads to greatly reduced values for all unit properties except the intrinsic coercive force. This entire situation is not well understood at the present time. From the constriction noted in hysteresis loops, however, it is apparent that one or more solid-state reactions are occurring in the temperature interval studied. Therefore, chamber cooling will continue to be utilized for the pre-production pilot line.

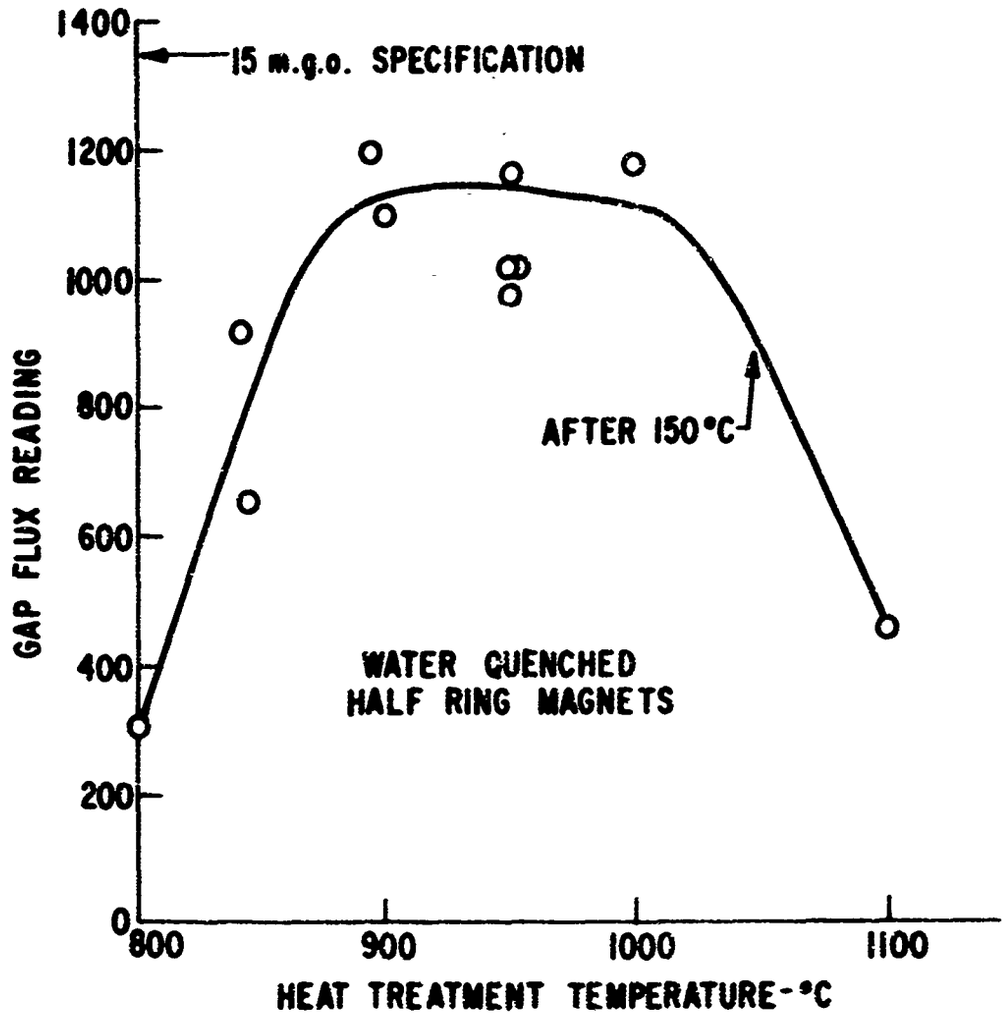

Figure 43 Magnetic quality of water quenched half-ring magnets after 150°C exposure.

TABLE XXXVIII

Magnetic Properties of Water-Quenched Test Bar Specimens

Specimen No.	Heat Treatment Temperature[a] (°C)	B_r (kG)	H_c (kOe)	H_{ci} (kOe)	H_k (kOe)	H_d@ B/H-1/2 (kOe)	$(BH)_{max}$ (MGOe)
AF-125-1	1100	6.275	1.525	2.350	--	--	3.2
AF-125-1A	950	6.275	4.600	8.175	--	--	6.6
AF-139-1	900	5.150	2.400	12.250	--	--	2.2
AF-140-1	800	6.500	1.550	1.675	--	--	1.8
AF-153-1	900[b]	8.525	7.700	14.400	7.975	5.400	17.0

(a) Specimens water quenched.

(b) This specimen was chamber cooled.

D. Pre-production Pilot Line Operation

The ultimate objective of Phase III work was the construction of a pre-production pilot line capable of producing 1000 full-ring magnets per month, per eight-hour shift. This capacity was to be demonstrated by producing 250 fully qualified ring magnets. In terms of the unit count in this report that is 500 half-ring magnets per week or about 12 per hour. Such a line was built and was operated during February and March of 1971. Five hundred fully qualified half-ring magnets were built and shipped to AFML-MATE in May 1971.

In the following sections we will discuss the actual pilot production run in terms of the unit operations outlined earlier.

Weigh Powder and Pack Tooling. The powder used was from lot L-25 described in Section VI. Forty-four billets were prepared. Each billet weighed 210 grams and was expected to yield 18 half-ring magnets. The production rate achieved exceeded 75 half-ring magnets per hour.

Align in Superconductor. All billets were aligned at 60 kOe applied field strength. The production rate achieved exceeded 100 per hour.

Isostatic Press. Due to temporary equipment limitations this portion of the pilot run was unbalanced. Two different presses were used. The billets were first pressed at 100 kpsi at Edmore. They were then transported to R&DC for final pressing at 200 kpsi. Had the pressing been done in the 200 kpsi press now available at Edmore the production rate would have exceeded

75 per hour. Four of the billets were scrapped at this stage as a result of leaks occurring during pressing. This problem was traced to faulty tooling.

Green Grind. The outer diameter of all billets was ground to 1.070 inches. This led to a sintered diameter of 1.045 inches. Approximately 0.25 inch was ground from the length of each billet in order to square the ends and chamfer the edges. The production rate exceeded 36 per hour.

Sinter. The billets were sintered in argon at temperatures ranging from 1112° to 1120°C. The typical sintered density ranged from 7.57 to 7.90 g/cm^3. The production rate exceeded 14 per hour per furnace.

Finish Machine. Finish machining consisted of grinding the outer diameter to a dimension within the specified tolerance. Production rates exceeded 50 per hour.

Slice into Half-Rings. The slicing was carried out using diamond cutting wheels. The magnets were sliced to the final dimensions. The production rate for a single machine was in excess of 14 per hour.

Clean and Inspect. The magnets were ultrasonically cleaned and checked on a go-no-go basis for dimensional tolerance.

Heat Treat. As described previously it was found necessary to heat treat the magnets. All magnets were heated and cooled from a temperature of 867° to 877°C.[4] It was subsequently learned that slightly better properties could have been obtained if this temperature were somewhat higher. The production rate here was limited by the number of available furnaces to about 10 per hour.

Magnetize. The half-rings were magnetized in an electromagnet capable of 35 kOe peak field. Rates of over 100 per hour were noted.

Stabilize and Test. All magnets were stabilized at 150°C and tested on a go-no-go basis. Using a minimum passing point of 15 MGOe energy product about 40% of the magnets passed. The remainder were remagnetized and stabilized at 120°C. All passed at this stage. Stabilization and testing rates approached 100 parts per hour.

Package and Ship. This was a routine operation performed by hourly help. All magnets were individually boxed in foam-lined boxes. Production rate exceeded 100 per hour.

The requirement was for production of 500 fully qualified half-ring magnets. We chose to perform 100% testing at all stages of production. Figure 44 shows a histogram depicting the quality of the 500 magnets which were shipped to AFML-MATE. The range of property variation is from 14 to 19

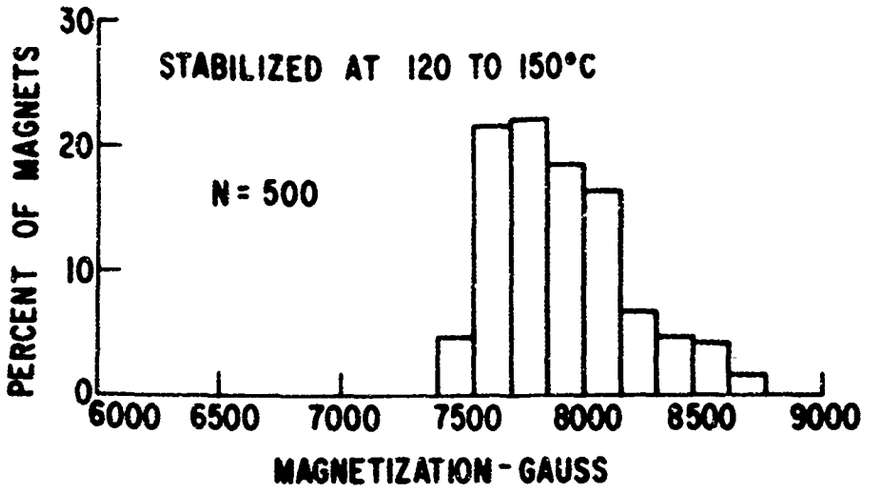

Figure 44 Summary of 500 half-ring magnets produced in the pre-production pilot line operation.

MGOe minimum estimated energy product. Note that all of these magnets were stabilized at at least 120°C. From prior study one would then expect the maximum irreversible temperature loss upon heating to 150°C to be less than 10%. In fact, 40% of the magnets will exhibit no loss upon reheating to 150°C.

We believe that the magnets shipped to AFML-MATE exceeded all requirements set in the contract.

REFERENCES

1. M. G. Benz and D. L. Martin, "Initial Observations: Cobalt-Mischmetal-Samarium Permanent Magnet Alloys," J. Appl. Phys. 42, 1534 (1971).

2. M. G. Benz and D. L. Martin, "Cobalt-Mischmetal-Samarium Permanent Magnet Alloys: Process and Properties," J. Appl. Phys. 42 (June 1971).

3. D. L. Martin and M. G. Benz, "Magnetization Changes for Cobalt-Rare Earth Permanent Magnet Alloys when Heated up to 250°C," Intermag. Conf., Denver, Colo., April 13-16, 1971.

4. D. L. Martin and M. G. Benz, "Magnetization Changes for Cobalt-Rare Earth Permanent Magnet Alloys when Heated up to 650°C." General Electric TIS Report No. 71-C-186, June 1971. Submitted to IEEE Trans. Magnetics.

SECTION VIII

Phase IV--Microwave Device Application of Co_5Sm Magnets (Hughes Aircraft Co.)

As stated in Exhibit A of the contract work statement the objective, criteria, and approach for this phase are:

- Objective. The objective of this phase is to demonstate the superior functional characteristics of Co_5Sm traveling wave tubes.

- Criteria and Approach. A minimum of five (5) Hughes 641H traveling wave tubes, shall be obtained for evaluation of the Co_5Sm material, and the performance of these tubes shall be compared with that of other state-of-the-art tubes. To ensure Air Force System applicability, the Co_5Sm TWT's shall be evaluated according to MIL-5400 Class II requirements including:

(1) Humidity	(4) Vibration
(2) Salt Spray	(5) Temperature
(3) Shock	(6) Altitude

The work for this phase was done by the Electron Dynamics Division of the Hughes Aircraft Co. on subcontract to the General Electric Company, Research and Development Center (Purchase Order 002-111517).

The report prepared by the Hughes Aircraft Co. covering this work is included as the balance of this section.

A. Objective of the Program

The purpose of this part of the project was to perform evaluation experiments of cobalt-samarium magnets produced by the General Electric Company. The project was divided into two phases.

The first phase was an evaluation of the magnets by themselves (i.e., not focusing a TWT). This phase consisted of a study to determine the reversible and irreversible temperature characteristics of the material.

The second phase consisted of evaluation of cobalt-samarium magnetic focusing arrays on Hughes Aircraft Co. traveling wave tubes. The tube type selected for these experiments was the 641H. It has been in high volume (i.e., several thousand) production, yet this tube is considered to be a state-of-the-art device which incorporates many recent developments in TWT design.

Another purpose of this project was to demonstrate the numerous advantages of the new material, Co_5Sm, on present and future traveling wave tube designs.

B. Temperature Studies

A periodic permanent magnet stack assembly was designed for preliminary evaluation of the Co_5Sm magnets. The outer diameter of the array was designed to accommodate the magnet diameter (0.625 inch) of the first magnet shipment (lot PV 648B). Figure 45 lists all the pertinent dimensions of the stack. A array of eleven magnets and twelve pole pieces was constructed and the axial magnetic field was measured at room temperature. The following is a summary of the theoretical calculation and actual measurements of this stack.

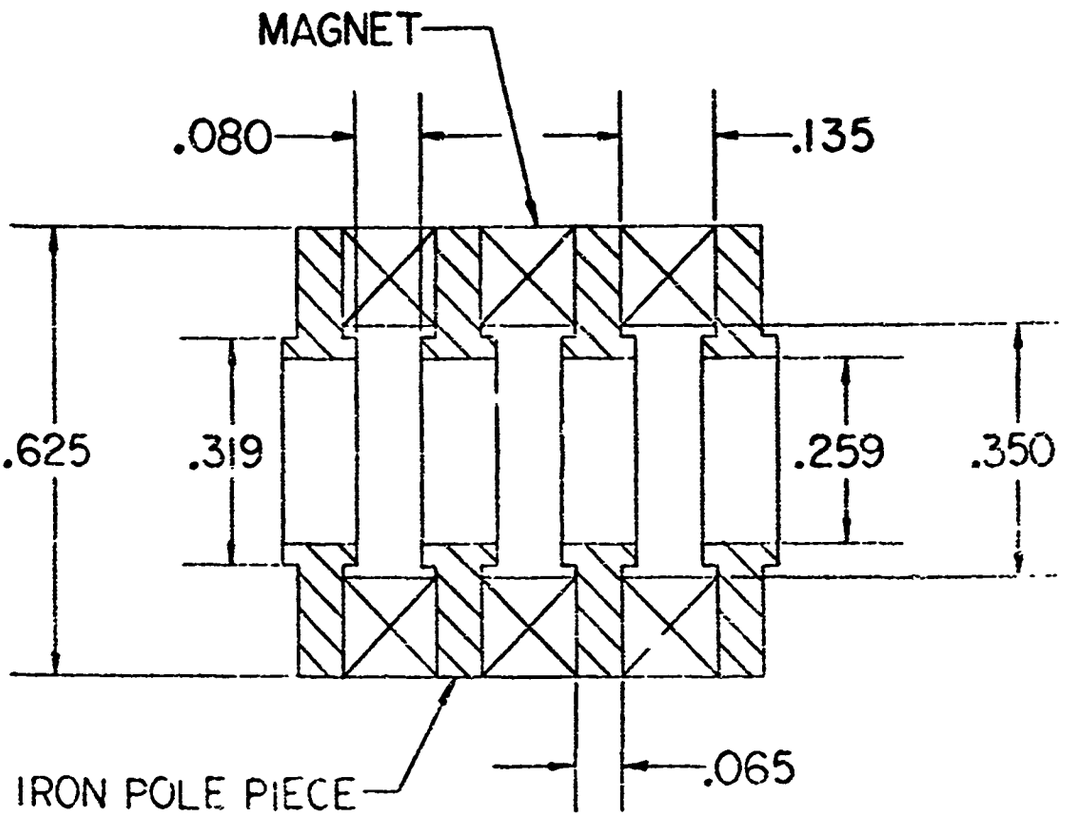

Figure 45 PPM array used in the temperature study.

THEORETICAL

Load line slope (B/H)	= -1.21
H_d	= 3500 Oe (based on lot PV 648B)
B	= 1875 gauss
B_{pp}	= 10,400 gauss max.

MEASURED

B_{peak} = 1870 gauss

The method and theory used to determine the calculated values is included in Appendix I. The peak magnetic field, B, is calculated by assuming an infinitely long array of magnets and pole pieces. Since the stack of interest was relatively short, end effects lowered the field produced by the outside magnets (Fig. 46). The field value quoted, therefore, is for the cell at the arrays center.

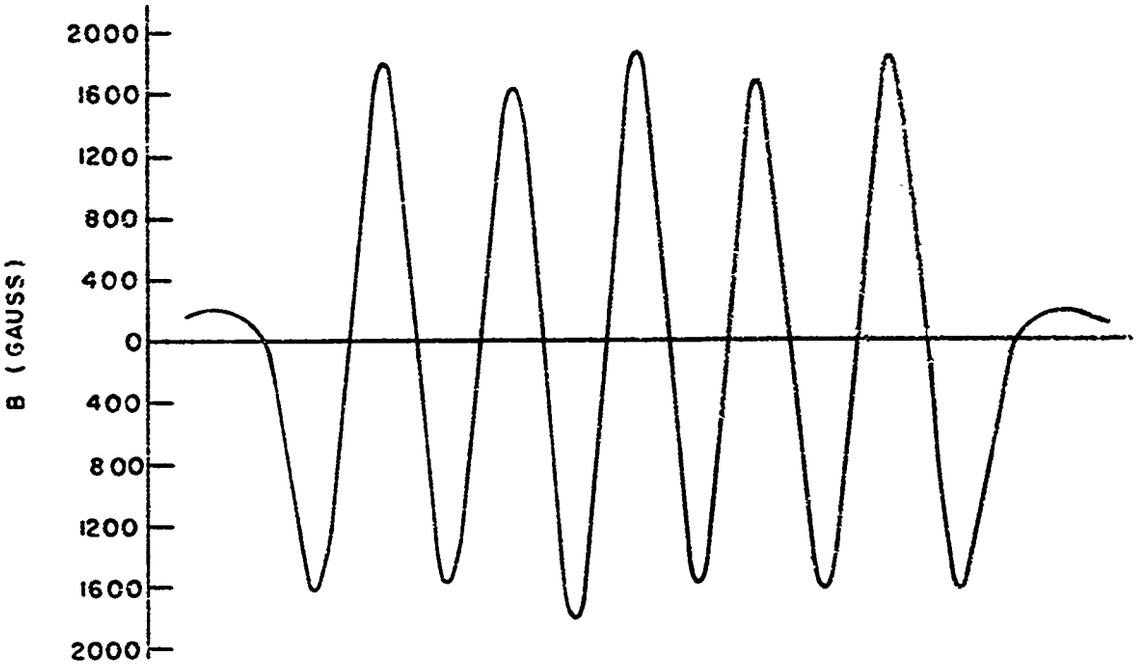

Figure 46 Axial magnetic field, B, in gauss versus axial position produced by the array in Fig. 45.

The same magnet stack was then subjected to many temperature cycles to determine both the reversible and irreversible temperature coefficients. In order to make measurements at elevated temperature, a search coil in conjunction with an integrating fluxmeter was used to measure the axial magnetic field. This kind of device was chosen because its performance is independent of temperature. The array was cycled from 24° to 100°C in increments of 25°C. This was repeated four times. There was a significant irreversible loss observed after the first cycle, but irreversible losses during subsequent cycles were unmeasurably small. In summary, there was

a complete recovery of magnetic field in cycling from 24° to 100°C, then back to 24°C after the initial loss had been established. The stack was then subjected to additional cycles from 24° to 175°C. As before, an irreversible loss was observed after the first cycle, but none was observed after each of the three subsequent cycles. During all cycles the values of axial magnetic field were recorded at each temperature increment so that the reversible temperature coefficient could be calculated. A summary of the reversible and irreversible temperature coefficient is listed below.

NOTE: These values were measured on a stack of load line slope (B/H) equal to 1.21. They are therefore only valid in the vicinity of this value.

TEMPERATURE COEFFICIENTS

(Load Line Slope = -1.21)

Reversible

-0.042% per °C

Irreversible

-4.4% from 24°C to 100°C
-7.9% from 100°C to 175°C
-12.3% from 24°C to 175°C

C. Alnico 5 Focused 641H

The Hughes Model 641H TWT was selected as the test vehicle for the evaluation of cobalt-samarium magnets. It will become evident during the following discussion that the 641H is ideally suited for this purpose.

The 641H as produced prior to this contract is a multi-octave, helix type, PPM focused tube. The general tube parameters are outlined in Table XXXIX.

Figure 47 shows the typical performance of this tube over its band of operation. This broad frequency characteristic coupled with the tubes present duty cycle capability of 10% immediately identifies it as an advanced design. The tube, although it has been in high volume production for a sufficient length of time to allow for total quantities in the thousands to have been produced, is state-of-the-art and incorporates many of the recent developments in TWT design.

TABLE XXXIX

General Tube Parameters--Alnico 5 Focused 641H

Parameter	Value
Power level	2 kW nominal
Frequency band	Multi-octave 3.5 to 10.6 GHz
Duty cycle	10%
Focusing	Radial periodic permanent magnet
Diameter vacuum assembly/package	1 3/4 inches/2 5/8 inches
Length	14 1/2 inches
Weight	8 3/4 lb
Cooling	Dielectric oil

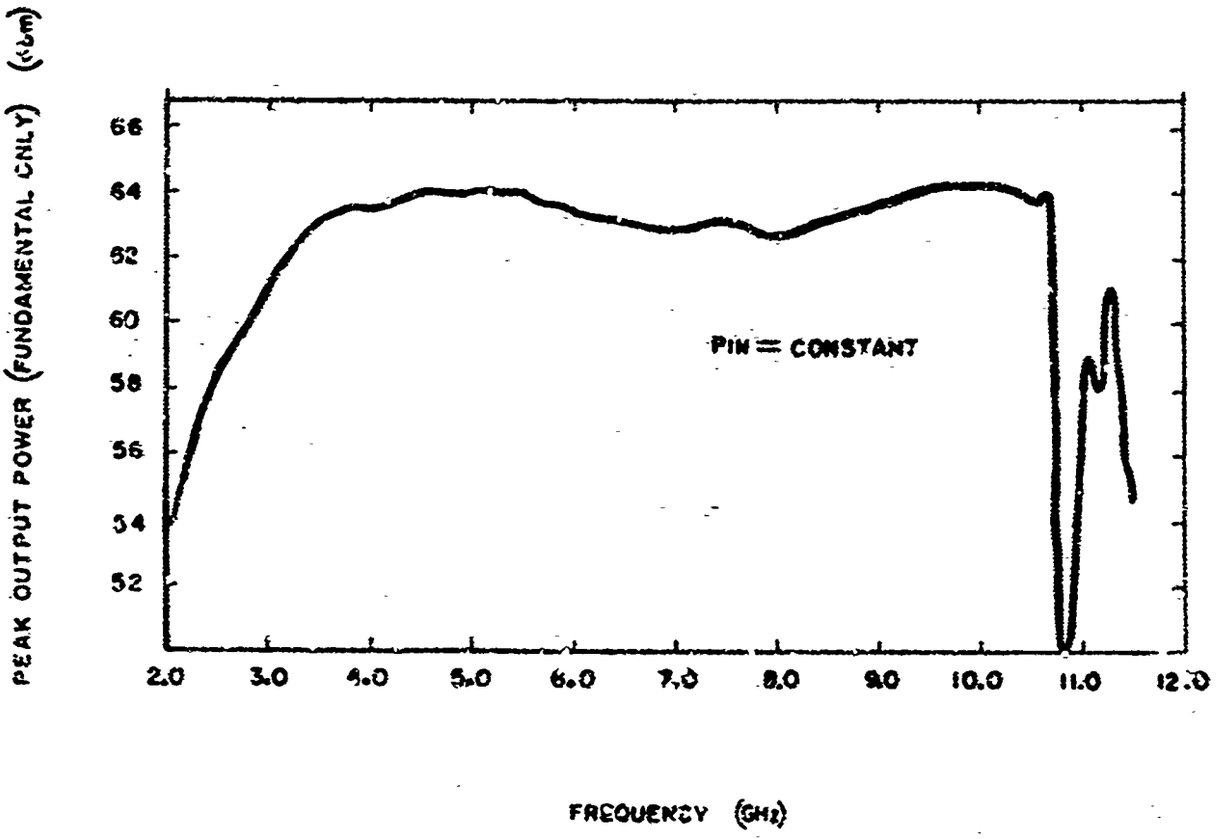

Figure 47 Typical performance output power vs frequency for the radially focused Hughes Model 641H.

Figure 48 is a photograph showing the tube in its external configuration while Fig. 49 shows the basic vacuum assembly removed from its package shell. The items shown in Fig. 49 are a basic vacuum assembly, a vacuum assembly with magnet bars attached, and a typical magnet bar. From this photo the complex nature of the focusing structure is apparent. This kind of structure was required because of the inferior characteristics of magnetic materials available prior the advent of Co_5Sm magnets. During the development of this tube the field requirements were such that the simpler axial PPM stack could not be utilized without the use of cobalt-platinum. The high cost of cobalt-platinum made this unfeasible. With Alnico 8 or barium ferrite magnets the available field and $\lambda p/L$ (see Appendix I) were such that satisfactory focusing could not be obtained. The development of the radial structure utilizing Alnico 5 magnets shown here allowed the use of a magnetic period of 0.480 resulting in a $\lambda p/L$ of approximately 2.5. This value, while usable, is considerably less than optimum. In addition, this radially PPM stack is quite complex and relatively difficult to manufacture.

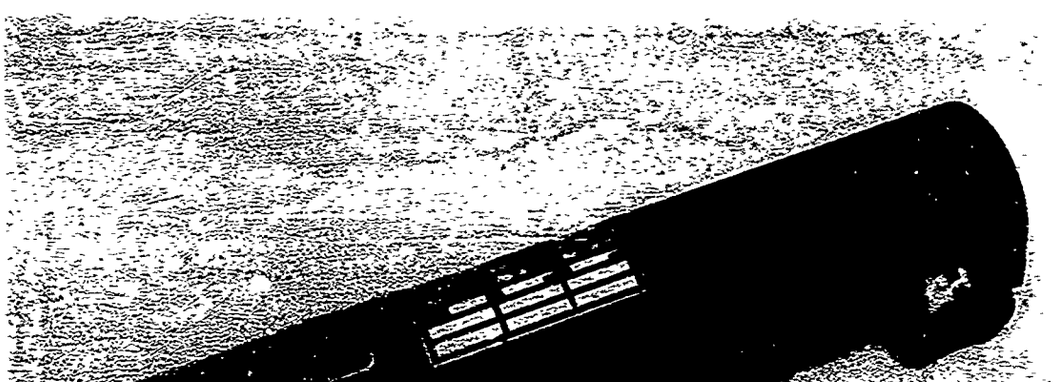

Figure 48 Hughes Model 641H traveling wave tube.

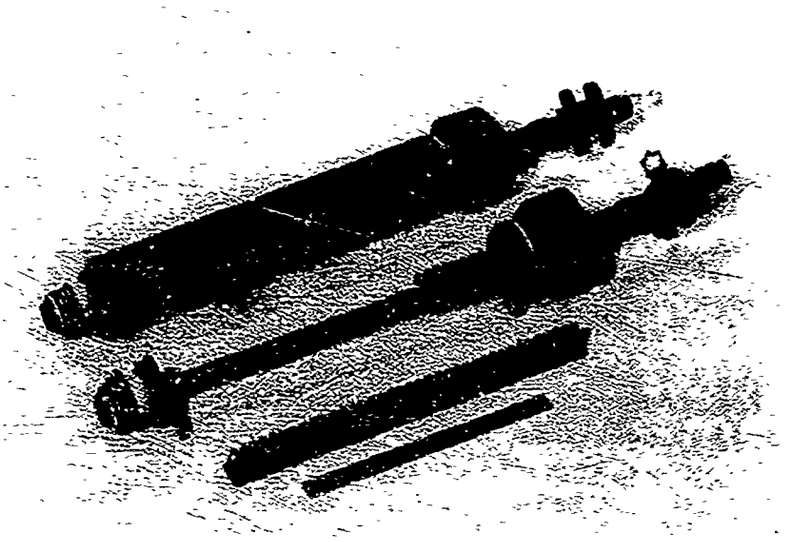

Figure 49 Photograph of the radially focused 641H vacuum assembly with and without magnets.

As noted in Table XXXIX, the weight of the tube in its radially focused configuration is 8 3/4 lb. The distribution of this weight is detailed below in Table XL:

TABLE XL

Distribution of Weight--Alnico 5 Focused 641H

Component	Approx. Wt (lb)
Vacuum assembly	1.00
Pole pieces	0.08
Magnet bars (7)	3.19
Magnet bar support sleeve	1.75
Package shell and end caps	2.50
Connectors/fittings	0.25
Total	8.77

The radial focused 641H tube has been in production for some time. As a result large amounts of extremely accurate and dependable data have been accumulated. Thus this particular tube is in the somewhat unique position of representing a device that is at the same time both state-of-the-art and well defined and predictable. It is therefore ideally suited for evaluating

cobalt-samarium magnets. The data shown in Fig. 47 are the result of a long series of tests that were undertaken to determine the exact capabilities of this tube. Data were taken in many areas of performance in addition to power and bandwidth.

D. Co_5Sm Focused 641H

The Co_5Sm focused 641H utilizes a conventional axial PPM focusing structure. The advantage of the simplicity of this type of stack is shown in Figs. 50 through 52. The tube shown in Figs. 50 and 51 is in the 641H modified to utilize an axial PPM stack of Co_5Sm magnets and Fig. 52 in a schematic of an axial stack. It is obvious from the photos and drawing that distinct advantage are displayed by the axial structure. In particular, the entire focusing structure is self-jigging on the vacuum barrel. The magnets are simple cylindrical shapes and require only that the dimensions of the opposite flat faces be accurately controlled. The pole pieces are also simple, uniform cylindrical shapes and are identical to each other.

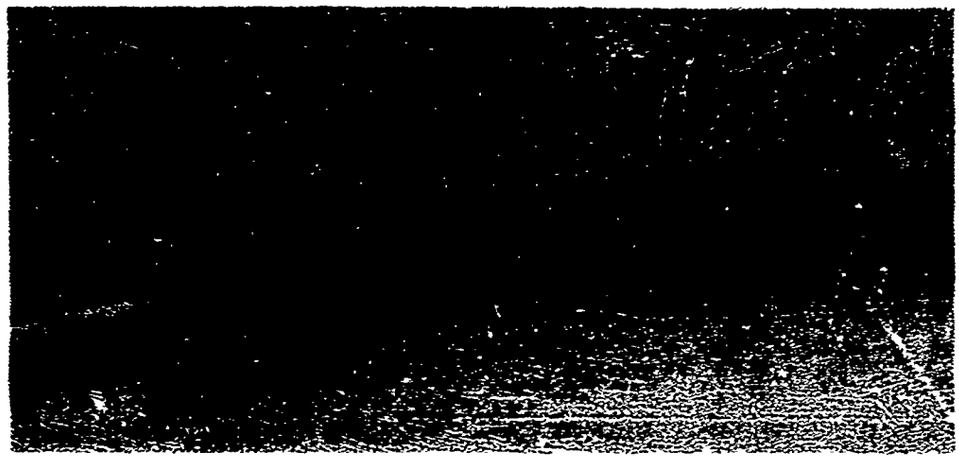

Figure 50 Photograph of the axially focused 641H vacuum assembly without magnets.

The incorporation of the cobalt-samarium magnet stack resulted in the reduction of the diameter of the focused vacuum assembly from 1 3/4 inches to 1 inch (see Fig. 53) and allowed a significant reduction in the total weight of the completed tube. Table XLI indicates the distribution of weight and the weight saved by substituting the Co_5Sm array for the Alnico 5 radially focused stack. The outside package on this tube, as well as the support sleeve, is identical to that used on the radially focused tube, and so the entire weight saving demonstrated on the axially focused tube is the result of the simpler magnet stack.

Figure 51 Photograph of the axially focused 641H vacuum assembly with magnets.

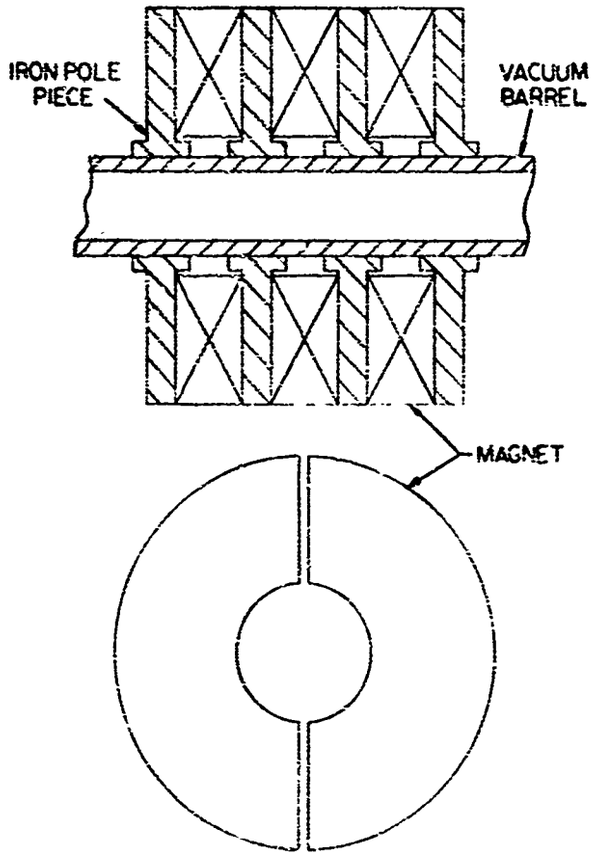

Figure 52 Schematic of an axial PPM stack and a single pair of magnets.

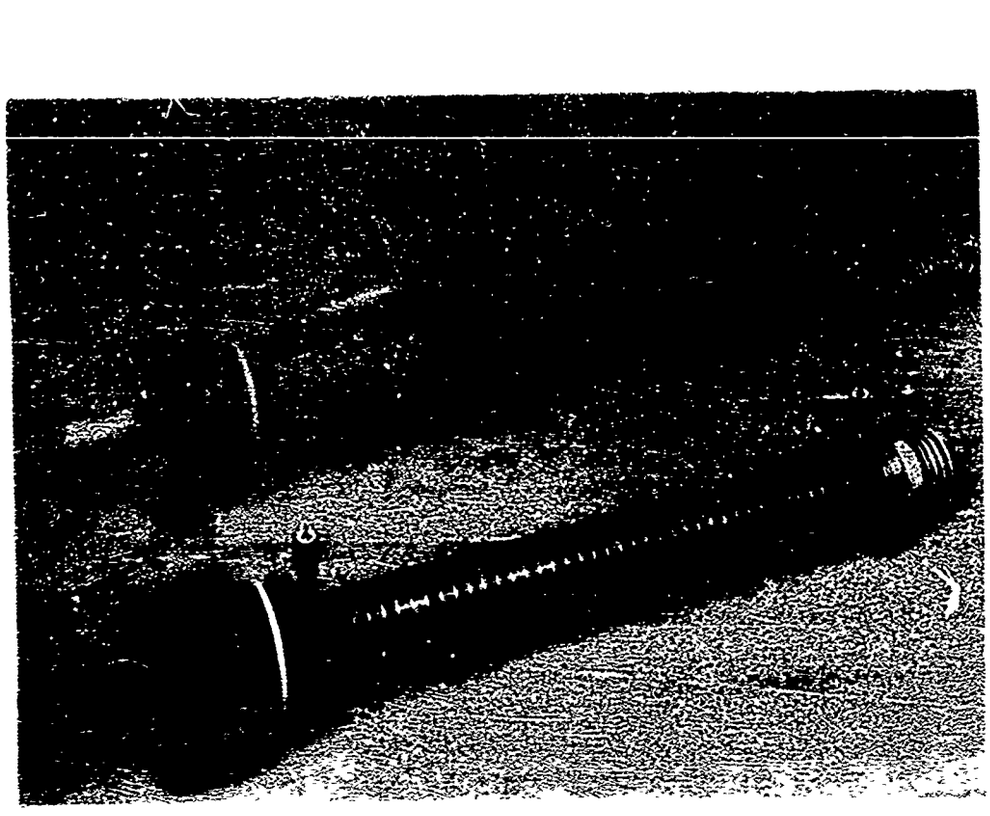

Figure 53 Radially focused 641H (upper) and axially focused 641H (lower).

TABLE XLI

Distribution of Weight and Weight Saving--Co_5Sm Focused 641H

Component	Co_5Sm Tube Weight (lb)	Saving (lb)
Vacuum assembly	1.00	None
Pole piece	0.70	0.62 (increase)
Magnets and clamps	1.70	1.49
Support sleeve	1.75	None
Package sleeve and end caps	2.50	None
Connectors/fittings	0.25	None
Total	7.90	0.87

This represents a savings of approximately 10%.

In addition to the weight reduction due to the magnets themselves, it would also be possible to further reduce the total weight by redesigning the tube package. The magnet bar support sleeve, which is essential to the radially focused tube package, could be eliminated from the axially focused tube package by a redesign. This would reduce the tube weight by an additional 20%, bring the total weight reduction made possible by the Co_5Sm material to 30%.

In addition to the physical advantages, significant improvements in the electrical performance and the maximum available magnet field were predicted. As previously noted the highest $\lambda p/L$ that can be obtained with previously available magnet material is approximately 2.5. The axial cobalt-samarium structure used allowed $\lambda p/L$ to be increased to 3.0, representing an increase of 20% in their critical focusing parameter. Furthermore, the maximum available magnetic field was increased from the 1800 gauss of the radially focused tube to 3000 gauss.

During the testing of the tubes, it was determined that the best focusing was obtained with a peak axial field of 2500 gauss. This result makes it possible to further improve the tube from two standpoints. First, the diameter of the magnets could be reduced from 1.0 inch to 0.75 inch. This also represents a reduction in tube weight. Or, second, $\lambda p/L$ could be increased to 3.6 by reducing the magnet thickness and therefore the magnetic period, L. A combination of these two improvements would also be possible. Essentially, the improvements to the 641H which are possible because of Co_5Sm are a weight reduction of at least 30%, an increase in the critical $\lambda p/L$ focusing parameter of 20% to 44% which would improve beam transmissions, and a mechanically simple focusing structure.

E. Performance of the Tubes

The contract specified fabrication of five tubes with magnets supplied by General Electric. The tubes were to be tested according to an Acceptance Test Procedure (ATP). The ATP (see Appendix II) is divided into two parts: Quality Conformance Inspection, Part 1 (QCI-1), to be performed on all five tubes; and QCI-2, to be performed on three tubes. QCI-1 consisted of a set of electrical measurements which determined the operating currents and voltages of the tube necessary for the specified power output. These data were taken with the tube operating at 10% duty.

QCI-2 is a series of environmental tests designed to evaluate the reliability of the tube under a variety of environmental operating conditions and are summarized below:

(a) Burn-in. The tube is temperature cycled from -40° to 90°C. Five cycles are included extending over a period of 50 hours.

(b) Shock Test. The TWT, while nonoperating, is subjected to 18 impact shocks having a magnitude of 15 g's and a duration of 11 milliseconds.

(c) Salt Spray Test. The tube, while nonoperating, is subjected to a fog mist containing 5% sodium cloride at a temperature of 35°C for 48 hours.

(d) Vibration Test. The tube, while operating, is subjected to vibrations of 5 to 2000 Hz with an acceleration of 2.6 to 10 g's.

(e) Temperature-Altitude Tests. The TWT is stabilized at -62°C and then checked for satisfactory operation after a three-minute warmup time allowing the temperature to rise to -40°C and with a pressure equivalent to an altitude of 70,000 feet. The tube is then operated at +120°C for four hours with the pressure at room ambient and then again at a pressure of 70,000 feet for four hours.

1. Tube No. 1

Construction was begun on the first tube after the evaluation of the magnet material itself had been completed. An optimum d-c beam transmission of 95% was established with a peak axial magnetic field of approximately 2500 gauss. However, for best r-f performance the d-c beam transmission was reduced to 92%. Under these operating conditions, r-f defocusing reduced transmission to 77%. This result represents a significant improvement over the previous radially focused tubes. The latter typically demonstrated a d-c beam transmission of 84% and an r-f defocused transmission of 63%.

The r-f characteristics of this tube were good. The output power level was well above the specified 61 dBm minimum with a 37 dBm r-f drive across the frequency range of 4 to 8 GHz. In fact, the output power level almost achieved 2 kw across the frequency range. These data are summarized in Fig. 54.

The 50-hour burn-in and the temperature-altitude test were conducted on this tube. The 50-hour burn-in was successfully completed, however, during the temperature-altitude test with the tube operating at 120°C excessive r-f defocusing caused the helix to melt. The tube was dismantled in order to measure the magnet field of the focusing stack. The field of a number of magnets had degraded as shown in Fig. 55. In fact, five magnet pairs were found to produce between 950 and 1250 gauss on the axis, whereas the majority of the magnet pairs produced between 2250 and 2500 gauss.

A series of experiments was undertaken to determine the temperature which produced such a large irreversible loss.

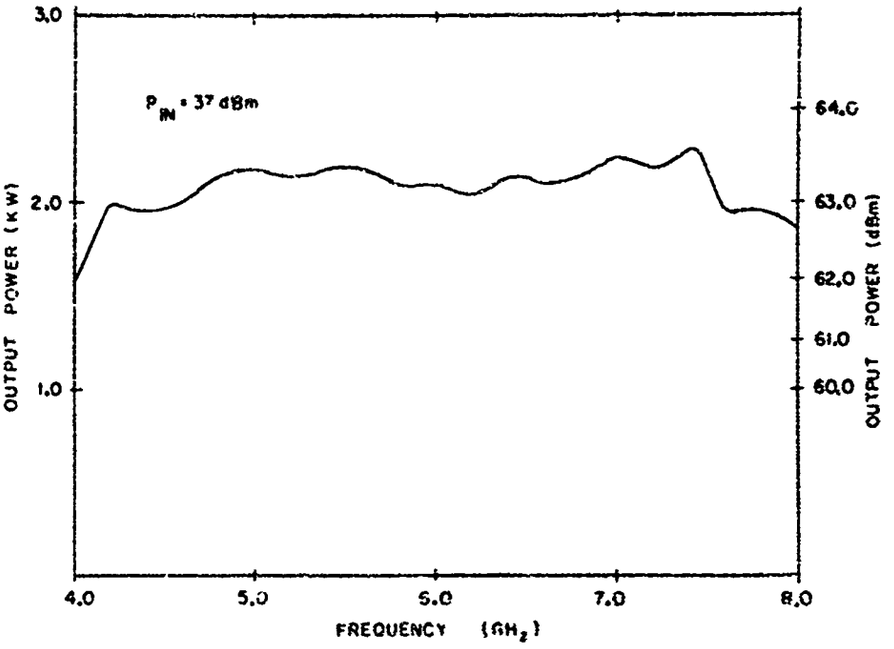

Figure 54 Output power versus frequency for the 641H, No. 1.

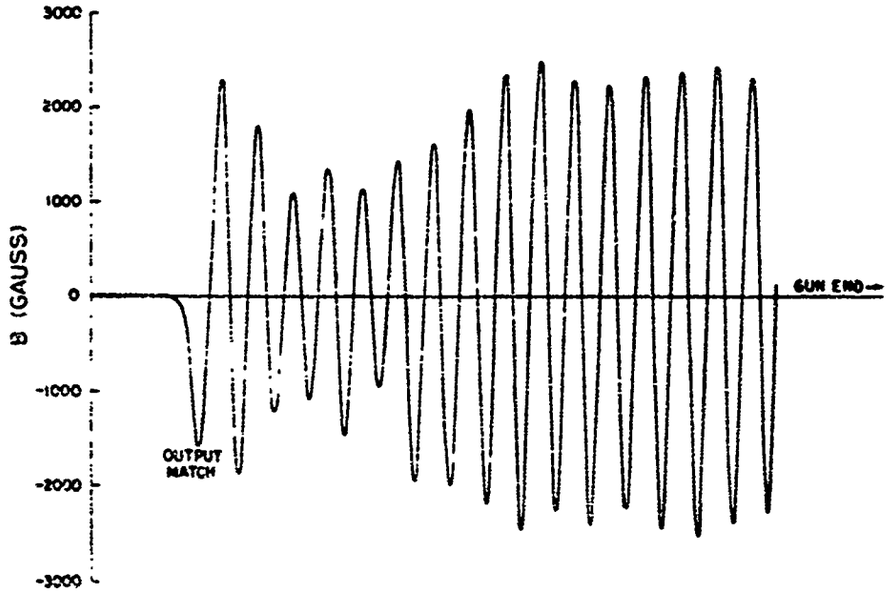

Figure 55 Axial magnet field, B, versus axial position measured on tube No. 1 after the helix was melted.

A small array consisting of the output match magnet pair and the last seven circuit magnet pairs was recharged as shown in Fig. 56. This stack was temperature cycled to 150°C and the magnets were found to exhibit an irreversible loss ranging from 3.1% to 33.2% (Fig. 56). It should be noted that the load line slope (B/H) for this stack is 0.5 compared with the slope of 1.21 for the stack used in the preliminary temperature study (part B). A subsequent cycle to 175°C produced additional magnetic field losses (Fig. 57) making the total irreversible loss 15.3% to 52.8% for the eight magnet pairs tested. (The magnets which were used on tube No. 1 were from the first lot, delivered by the General Electric Company.) These experiments showed that it was necessary to temperature cycle the magnets after their field strengths had been adjusted to the proper value. In all subsequent tubes the magnets were temperature cycled from room temperature to 160°C after final field adjustments were made. None of the magnets was magnetized or demagnetized after the final 160°C cycle.

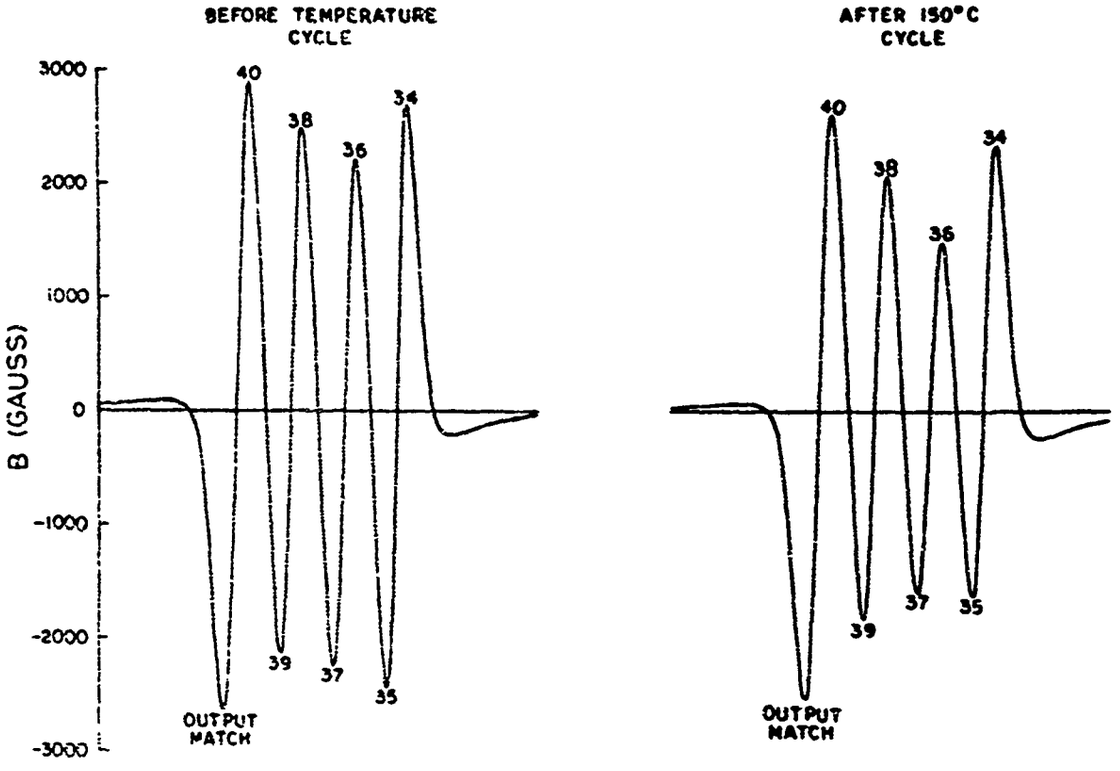

Figure 56 Axial magnetic field, B, versus axial position produced by the last eight magnet pairs from tube No. 1 before temperature cycle and after the 150°C cycle.

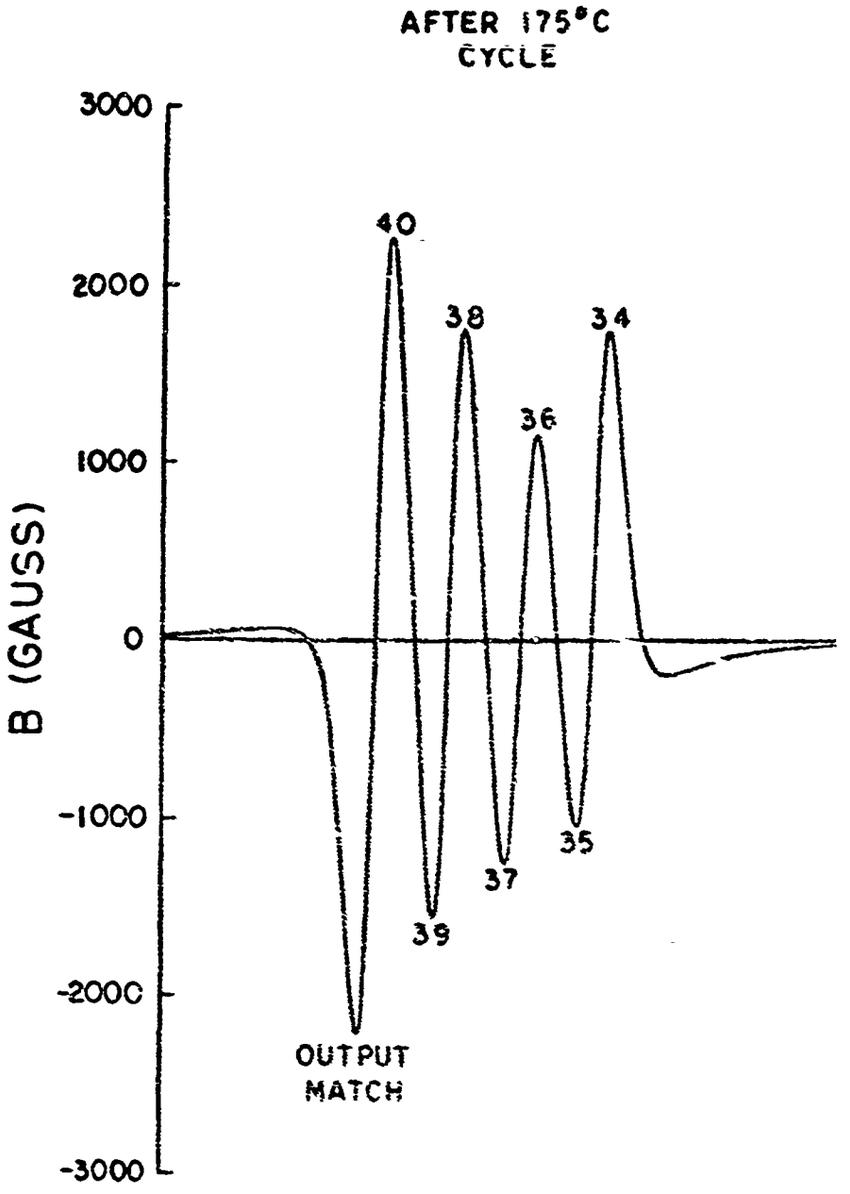

Figure 57 Axial magnetic field, B, versus axial position provided by the last eight magnet pairs from tube No. 1 after the 175°C temperature cycle.

2. Tube No. 2

The second tube constructed was focused using magnets from the second lot delivered by the General Electric Company. The beam transmission and power output were similar to those of tube No. 1, under air-cooled condition. No significant degradation in focusing was observed during operation at a duty cycle of 3.3%. However, the first three turns of the helix were melted. It is

likely that a failure of the modulator caused it to operate CW for a short period of time and melt the helix. This kind of modulator failure is equivalent to operating the tube at 100% duty for a short time. After the helix had been severed, the tube still focused well, which indicates that the failure was not caused by the magnets.

3. Tube No. 3

Tube No. 3 was focused with the fifth lot of magnets. The tube demonstrated a d-c beam transmission of 90% and defocused to 74% with r-f drive. Data taken both air-cooled and oil-cooled indicated that the tube delivered sufficient output power across the frequency range of 4 to 8 GHz. These data are summarized in Fig. 58.

This was the second tube subjected to environmental testing. All five environmental tests were completed according to the ATP with the exception of paragraph 5.6.3, vibration along the major horizontal axis. A large resonance was observed at a frequency of 860 Hz. This problem was the result of modifications to the package to accommodate the Co_5Sm magnet array and had nothing to do with the magnets themselves. In order to avoid the possibility of damage to the tube, paragraph 5.6.3 was not completed along the major horizontal axis. It was, however, completed along the other

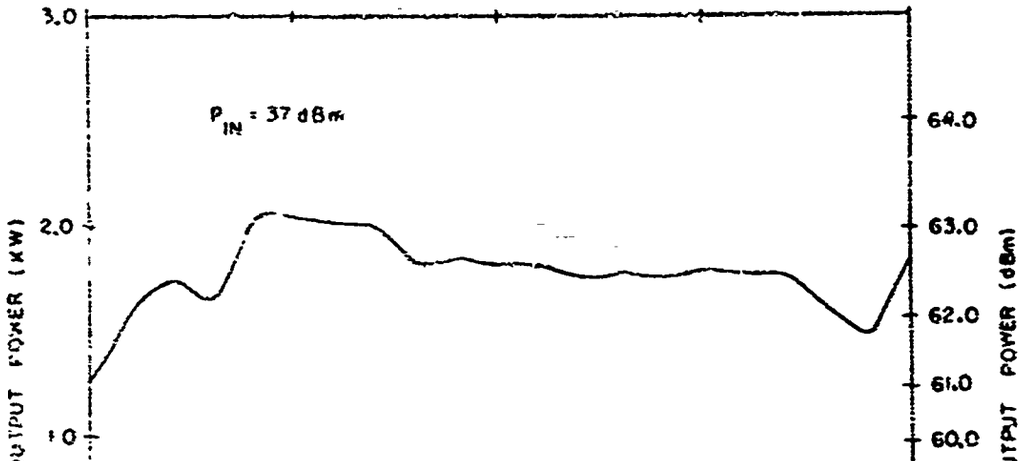

Figure 58 Output power versus frequency for the 641H, No. 3.

two axes. It was later determined that this resonance could be minimized by shoring up the collector end cap to effectively reduce the motion to a safe level. This was done on subsequent tubes.

During the temperature-altitude test tube No. 3, unlike tube No. 1, performed well. The only significant increase in body current occurred when the tube was operated at +120°C. An increase in body current in a normal phenomenon during high-temperature operation and the value measured were well within the acceptable limits. When the tube was cooled to ambient the body current returned to its original value. This indicates that the degraded transmission at +120°C was due only to reversible temperature loss and that cycling the magnets to 160°C had stabilized them.

4. Tube No. 4

The fourth tube built was focused with the magnets from General Electric's lot #4. A d-c beam transmission of 88% and an r-f driven beam transmission of 71% was achieved on this tube. The output power was greater than 61.0 dBm across the frequency range 4 to 8 GHz, and the minimum point of 61.1 dBm occurred at low band edge (4.0 GHz). The output power measured at a duty of 10% is plotted in Fig. 59.

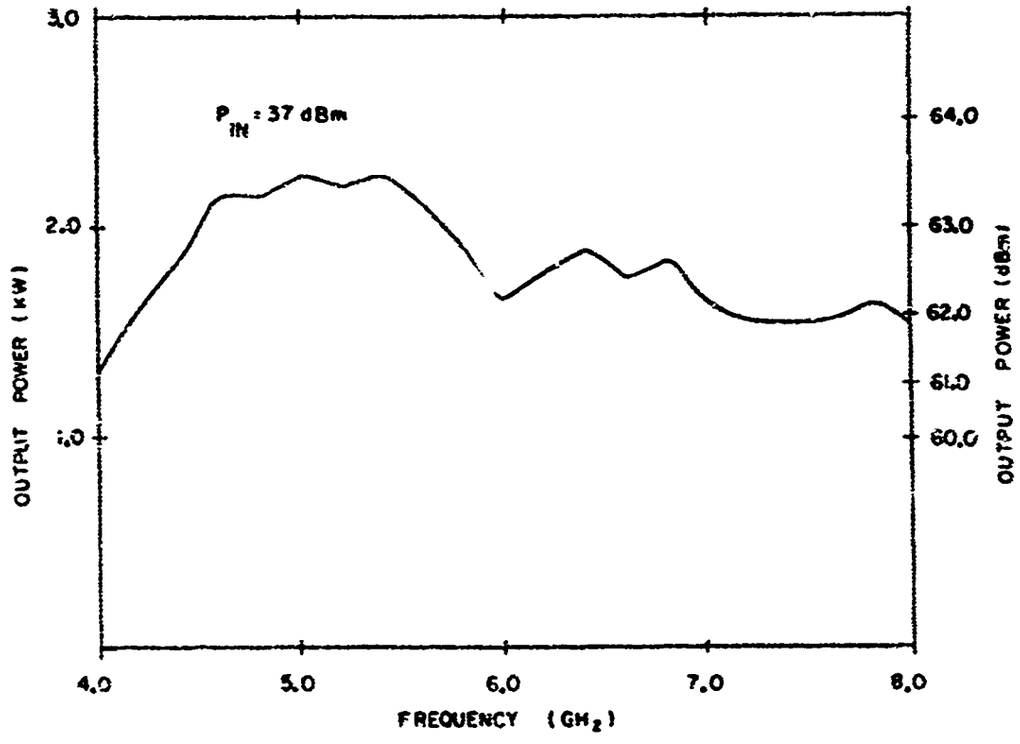

Figure 59 Output power versus frequency for the 641H, No. 4.

Tube No. 4 was the third tube to be subjected to the environmental tests. During vibration along the minor horizontal axis, the tube demonstrated severe modulation of the cathode current and r-f power output. However, the tube performed normally when the vibration was terminated. The vibration test was discontinued at this point in order to prevent further damage which would prohibit temperature-altitude tests. The cause of the severe modulation may have been due to loose internal gun parts, since an inspection of the leads between the vacuum assembly and the external package proved negative.

The temperature-altitude test was then successfully completed. The body current did not significantly increase during this test or during the 50-hour burn-in.

5. Tube No. 5

Tube No. 5 was focused using the magnets which were previously employed on tube No. 2 (which failed). This tube (i. e., No. 5) demonstrated a maximum body current similar to that of tube No. 4, a maximum value of 0. 460 amp. Tube No. 4 was operated oil-cooled at 10% duty and data were taken in accordance with QCI-1. All specifications were met during this test. A plot of output power versus frequency is included on Fig. 60. No environmental tests were conducted on this tube.

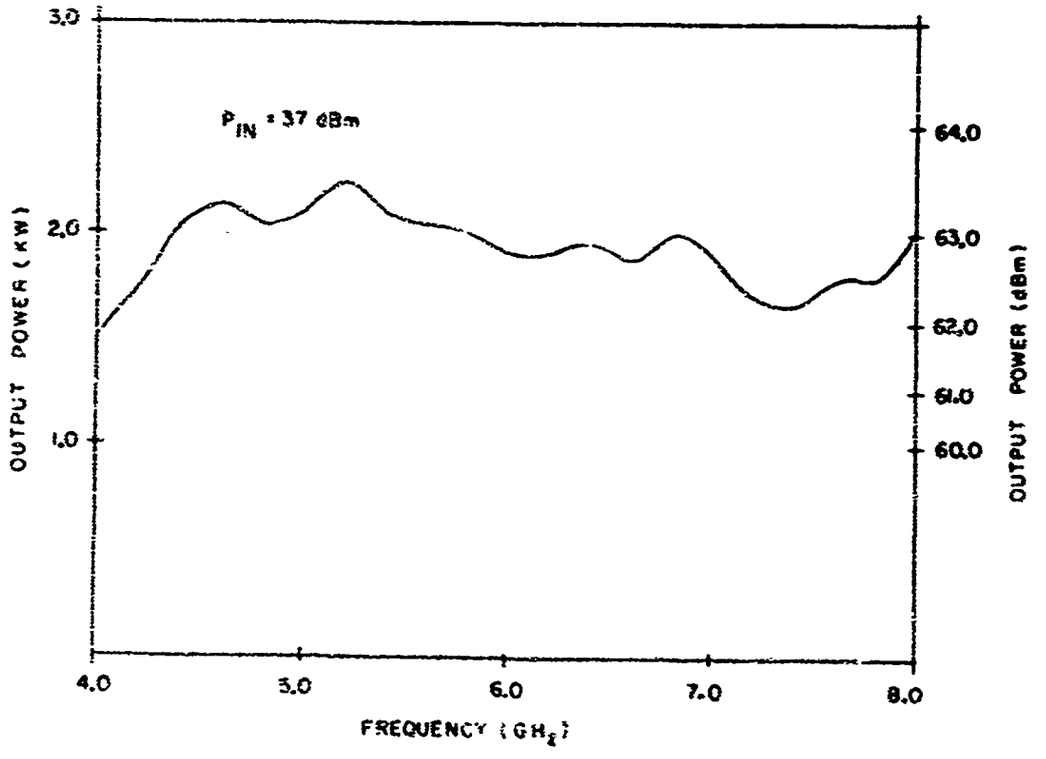

Figure 60 Output power versus frequency for the 641H, No. 5.

6. Tube No. 6

Magnets from General Electric's lot #3 were installed on this tube. However, the tube developed a vacuum leak at the braze between the input r-f port and the tube barrel. At this point the tube was judged unsatisfactory and the magnets were removed for later installation on tube No. 8.

7. Tube No. 7

This tube developed vacuum leaks at both input and output r-f port brazes during evacuation. Magnets were not installed on this tube.

8. Tube No. 8

The magnets from lot #3 were installed on tube No. 8. A d-c beam transmission of 89% and an r-f defocused transmission of 73% were achieved. The tube delivered a maximum of 63.1 dBm of output power with a 37 dBm drive level and a minimum of 61.0 dBm across the frequency range of 4 to 8 GHz. These data are included in Fig. 61.

Table XLII is a summary of the data taken on the six tubes which were focused and tested.

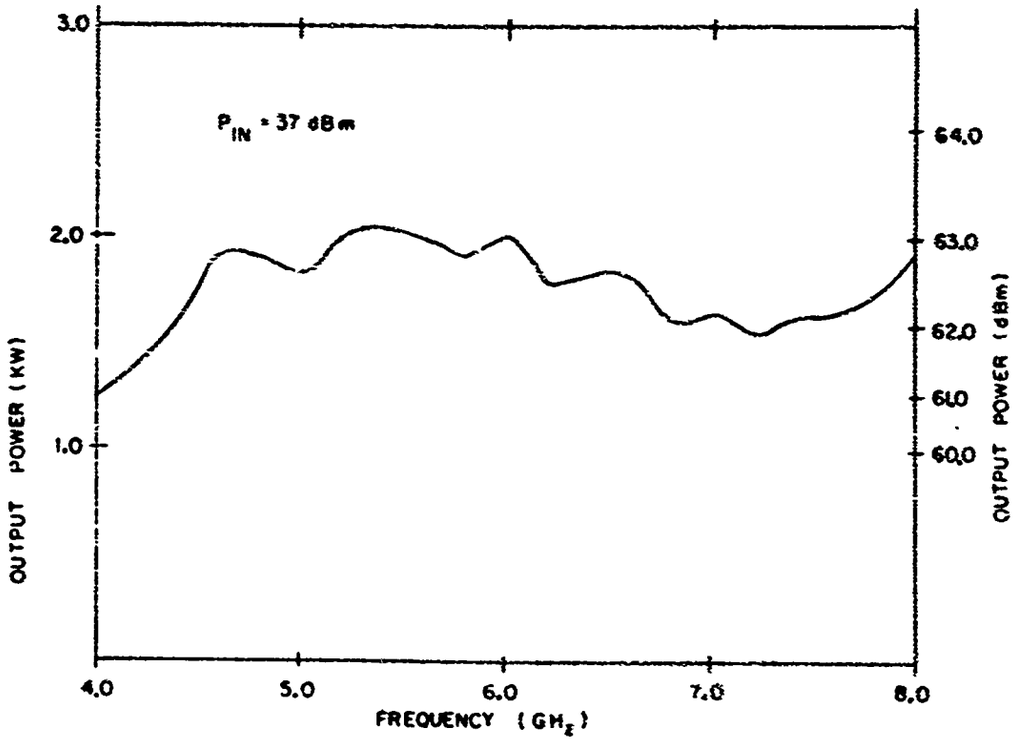

Figure 61 Output power versus frequency for the 641H, No. 8.

TABLE XLII

Summary of Data Taken on Six Co_5Sm Focused Tubes

TEST NO.	1	2	3	4	5	8
SERIAL NUMBER	C1062	--	C1065	C1063	C1064	C1061
MAXIMUM AIR-COOLED DUTY	3%	3.3%	4%	4%	4%	4%
MAXIMUM OIL-COOLED DUTY	10%	--	10%	10%	10%	10%
MINIMUM OUTPUT POWER (dBm)	62.0	62.0	61.0	61.1	61.8	61.0
MAXIMUM OUTPUT POWER (dBm)	63.6	64.0	63.1	63.5	63.5	63.1
DC BEAM TRANSMISSION	92%	90%	90%	88%	90%	89%
RF BEAM TRANSMISSION	77%	78%	74%	71%	70%	73%
ENVIRONMENTAL TESTS	Yes	No	Yes	Yes	No	No
MAGNET LOT NUMBER USED	1	2	5	4	2	3
DELIVERED TO GENERAL ELECTRIC CO.	Yes	No	Yes	Yes	Yes	Yes

F. Conclusions

During this magnet evaluation program, a series of experiments were conducted to measure the reversible and irreversible temperature coefficients of cobalt-samarium magnets. Eight Model 641H traveling wave tubes were constructed of which six were tested. One tube was lost during the preliminary test and one during environmental tests. Three of the six tubes underwent a series of environmental tests. Five tubes were delivered of which four were operational.

Measurements of the reversible and irreversible temperature coefficients were made on a PPM array of 0.625 inch outer diameter. These magnets exhibited a reversible loss of 0.042% per °C for a load line slope (B/H) of 1.21. The irreversible losses measured were 4.4% from 24° to 100°C, 7.9% from 100° to 175°C for a total of 12.3% from 24° to 175°C. Although tests of this type were not conducted on the 1.0 inch outer diameter magnets used on the tube, the later lots exhibited considerably lower irreversible losses.

The use of Co_5Sm in an axially oriented array allowed significant improvements in the maximum available magnetic field and the focusing parameter $\lambda p/L$. The previously used radial Alnico 5 array produced a peak axial magnetic field of 1800 gauss while the axial Co_5Sm stack produced 3000 gauss. $\lambda p/L$ for the Co_5Sm tube was 3.0, as compared to a value of 2.5 for the Alnico 5 tube.

The average d-c beam transmission for the Co_5Sm focused tube was 90% as compared to 84% for the Alnico 5 focused tubes. R-f defocusing reduced the transmission to an average of 75% for the Co_5Sm focused 641H, while the Alnico 5 focused 641H typically demonstrated an r-f transmission of 63%. To obtain this transmission it was necessary to utilize only 2500 gauss of the 3000 gauss which was available. In addition to the improved beam transmission, the Co_5Sm magnet material allowed a significant reduction in the weight of the tube. The axially focused 641H weighed 7.9 lb, whereas the radially focused tube weighed 8.75 lb.

Co_5Sm also provides the opportunity for further improvements to the 641H. Since only 2500 gauss of the 3000 gauss available was necessary for best focusing a redesign of the magnet stack in one of two ways is possible. The magnet period, L, could be reduced enough to increase $\lambda p/L$ to 3.6 yet still maintain an axial peak field of 2500 gauss. The other possibility is to reduce the outer diameter of the magnets to 0.750 inch. This change represents a decrease of approximately 50% in the weight of the magnets.

The radially focused tube required an inner support sleeve as part of the package which was also used on the axially focused tube. However, the support sleeve was not essential to the axial focusing structure. A redesign of the package to eliminate this sleeve could have further reduced the tube weight

by approximately 1.75 lb. That is, the use of Co_5Sm on the 641H tube reduced the weight by 10% and provided the opportunity for an additional 20% reduction with a suitable package redesign.

Because of the failure of tube No. 1 during environmental test, it was determined that the magnets had to be stablized at 160°C after they had been adjusted. If they were not stabilized, the high temperature encountered during the environmental tests would demagnetize the magnets enough to cause sufficient defocusing to melt the helix. All subsequent magnets were treated in this way and no further problems of this nature were encountered.

The process of installation of magnets on the tubes and focusing requires frequent handling of the magnets. It was found that because of the brittleness of the Co_5Sm material, extreme care was necessary to prevent breakage. This problem was, however, minimized as experience with the material increased.

REFERENCES

1. Hughes Aircraft Company, Electron Dynamics Division "Technical Proposal for Samarium-Cobalt Focused Traveling-wave Tube," RFP F33615-69-R-2444, General Electric Company (June 1969).

2. J. E. Grant, M. G. Benz, and D. L. Martin, "A 2 kW, Multi-Octave TWT Focused with Cobalt-Samarium Magnets," General Electric Technical Information Series (Jan. 1971).

3. M. G. Benz et al., "Manufacturing Methods and Technology for Processing Cobalt-Samarium Magnets," Interim Technical Report IR-612-9A(4), Contract No. F33615-70-C-1098, Air Force Materials Laboratory, Air Force Systems Command, Wright-Patterson Air Force Base, Ohio (Nov. 1970).

4. F. Sterzer and W. W. Siekanowitz, "The Design of Periodic Permanent Magnets for Focusing of Electron Beams," RCA Rev., Vol. 18, pp. 39-59 (March 1957).

5. Hughes Aircraft Company, Electron Dynamics Division, "Monthly Progress Reports 1 - 15," Contract No. F33615-70-C-1098, General Electric Company.

APPENDIX I

PERIODIC MAGNETIC FOCUSING DESIGN

Periodic permanent magnetic focusing has proved to be a useful method of constraining electron beams. PPM focusing has a significant weight advantage over uniform field focusing. Typically, a solenoid and its associated power supply can be replaced by a periodic permanent magnet assembly weighing one-tenth of the solenoid. Even though field adjustment is more critical with periodic focusing, and degradation of beam transmission due to r-f defocusing is more severe than when employing an electromagnet, PPM focusing is extensively used for pulse traveling wave tubes. Presently the beam transmission of the PPM focused traveling wave tubes is about 90% during r-f operations.

PEAK MAGNETIC FIELD AND MAGNET PERIOD

The theoretical uniform magnetic field, B_b, required to confine an ideal electron beam is given by:

$$B_b = 327 \frac{I^{1/2}}{V^{1/4} r_b} \text{ gauss,} \qquad \text{(VIII-1)}$$

where I is the beam current in amperes, V is the beam voltage in volts, and r_b is the average beam radius in inches. The derivation of Equation (VIII-1) assumes that all electrons leave the cathode with a zero component of transverse velocity and follow well defined trajectories which do not cross. In general, these assumptions are only approximately valid, and consequently most beams require more field than that calculated by Equation (VIII-1). Usually the required field is more closely approximated by:

$$B = 2B_b \qquad \text{(VIII-2)}$$

When a PPM stack is used, it is desirable to design the structure so that the field produced is a sine function. Since the root mean square of a sine is $1/\sqrt{2}$, the maximum value, B_{peak}, of a sinusoidal PPM field which is equivalent to the uniform field calculated by Equation (VIII-2) is given by:

$$B_{peak} = \sqrt{2}\, B$$

$$= 925 \frac{I^{1/2}}{V^{1/4} r_b} \text{ gauss.} \qquad \text{(VIII-3)}$$

An equally important focusing parameter is the ratio of the plasma wavelength, λp, associated with the electron beam, to the magnet period, L, given by

$$\frac{\lambda p}{L} = 0.0359 \frac{V^{3/4} r_b}{I^{1/2} L} \text{ inches.} \qquad \text{(VIII-4)}$$

The variable L is defined in Fig. 62. Spatial periodic magnetic field variations cause corresponding variations in the beam diameter called "scalloping" or "ripple" which can adversely affect the focusing characteristics of the tube. The ratios $\lambda p/L$ primarily determines the amount of ripple which may occur. An increase in $\lambda p/L$, which is equivalent to a reduction in magnetic period, reduces the beam ripple. Unfortunately, the peak axial magnetic field obtainable in a PPM stack is a direct function of the magnetic period. That is, a reduction in period will also result in a corresponding reduction in magnetic field. Best focusing characteristics can be achieved by designing a magnet structure with the smallest period, yet consistant with Equation (VIII-1) and available magnetic materials. $\lambda p/L$ for most tube designs lies between two and five. A value below three is considered marginal with best results above 3.5. However, until the introduction of Co_5Sm many state-of-the-art tube designs were forced to operate with a low $\lambda p/L$ because of the relatively low energy products and coercive forces of previously available permanent magnets.

PERMANENT MAGNET DESIGN[4]

Once the peak field and the magnetic period have been determined, from Equations (VIII-3) and (4), the dimensions of a magnet system to provide the required field is to be determined. Figure 62 shows a magnet structure of the single period magnetic focusing.

The peak field on the axis of an infinitely long magnetic structure of the type shown in Fig. 62 is given by

$$B_m = \frac{H_d T}{g} \sum_{m=1}^{\infty} \frac{1}{m} f_1\left(\frac{m d_1}{L}\right) \sin\left(\frac{m\pi g}{L}\right) \qquad \text{(VIII-5)}$$

$$m = 1, 3, 5, 7$$

where T, g, d_1 and L are dimensions shown in Fig. 62 and H_d is the magnetic intensity, in oersteds, of the magnetic material used.

The function $f_1 (md_1/L)$ versus md_1/L is plotted in Fig. 63. Equation (VIII-5) was based on the assumption that the pole pieces are not saturated. For most practical structures the series in Equation (VIII-5) converges very rapidly, and is usually sufficient to evaluate only the term for $m = 1$.

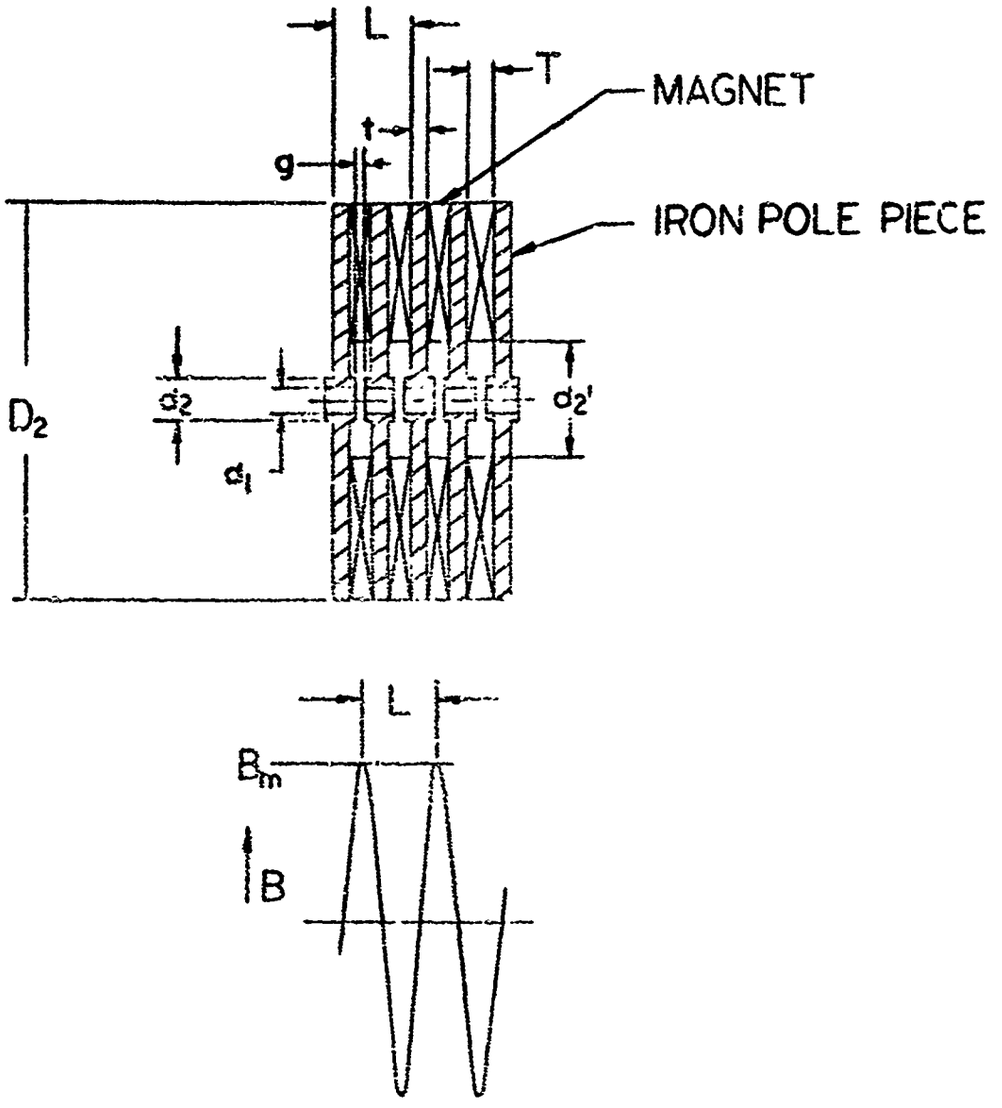

Figure 62 Axial magnetic focusing structure and magnetic field distribution.

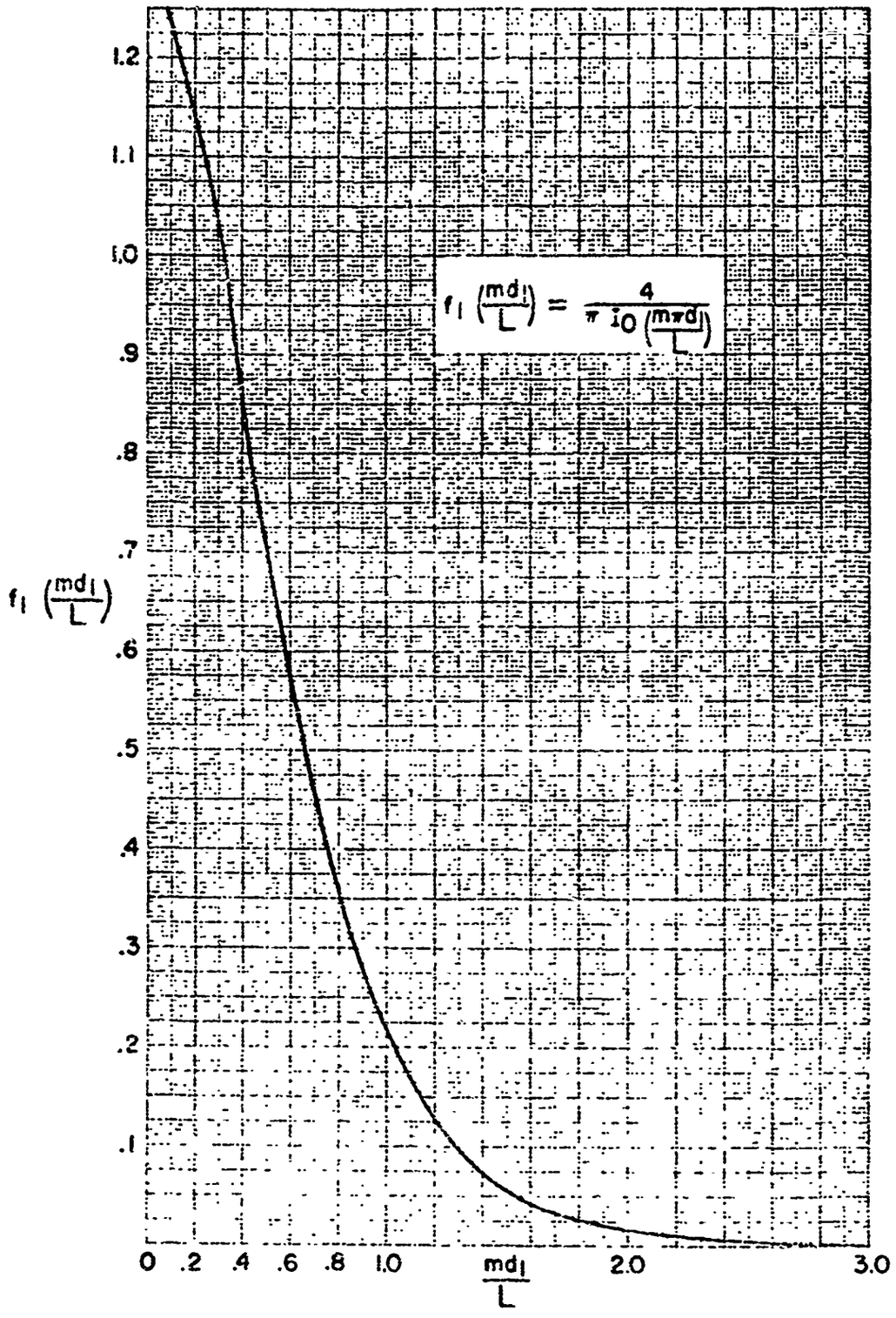

Figure 63 Plot of $f_1\ (md_1/L)$ versus md_1/L as used in Equation (VIII-5).

To determine the value of H_d in Equation (VIII-5), the total permeance P_t, of the magnetic circuit, must be calculated. To simplify the calculation the magnetic circuit is divided into three flux paths as shown in Fig. 64.

In the simplified design, two distinct and uniform fields are assumed for flux path I. The permeance of path I is given by

$$P_1 = p_1' + p_1''$$

$$= 0.785 \frac{d_2'^2 - d_2^2}{T} + 0.785 \frac{d_2^2 - d_1^2}{g} \text{ inch} \qquad \text{(VIII-6)}$$

The permaneance of path II is given by

$$P_2 = \sum_{m=1}^{\infty} \frac{Ld_1}{gTm^2} f_2 \left(\frac{md_1}{L}\right) \sin \left(\frac{m\pi g}{L}\right) \text{ inch} \qquad \text{(VIII-7)}$$

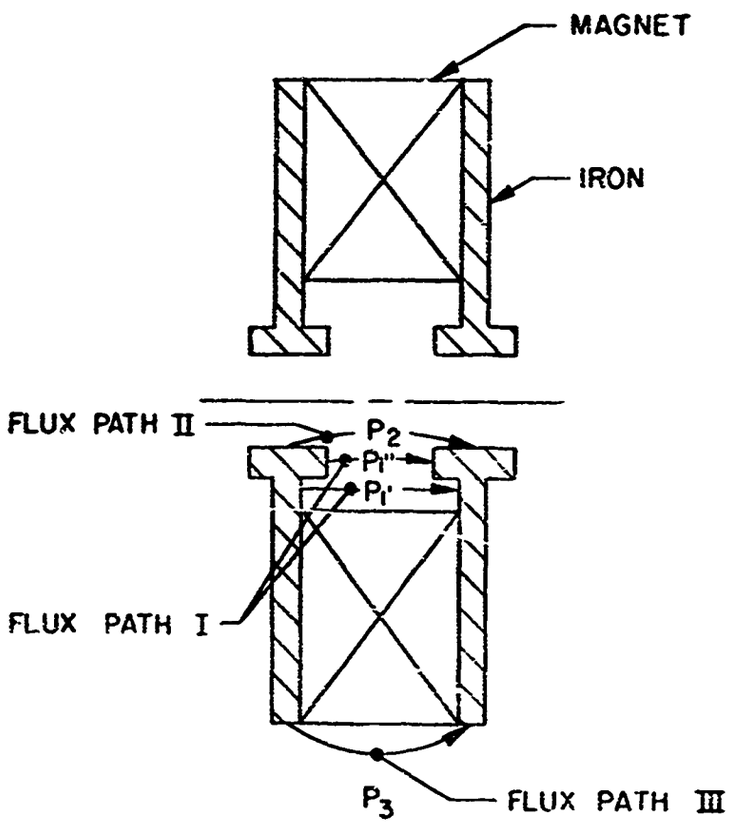

Figure 64 Manner in which external magnetic circuit is divided into three flux paths for calculation of total permeance.

and the permeance of path III is given by

$$P_3 = \sum_{m=1}^{\infty} \frac{LD_2}{Tm^2} f_3\left(\frac{mD_2}{L}\right) \sin\left(\frac{m\pi T}{L}\right) \text{ inch} \qquad \text{(VIII-8)}$$

The function $f_2\ (md_1/L)$ versus md_1/L and $f_3\ (mD_2/L)$ versus mD_2/L are plotted in Figs. 65 and 66, respectively.

The total permeance, P_T is given by

$$P_T = P_1 + P_2 + P_3 \text{ inch} \qquad \text{(VIII-9)}$$

From the following relation

$$-\frac{B_d}{H_d} = \frac{T}{A_c} P_T \qquad \text{(VIII-10)}$$

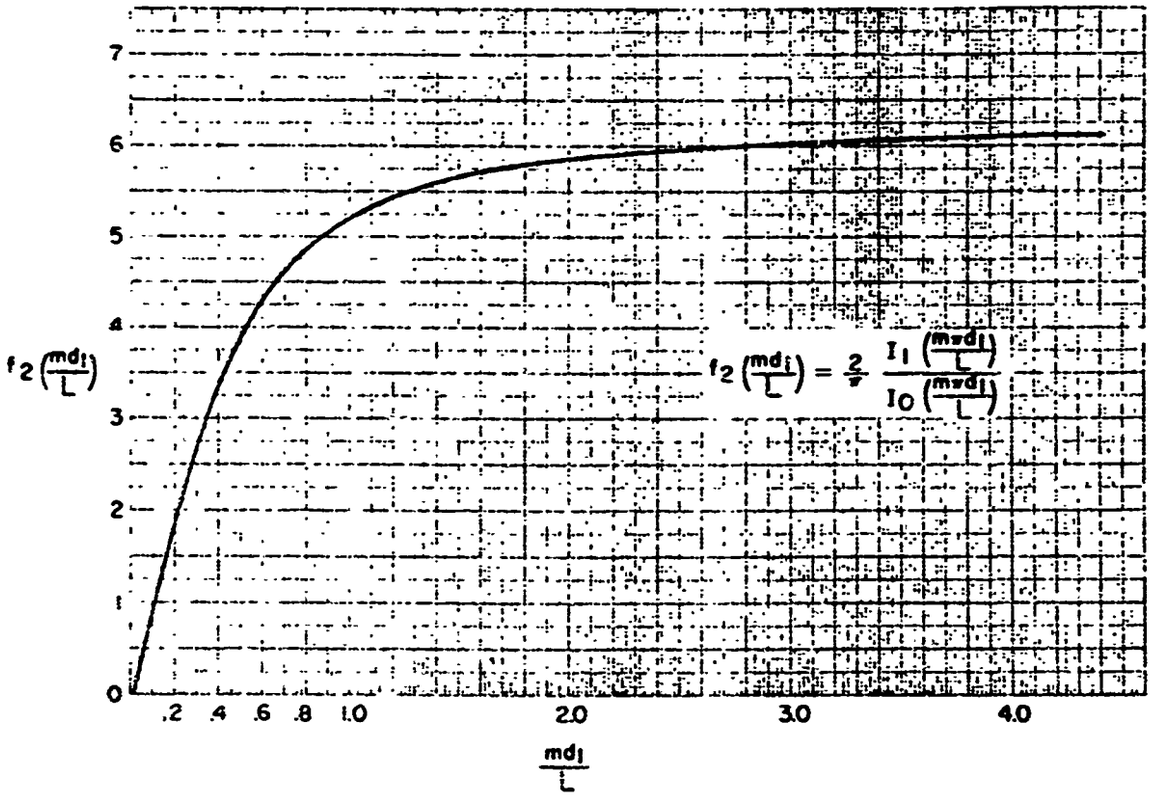

Figure 65 Plot of $f_2\ (md_1/L)$ versus $f_3\ (md_1/L)$ as used in Equation (VIII-7).

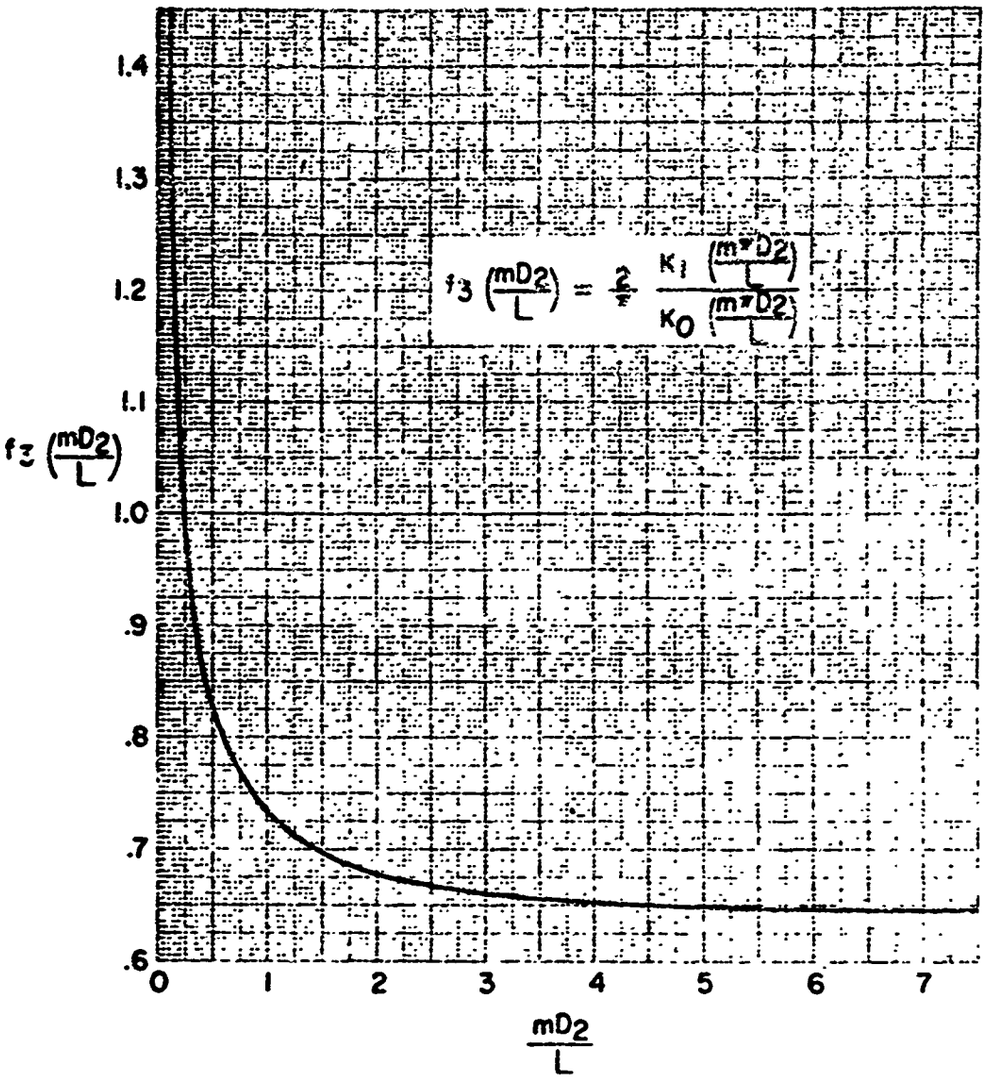

Figure 66 Plot of $f_3\,(mD_2/L)$ versus $f_3\,(mD_2/L)$ as used in Equation (VIII-8).

where

B_d = magnetic flux density of the magnet in gauss

T = $L/2 - t$ inch

A_c = cross-sectional area of the magnet

= $0.785\,(D_2^2 - d_2'^2)$ inch^2 .

A load line having a slope of B_d/H_d determined from Equation (VIII-10) drawn from the origin of the demagnetization characteristics (B_d versus H_d) of the magnetic material will intersect the demagnetization curve at the operating point and give H_d. Figure 67 shows plots of demagnetization curve for cobalt-samarium. As an example, a load line is plotted in the figure. Substituting the value of H_d into Equation (VIII-5), the peak field B_m is determined.

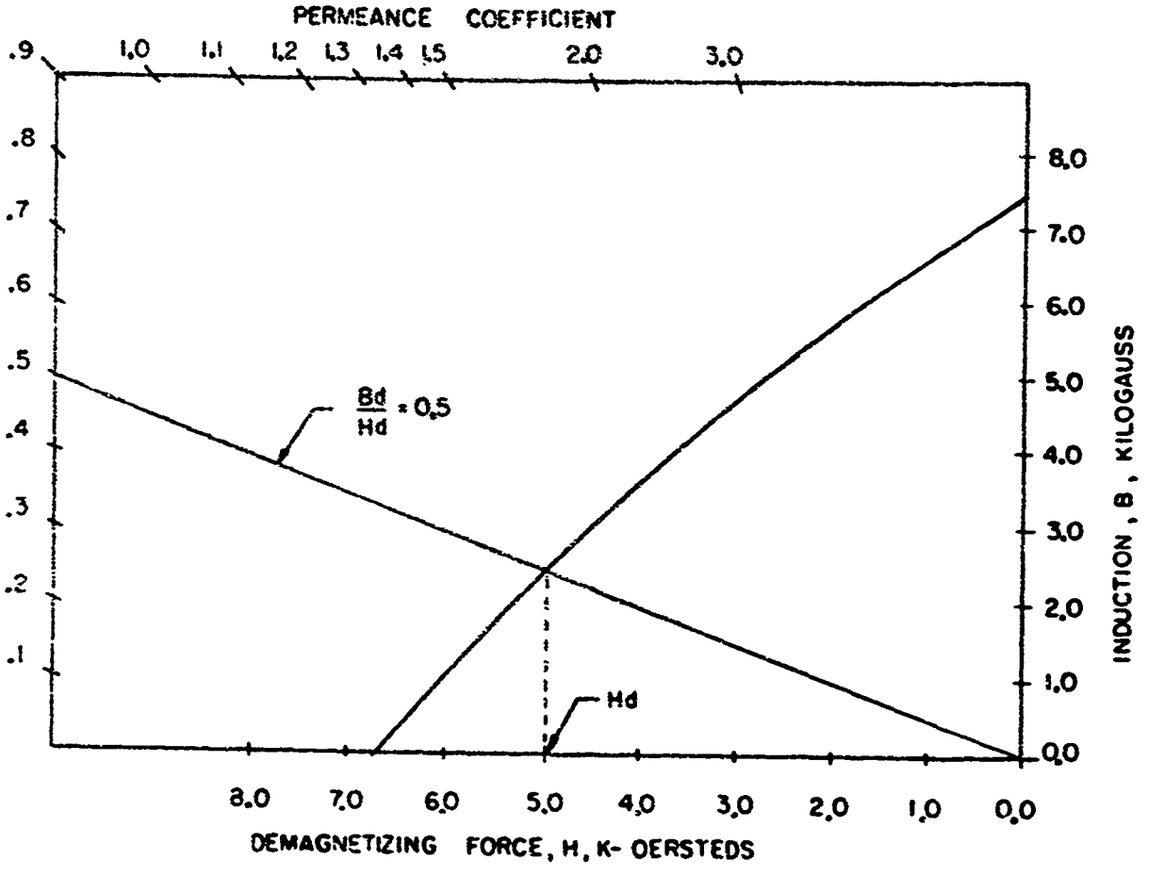

Figure 67 The demagnetization curve of Co_5Sm with sample load line plotted.

APPENDIX II

641H ACCEPTANCE TEST PROCEDURE

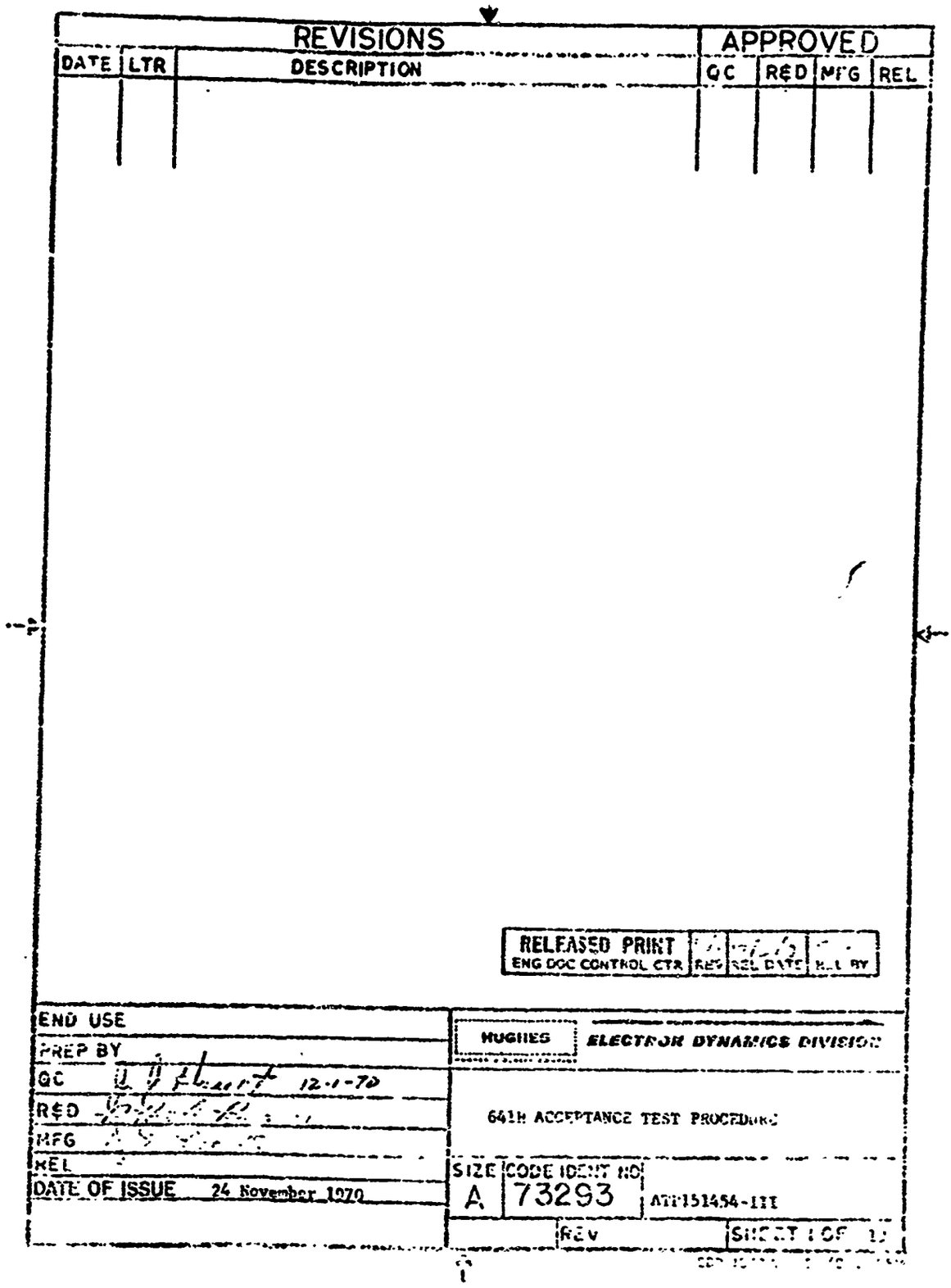

REVISIONS			APPROVED			
DATE	LTR	DESCRIPTION	QC	R&D	MFG	REL

RELEASED PRINT
ENG DOC CONTROL CTR | REV | REL DATE | REL BY

END USE
PREP BY
QC 12-1-70
R&D
MFG
REL
DATE OF ISSUE 24 November 1970

HUGHES ELECTRON DYNAMICS DIVISION

641H ACCEPTANCE TEST PROCEDURE

SIZE	CODE IDENT NO	
A	73293	ATP151454-111

REV | SHEET 1 OF 12

1.0 SCOPE

The purpose of th.s document is to delineate the acceptance tests to be performed on each delivered unit.

2.0 APPLICABLE DOCUMENTS

The following documents form a part of this document to the extent specified herein.

Drawings, HAC - EDD

B105442 Outline and Mounting Drawing

3.0 REQUIREMENTS

Acceptance tests shall be conducted at Hughes Aircraft Company, Electron Dynamics Division (EDD) or other test facilities approved by EDD.

3.1 Test Results

The results of acceptance tests shall be recorded on customer test data sheets which are controlled by this procedure and revisions hereto.

All entries made during acceptance testing must be in ink. Deletions and/or corrections to the data sheets shall be made by ruling out the appropriate portions of the test data and inserting the corrections. Ruled-out data must remain legible and be signed and dated by the person making the correction.

Completed data sheets shall be signed or stamped by the person performing the test and EDD Quality Assurance.

3.2 Preparation of Data

One copy of test results (customer test data sheets) shall be shipped with each unit.

3.3 Test Sequence

The order of test paragraphs as listed does not represent the required sequence of tests. Functional and environmental tests may be performed in any sequence. To facilitate testing, steps from one Functional Test paragraph may be performed in conjunction with steps from any other paragraph at the option of Hughes EDD.

3.4 Standard Test Conditions

Ambient test conditions for conducting acceptance tests shall be as indicated below unless otherwise specified.

A. Temperature, 50°F to 95°F

B. Relative Humidity, 90% RH or less

C. Barometric Pressure, Prevailing Laboratory Pressure

3.5 Environmental Test Tolerances

A. Vibration Amplitude	± 10%
B. Vibration Frequency	± 2%
C. Temperature	± 5°F
E. Test Time Duration	± 10%

3.6 Failure

Performance degradation during environmental exposures of burn-in will not necessarily constitute a failure. However, any performance degradation beyond the limits specified herein, will constitute a failure.

4.0 QUALITY CONFORMANCE INSPECTION, PART 1 (QCI-1)

The following tests shall be performed on each traveling wave tube (TWT), test data shall be recorded as specified in the individual test paragraph.

4.1 Operating Procedure

Install tube in test fixture, connect hydraulic lines, RF leads and DC leads. Caution Note: Only Parker No. 5-017 144905 "O" Rings are to be used at both ends of the DC lead assemblies.

4.1.1 Whenever connections are made to the oil fittings or Electrical connections the following limitations apply:

The total effective moment of torque or other distorting force which may be applied at the points where the hydraulic adapter or high voltage adapter fittings join the tube cover package, shall not exceed 30 inch pounds.

4.1.2 Turn-on of the tube shall always be as follows:

1. Supply coolant
2. Apply heater voltage
3. Apply grid bias voltage
4. Apply cathode voltage
5. After 3 minutes delay apply grid pulse voltage

4.2 Test Conditions

Tests shall be performed at room ambient temperature unless otherwise specified. Data is to be recorded at 200 Mc intervals from 4 to 8 GHz unless otherwise specified. The allowable range of electrical inputs shall be as follows:

	Min.	Max.	Units	Symbols
Heater voltage	6.03	6.27	V_{rms}	E_f
Heater current	2.4	3.5	A	I_f
Cathode voltage	-9.5	-10.5	kVdc	E_k
Grid Bias voltage (referred to cathode)	-160.0	-150.0	Vdc	E
Grid pulse voltage (referred to bias)	250	400	V	e_c
Peak grid current	---	400	ma	i_c
Peak helix current	---	833	ma	i_w
Pulse width	4.75	5.25	usec	T_p
Peak collector current	---	1.0	A	i_b
Duty	---	10.0	%	Du
Peak Cathode Current	---	2.1	A	i_k

NOTE: 1. Tests shall be performed with collector referred to cathode at 6.0 kVdc ± 5%.

2. All tests are to be performed at 10% duty cycle with the exception that environmental tests will be performed at 4% duty cycle.

4.3 Visual and Mechanical

Visual and dimensional inspection shall be performed to determine compliance to B105442

4.4 Electrical

These tests shall be performed with the TWT operating at nameplate voltages (eg those operating voltages selected for optimum performance) unless otherwise specified.

4.4.1 Heater Current

Three minutes after application of 6.15 V to the heater of the tube, the measured heater current shall be in the range 2.4 to 3.5 amperes. Record.

4.4.2 Cathode Voltage

With the electrode potentials adjusted to nameplate values, the measured cathode voltage shall be in the range from -10.5 to -9.5 kVdc. Record.

4.4.3 Cathode Current

With nameplate electrode potentials applied to the tube, the

4.4.3 Cathode Current (Cont.)

cathode current shall not exceed 2.1 amperes. (Cathode current (i_k) = $i_c + i_g$)

4.4.4 Grid Voltage

With the electrode potentials adjusted for nameplate values, the peak grid pulse voltage shall be in the range from 250 to 400 volts when measured with respect to the grid bias which shall be -150.0 Vdc to -160.0 Vdc. Record.

4.4.5 Grid Current

With nameplate values applied to the tube, the measured peak grid current shall not exceed 400 milliamperes. Record.

4.4.6 Peak Helix Current

With nameplate electrode potentials applied to the tube, the peak helix current shall not exceed 833 milliamperes. $i_w = i_k - (i_c + i_b)$. Record.

4.4.7 Peak Collector Current

With nameplate electrode potentials applied to the tube, the measured collector current shall not exceed 1.80 amperes. Record.

4.4.8 Power Output with 37 dbm Drive

The tube shall be operated with nameplate electrode potentials applied. With an input signal level of 37 dbm, the power output shall be a minimum 61 dbm. Record. Measurements shall be made at frequencies from 4 to 8 GHz at 200 Mc intervals.

4.4.9 Input and Output VSWR (Nonoperating)

The VSWR at the input of the tube shall be less that 2:1 and at the output, less than 2.5:1 in the frequency band of operation. The maximum input and output VSWR shall be measured and recorded.

5.0 QUALITY CONFORMANCE INSPECTION, PART 2 (QCI-2)

The following tests shall be performed on a minimum of three (3) tubes. Each tube selected for these tests shall be tested in accordance with the requirements of QCI-1 prior to the performance of QCI-2.

5.1 Environmental Tests

All environmental tests shall be conducted in accordance with the procedures of specification. MIL-T-5422 as modified by this procedure.

5.2 Electrical

These tests shall be performed with the TWT operating at nameplate voltages (eg those operating voltages selected for optimum performance) unless other wise specified.

5.2.1 Beam Current at Cutoff

With nameplate electrode potentials applied to the tube except grid pulse voltage equals zero, and grid bias at -150.0 Vdc. The beam current shall not exceed 500 a.

5.2.2 Stability

The tube shall be operated with nameplate electrode potentials applied. With either or both the input and output of the tube connected to circuits having a maximum mismatch ratio of 4:1. The tube's total noise and spurious power output shall not exceed 10 dbm measured through a 4 to 8 GHz band pass filter.

5.2.3 Grid Capacitance

This test shall be performed with the tube non-operating. The grid cathode capacitance shall not exceed 25 $\mu\mu$ f. The grid anode capacitance shall not exceed 20 $\mu\mu$ f. These capacitances are determined by measuring combinations of grid-anode, grid-cathode, and cathode-anode capacitance and calculating grid-cathode and grid-anode capacitances. The grid-anode and cathode-anode capacitance is found by connecting the grid terminal to the cathode terminal and measuring this combination capacitance with respect to anode (ground). This shall be designated reading M1. The grid-cathode and grid-anode capacitance is found by connecting the cathode terminal to anode ground and measuring the grid terminal capacitance with respect to anode (ground). This reading shall be designated M2. The grid-cathode and cathode-anode capacitance is found by connecting the grid terminal to anode ground and measuring the cathode terminal capacitance with respect to anode ground. This reading shall be designated M3. The grid-cathode capacitance (Cgk) is calculated from the following:

$$Cgk = \frac{M_3 + M_2 - M_1}{2}$$

The grid-anode capacitance (Cga) is calculated from the following:

$$Cga = \frac{M_1 + M_3 - M_2}{2}$$

5.2.3 Grid Capacitance (Cont

The heater termina[illegible] nnected to the heater cathode terminal during [illegible] cests.

5.3 50 Hours Burn-in (Tem[illegible] ure Cycling)

The tube shall be o[illegible] d with nameplate voltages applied and temperature cycled in the following manner:

In one hour the temperature of the input coolant shall be elevated to +90°C. The temperature of the input coolant will then be lowered to -40°+0°C in one hour. This cycle per Fig. 69. will be repeated until 5 cycles are completed, then input coolant temperature is to be raised to 90°C and maintained for 10 hours minimum.

5.3.1 At the start of burn-in while at ambient temperature, and at the middle and end of burn-in (while at +90°C), perform the tests of paragraph 4.4.8 at 4.0, 6.0 and 8.0 GHz. When performing RF tests at 6.0 GHz, record the helix, collector and cathode current.

5.4 Shock Test (Non-operating)

The tube shall be subjected to 18 impact shocks having a magnitude of 15g and a duration of 11±1 milliseconds. The intensity shall be within ±10% when measured with a filter having a bandwidth of 0.2 to 250 cycles per second, and the maximum "g" shall occur at approximately 5.5 milliseconds. The shocks shall be applied as follows in the numerical order shown in Fig. 70.

(a) Vertically, three shocks in each direction
(b) Parallel to the major horizontal axis, three shocks in each direction.
(c) Parallel to the minor horizontal axis, three shocks in each direction.

The above mentioned shocks shall be considered obtained when the tube is subjected to the shock tests by a shock machine as specified in specification MIL-S-4456, or a machine of equal performance.

5.4.1 Post Shock Test

After completion of the tests, the tube shall be carefully examined for evidence of mechanical failure and tested in accordance with paragraph 4.4.8 at F = 4.0, 6.0 and 8.0 GHz.

5.5 Salt Spray Test (Non-operating)

Tube DC connectors are to be closed with 3102052/89901/1 80901/1/12 USN caps. Tube RF connectors are to be closed with TNC weatherproof caps (or equivalent). Hydraulic fittings are to be closed with BS71394 Steel Caps. (Drain oil prior to test.)

5.5.1 General

The tube shall be supported from the bottom with the top inclined 15° from the vertical parallel with the principal direction of flow of fog through the chamber. The salt solution concentration shall be 5% sodium chloride (containing on a dry basis not more than 0.3% total impurities). The solution shall be prepared by dissolving 5 ± 1 parts by weight of salt in 95 parts by weight

5.5.1 General (Cont.)

of distilled or other water. The water used shall contain no more than 200 parts per million total solids. The solution shall be kept free from solids by filtration or decantation. The solution shall be adjusted to and maintained at a specific gravity o. from 1.0268 to 1.0413. The pH shall be maintained between 6.5 and 7.2 when measured at a temperature between 33.9° and 36.1°C. Only cp grade hydrochloric acid or sodium hydroxide shall be used to adjust the pH. The pH measurement shall be made electrometrically using a glass electorde with a saturated potassium-chloride bridge or by a colorimetric method such as bromoblue, provided the results are equivalent to those obtained with the electrometric method.

5.5.2 Operating Conditions

The temperature in the exposure core shall be maintained at $35 {}^{+1.1}_{-1.7}$ °C. Atomization shall be such that a suitable receptacle placed at any point in the exposure zone will collect from 0.75 to 2.0 milliliters of solution per hour for each 80 square centimeters or horizontal collecting area (10 cm dia) based on an average run of at least 16 hours. The solution thus collected shall have a sodium chloride content of from 4 to 6%. At least two clear fog-collecting receptacles shall be used, one placed near any nozzle and one placed as far as possible from all nozzles. Receptacles shall be fastened so they are not shielded by specimens and so that no drops of solution from specimens or other sources will be collected. The test shall run continuously for 48 hours with no interruption except for adjustment of the apparatus and inspection of the tube.

5.5.3 Post Salt Spray Test

At the completion of the exposure period, perform the tests of paragraph 4.4.8 at f = 4.0, 6.0 and 8.0 GHz. The tube shall be examined for any evidence of mechanical failure.
To aid in examination, tube shall be prepared in the following manner: salt deposits shall be removed by a gentle wash or dip in running water not warmer than 37.8°C and a light brushing using a soft hair brush or plastic bristle brush.

5.6 Vibration Test (Operating)

The tube shall be operated with nameplate voltage with the input signal adjusted to the small signal gain region at 6.0 GHz. The RF output pulse shall be monitored for modulation using a crystal and oscilloscope. Modulation of the RF output pulse due to vibration shall not exceed 20% maximum of the total output pulse.

5.6.1 Preliminary Procedure

Operation of the tube shall be continuous, and special care shall be taken to insure electrical continuity during vibration. The tube shall be securely mounted to fixture No. SP14537-31702 by means of the normal mounting screws torqued per MIL-E-4158 USAF

5.6.1 Preliminary Procedure (Cont.)

to 14 to 18 inch pounds. The RF connectors are to be safety wired, the hydraulic and high voltage fittings torqued to 30 inch pounds maximum and all leads and lines clamped to the fixture. Make such connections and instrumentation as necessary. Prior to resonance survey vibration, turn on the tube and make a reference run to check equipment.

5.6.2 Resonant Survey

Resonant modes of the tube (non-operating) shall be determined by varying the frequency of applied vibration slowly between 5 - 2000 cps at an acceleration level 50% lower than Fig. 68. Individual resonance surveys shall be conducted with vibration applied along each of three mutually perpendicular axes of the tube under test. Resonances shall be determined by the most practicable means, i.e., by 1) a stroboscope, 2) stethoscope, 3) a comparison of tube acceleration compared to table acceleration.

5.6.3 Resonance Vibration

With the tube operating, the table shall be vibrated in major horizontal axis (Fig. 70) at each of the indicated resonant points obtained in Paragraph 5.6.2, and at the amplitudes or accelerations of Fig. 68. Vibration shall be of 30 minute duration at each resonance. If more than four resonant modes are noted for any one plane the four most severe will be used. The RF output pulse shall be monitored and the maximum modulation recorded. At the completion of this step the tube shall be closely inspected for evidence of any mechanical failure.

5.6.4 Cycling

With the tube under test operating, the table shall be vibrated along a horizontal direction with the frequency varying between 5 and 2000 cycles per second at the amplitudes and accelerations as indicated in Fig. 68. The rate of frequency change shall be logarithmic and shall be such that a complete cycle (5 - 2000 - 5 cps) will consume 30 minutes. The test shall continue for the time specified in Table I. The RF output pulse shall be monitored and the maximum modulation recorded. At the completion of this step the tube under test shall be closely inspected for any evidence of mechanical failure.

5.6.4.1 Repeat paragraphs 5.6.3 and 5.6.4 with the axis of vibration changed to the minor horizontal. (Fig. 70)

5.6.4.2 Repeat paragraph 5.6.3 and 5.6.4 with the axis of vibration changed to the vertical. (Fig. 70)

5.6.4.2 (Cont.)

NOTE: In no case shall either the cycling time or the time for each resonant point be less than 30 minutes. The vibration test shall follow the schedule of Table I (time shown refers to one axis of vibration).

TABLE I

Number of resonances	0	1	2	3	4
*Total vibration time at resonance	-	30 min.	1 hr.	1-1/2 hrs.	2 hrs.
Cycling time (min.)	3 hrs.	2-1/2 hrs.	2 hrs	1-1/2 hrs.	1 hr.

* 30 minutes minimum at each point of resonance

5.6.3 Post Vibration Test

Perform the tests of paragraph 4.4.8 at f = 4.0, 6.0, and 8.0 GHz. Examine the tube for any evidence of mechanical failure.

5.7 Temperature - Altitude Test (Operating)

During this test nameplate voltages shall be applied to the tube. Whenever an R_F test is performed helix, collector and cathode current shall be recorded at 6.0 GHz.

Step 1. The tube shall be placed in the center of the test chamber making such connections and instrumentation as necessary to monitor the tube. Perform a reference run per paragraph 4.4.8 at 4.0, 6.0 and 8.0 GHz.

Step 1a. Store at -62°C until stabilized (tube non-operating). The tube temperature shall be taken as the average of the temperature measured at the two end caps.

Step 2. With the tube non-operating and coolant flowing, apply heater voltage. After 3 minutes, with input coolant temperature -40^{+0}_{-10} C apply the other electrode voltages. Adjust chamber pressure to 70,000 feet. Turn on tube and test per paragraph 4.4.8 at 4.0, 6.0 and 8.0 GHz. Tube shall be turned on and off a minimum of three times and checked for satisfactory operation immediately after the 3 minute warm-up period.

Note 1 Satisfactory operation immediately after the specified warm-up time shall be determined by data within specified limits for tests required in Step 2.

Note 2 All characteristics which are likely to be affected by low temperatures shall be checked first. Should the time required to complete the tests exceed 15 minutes beyond the warm-up time, input coolant temperature shall again be stabilized at -40^{+0}_{-10}°C and the operational check continued.

Step 3 With tube non-operating, adjust input coolant temperature to -10°C. Adjust chamber pressure to room ambient. After stabilization the chamber shall be opened, coolant flow removed and frost permitted to form on the tube. The chamber shall remain open long enough for the frost to melt but not long enough for the moisture to evaporate. The chamber shall then be closed, the tube turned on and tested per paragraph 4.4.8 at 4.0, 6.0 and 8.0 GHz. The tube shall be turned on and off at least 3 times and checked for satisfactory operation immediately after the 3 minutes warm-up period, while tube is still wet, not iced. Coolant temperature shall be -10°C during test.

Note 3 When the chamber is opened it is intended that frost will form; however, should the relative humidity of the air be such that frost will not form, an artificial means shall be used to provide the relative humidity necessary to have frost form.

Step 4 After completion of the cold test (Steps 2 and 3) and prior to starting the high temperature tests a reference run shall be made at room ambient temperature and pressure. The results obtained shall be compared to the results of the reference run made in Step 1.

Step 5 With the tube non-operating, adjust input coolant temperature to +120°C, adjust chamber pressure to room ambient. After stabilization turn on tube. The tube shall be operated continuously for 4 hours minimum, temperature readings shall be recorded every 30 minutes. At the end of the 4 hours while still at +120°C and ambient pressure, test per paragraph 4.4.8 at 4.0, 6.0 and 8.0 GHz.

Step 6 With the tube non-operating adjust chamber pressure to 70,000 feet with the input coolant temperature at +120°C. After stabilization turn on tube.. The tube shall be operated continuously for 4 hours, temperature readings shall be recorded every 30 minutes. At the end of the 4 hours while still at +120°C and 70,000 feet, test per paragraph 4.4.8 at 4.0, 6.0 and 8.0 GHz.

Step 7 Adjust input coolant temperature and chamber pressure to room ambient. After stabilization, test per paragraph 4.4.8 at 4.0, 6.0 and 8.0 GHz.

5.8 <u>Final Functional Test</u>

Repeat paragraphs 4.4.1 through 4.4.9.

HUGHES ELECTRON DYNAMICS DIVISION	SIZE A	CODE IDENT NO 73293	TP 151424
DATE OF ISSUE		REV	SHEET 12 OF 19

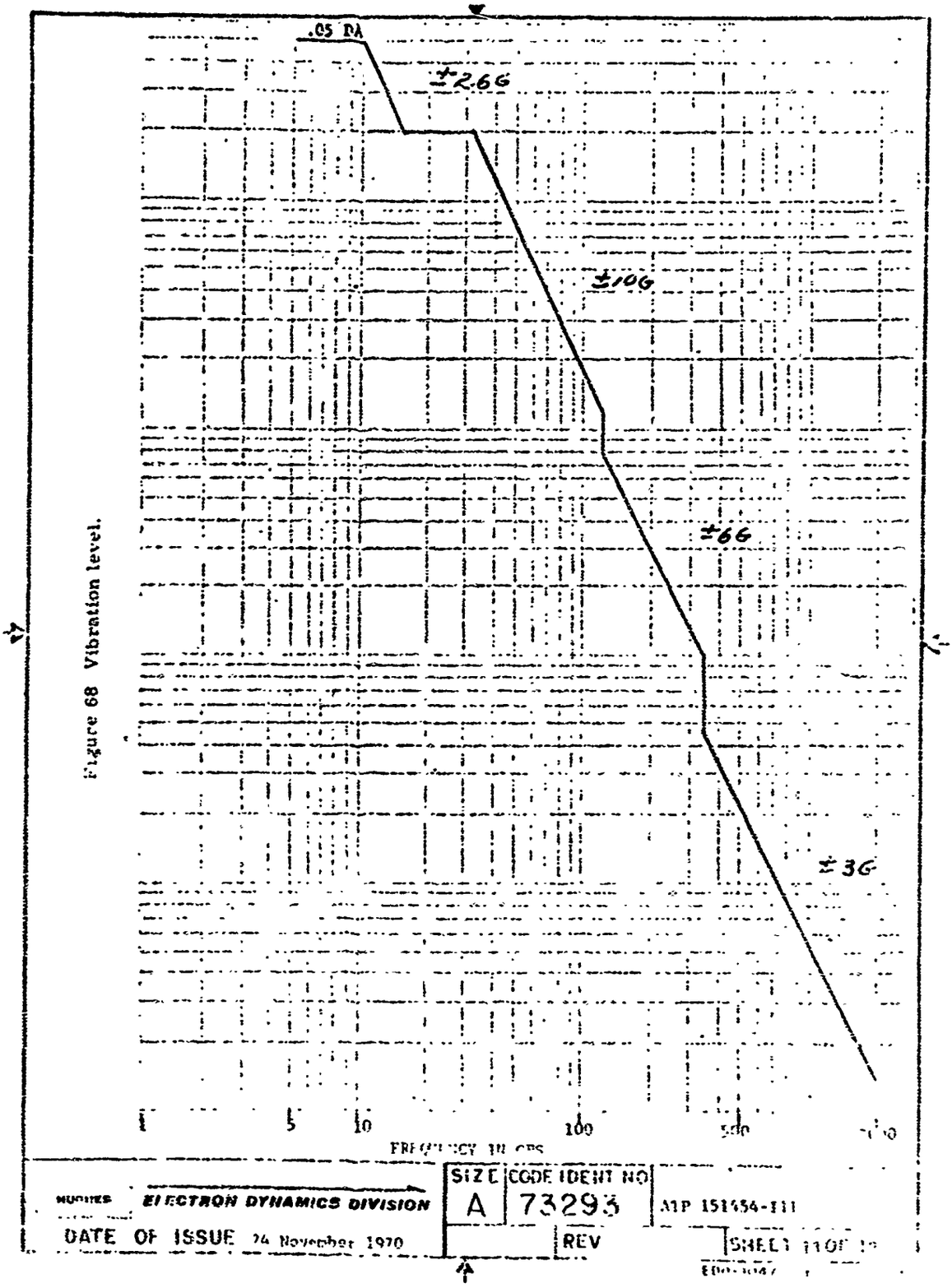

Figure 68 Vibration level.

NOT REPRODUCIBLE

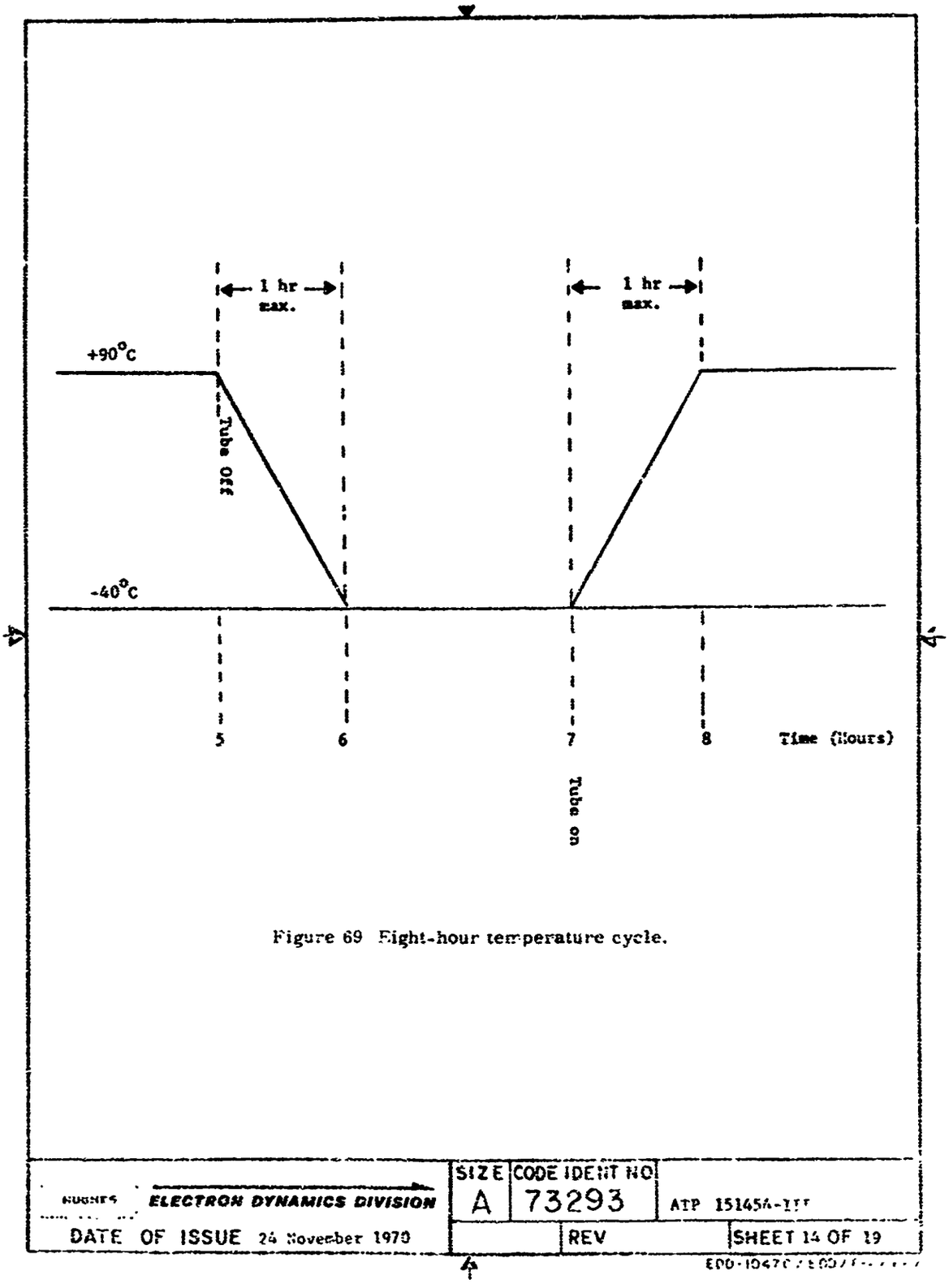

Figure 69 Eight-hour temperature cycle.

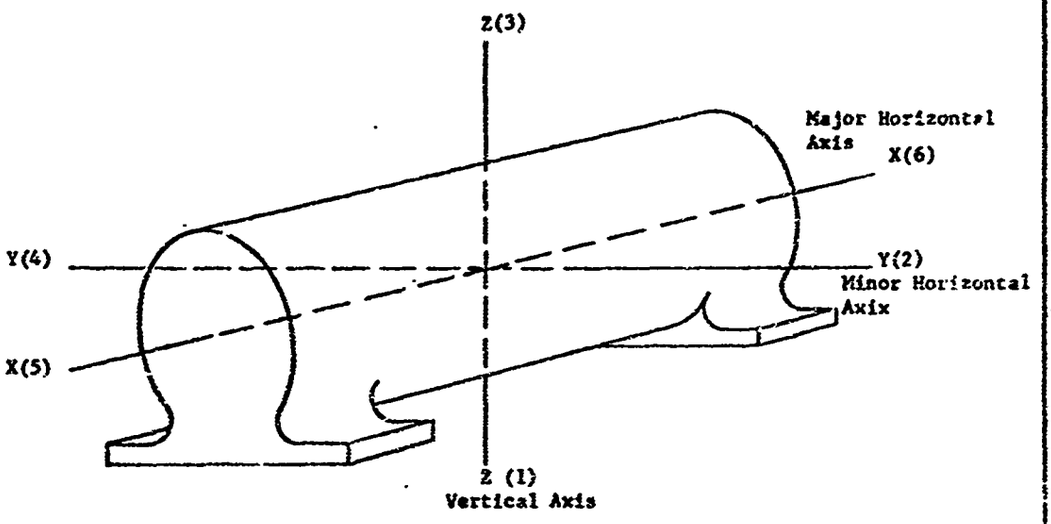

Figure 70 Numerical order and orientation of shock.

HUGHES ELECTRON DYNAMICS DIVISION	SIZE A	CODE IDENT NO 73293	ATP 151454-III
DATE OF ISSUE 24 November 1970		REV	SHEET 15 OF 15

EDD-1047C/E

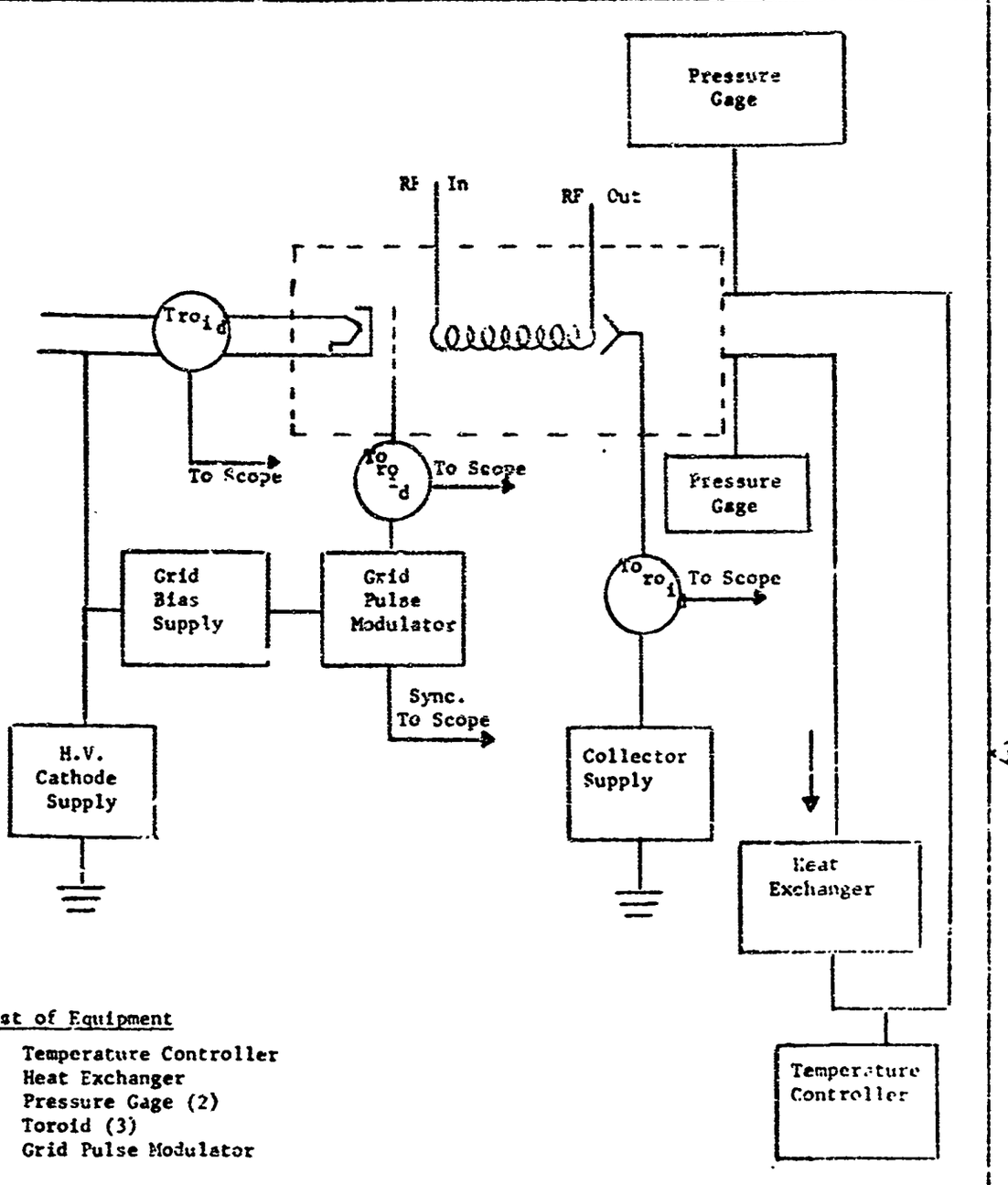

List of Equipment

1. Temperature Controller
2. Heat Exchanger
3. Pressure Gage (2)
4. Toroid (3)
5. Grid Pulse Modulator

(This item includes the heater isolation transformer, grid bias supply, grid pulse modulator, and high voltage cathode supply.)

*Note: Helix currents cannot be monitored when tube is packaged.

Figure 71 Coolant, pulse, and d-c operating circuit.

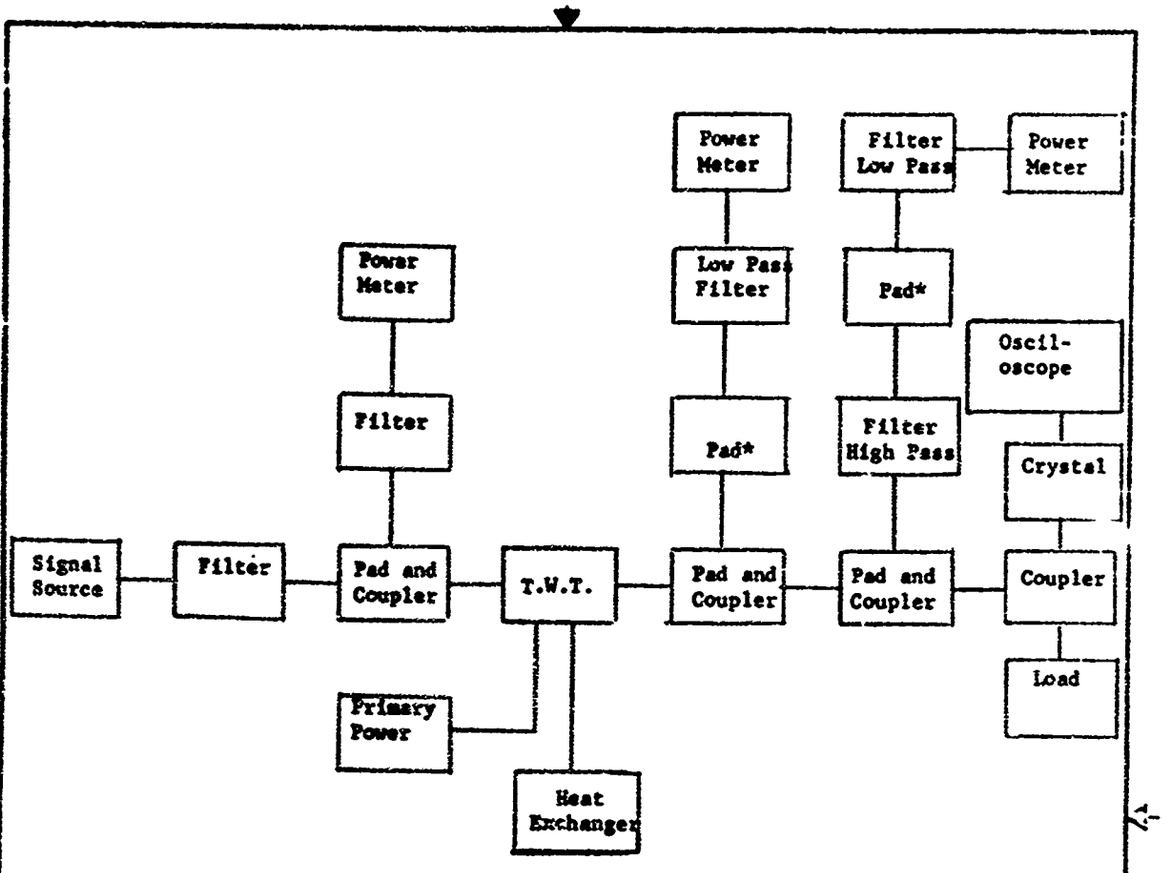

Figure 72

List of Equipment

Signal Source
Filer (4)
Pad and Coupler (3)
Power Meter (3)
Load
Primary Power Source
Heat Exchanger
Pad (2) * - attenuation dependent on duty cycle
Coupler
Crystal
Oscilloscope

HUGHES ELECTRON DYNAMICS DIVISION	SIZE A	CODE IDENT NO 73293	ATP 151454-III
DATE OF ISSUE 24 November 1970		REV	SHEET 17 Or 19

EDD-1047C/EDD/8-67 RS

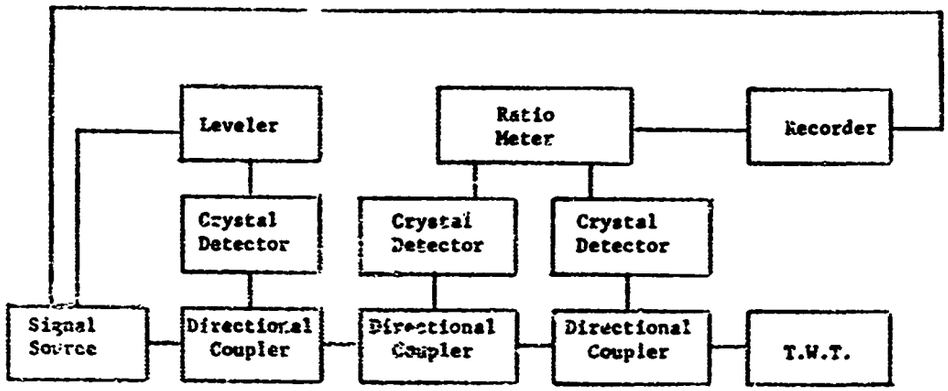

List of Equipment

Sweeping Power Supply and BWO
Directional Coupler
Crystal Detector
Leveler
Matched Directional Couplers (2)
Coax Detector (2)
Ratio Meter
Recorder

Figure 73 Cold VSWR block diagram.

HUGHES ELECTRON DYNAMICS DIVISION | SIZE A | CODE IDENT NO 73293 | ATP 151454-111

DATE OF ISSUE 24 November 1970 | REV | SHEET 18 OF 19

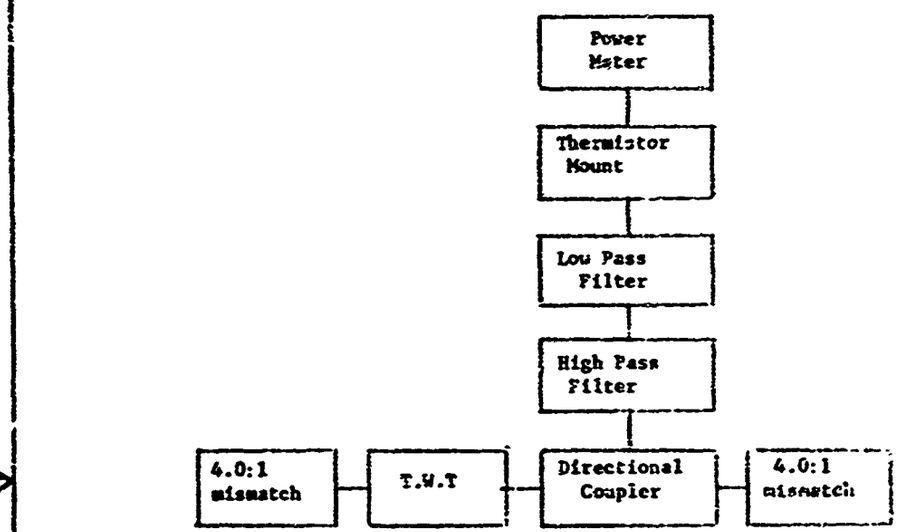

List of Equipment

4.0:1 mismatch (2)
Directional Coupler
High Pass Filter
Low Pass Filter
Crystal Detector
Thermistor Mount
Power Meter

Figure 74 Spurious power output block diagram.

HUGHES ELECTRON DYNAMICS DIVISION	SIZE A	CODE IDENT NO 73293	TP 15454-311
DATE OF ISSUE 24 November 1970		REV	SHEET 10 OF 14

SECTION IX

SUMMARY (M. G. Benz)

A pre-production pilot line capable of producing cobalt-samarium magnets has been established (Sections VI and VII).

The properties of magnets produced on this pre-production pilot line exceeded the target specifications for this program (Section VII).

The cost of magnets produced on this pre-production pilot line was approximately one fourth the cost the same size magnet would be if fabricated from cobalt-platinum.

Magnets produced on this pilot line have been used to fabricate traveling wave tubes (Section VIII and Ref. 1).

The performance of these tubes indicates that cobalt-samarium magnets are suitable for fabrication of traveling wave tubes; and, in fact, that they will allow significant advances in the state-of-the-art in the design of such tubes (Section VIII and Ref. 1).

Pre-Production Pilot Line

The individual steps utilized in the pre-production pilot line include melting, powder preparation, blending, alignment, pressing, sintering, heat treatment, shaping, and magnetizing.

Melts were prepared by induction melting. Two compositions were prepared for subsequent blending as powder to the desired final composition (approximately 62 to 63 wt % Co). The melt compositions were 66 wt % Co, 34 wt % Sm, and 40 wt % Co, 60 wt % Sm. These were chosen to take advantage of the multiphase approach to the sintering process. For this particular case, the 40 wt % Co alloy is partially liquid at the sintering temperature and we have referred to this as liquid-phase sintering (Section II and Ref. 2).

The cast ingots were reduced to powders in the 10μ size range by a series of steps which included jaw crushing, double-disk pulverizing, and milling in a fluid energy mill with nitrogen as the working gas. The two compositions were blended together at this stage to achieve the desired final composition (Section VI).

Next the blended powder was oriented in a magnetic field of 60 kOe and then compacted to a density of approximately 6.9 g/cm^3 by application of hydrostatic pressures up to 200 kpsi. (Relative density approximately 80%. Full density was taken as 8.6 g/cm^3 for this alloy.)

The oriented pressings were then further densified by means of a high-temperature diffusion-type sintering process. Following sintering, a thermal aging treatment was sometimes used to regain coercivity lost during sintering (Section VII and Refs. 3, 4).

The sintered bars were shaped into half-ring magnets by slicing and grinding, magnetized, and shipped. Following magnetizing, a thermal knockdown was sometimes used to bring the irreversible losses within the specified limit (Section VII and Ref. 4).

Properties

The properties of magnets produced on the pre-production pilot line in general significantly exceeded:

$(BH)_{max}$	15 MGOe
B_r	8.2 kG
H_c	-6.5 kOe
H_d (at B/H = -1/2)	-5.0 kOe
Irreversible loss after exposure to 150°C (B/H = -1/2)	less than 10%

The uniformity of the properties of magnets within each lot was high, and lot-to-lot variations were minimal for a pre-production pilot line at this stage in its development (Section VII).

Traveling Wave Tubes

Five traveling wave tubes were successfully fabricated and operated. Data gathered indicate that a significant advance in the state-of-the-art is possible.

Conclusion

The sequence of unit operations utilized in this program can be used to fabricate high-performance cobalt-samarium magnets. Furthermore, with some modifications, the same basic technology seems to lend itself to successful fabrication (on a research basis at least) of magnets containing rare earth elements other than samarium (Refs. 3, 5-8).

REFERENCES

1. J. E. Grant, M. G. Benz, and D. L. Martin, "A 2 KW, Multi-Octave TWT Focussed with Cobalt-Samarium Magnets," IEEE International Devices Meeting, Washington, D. C., Oct. 28-30, 1970.

2. M. G. Benz and D. L. Martin, "Cobalt-Samarium Permanent Magnets Prepared by Liquid Phase Sintering," Appl. Phys. Letters, 17, 176 (1970).

3. M. G. Benz and D. L. Martin, "Cobalt-Mischmetal-Samarium Permanent Magnet Alloys: Process and Properties," J. Appl. Phys., 42 (June 1971).

4. D. L. Martin and M. G. Benz, "Magnetization Changes for Cobalt-Rare Earth Permanent Magnet Alloys when Heated to 650°C, submitted to J. Appl. Phys.

5. D. L. Martin and M. G. Benz, "Cobalt-Rare Earth Permanent Magnet Alloys," Cobalt, 50, 11 (March 1971).

6. D. L. Martin and M. G. Benz, "Magnetic Properties of Cobalt-Rare Earth Magnets for Microwave Applications," IEEE Trans. Mag. (June 1971).

7. J. Tsui and K. Strnat, "Sintering of $PrCo_5$ Permanent Magnets," J. Appl. Phys., 42 (1971).

8. J. Tsui and K. Strnat, "Sintering of $PrCo_5$ Magnets with Pr-Co Alloy Addition," Intermag. Conf., Denver, Colo., April 13-16, 1971.

SECTION X

The Program Schedule Milestone Report (Item B001) being used for this program is included as Table XLIII.

TABLE XLIII

Manufacturing Methods and Technology for Production of Cobalt Samarium Magnets

CONTRACT NO. F33615-70-C-1098
PROJECT NO. 612-9

Milestone Status Report #

Phase I - Analysis
1. Analysis of Problem
2. Materials Processes - Powder preparations
3. Materials Processes - Magnet preparation
4. Selection of Microwave Device - Final Specifications
5. Magnet Characterization - Final Specifications
6. Preproduction Samples - 10

Phase II - Determination of Manufacturing Processes
7. Powder Process evaluation & Selection
8. Magnet Fabrication Evaluation & Selection

Phase III - Pilot Line Program
1. Pilot Line Construction - Powder
2. Pilot Line Construction - Magnets
3. Pilot Line Process Optimization Studies
4. Sample Magnets for TWT's
5. Pilot Line Production for TWT's
6. Pilot Line Production for AFML/MATB

Phase IV - Microwave Device Application of Co-Sm Magnets
1. Evaluation of Magnets in TWT's
2. Environmental Testing of Magnets & TWT's

Deliveries:
1. Data (Item 1AA)
2. Preproduction Samples - 10 (Item 1AB)
3. Pilot Production Magnets - 250 (Item 1AC)
4. Co-Sm TWT's - 5 (Item 1AD)
5. Status Display (Item 1AE)

Reports:
Monthly Letter
Quarterly Report
Final Report (Draft)
Final Report (Distribution)

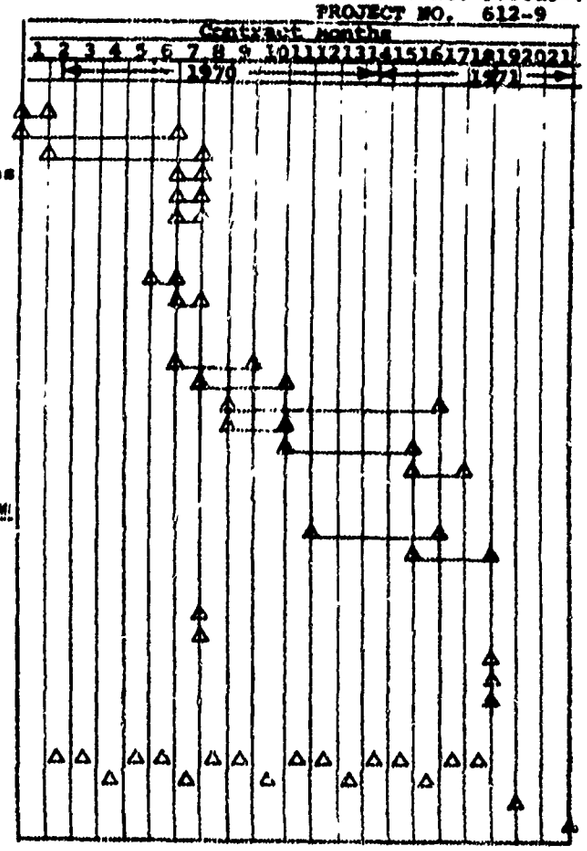

Legend
Scheduled event △
Time span △——△
Completed event ▲

General Electric Company
Research & Development Center

SECTION XI

Contract Work Statement: Exhibit A

A. PURPOSE AND OBJECTIVE

1. The purpose of this project is to make available cobalt-samarium magnets with specific physical and magnetic properties especially developed for application to traveling wave tubes (TWT's).

2. The specific objective of the project is to establish the manufacturing methods, processes, techniques, and special equipment for the economic fabrication of cobalt-samarium magnets in production quantities. Production capability will be demonstrated in a pilot line production. This effort is to establish low-cost fabrication techniques for quality, quantity, production of Co_5Sm Magnets applicable to traveling wave tubes and shall be adaptable to other devices.

B. SCOPE

The project is to be divided into four phases: I--Analysis; II--Determination of Manufacturing Processes; III--Preproduction Pilot Line; and IV--Microwave Device Application of Co_5Sm Magnets.

1. Phase I--Analysis

a. Objective - The objective of this phase is to analyze the problems associated with the establishment of manufacturing methods for the economical fabrication of cobalt-samarium magnets in production quantities and to formulate a production plan for providing Co_5Sm magnets.

b. Criteria and Approach

(1) The effort under Phase I shall be directed toward evaluation of the unit operations involved in manufacturing high-quality Co_5Sm magnets with respect toward their economics, reproducibility, and ease of transition into the magnet producing industry.

(2) The work in this phase shall be divided into the following tasks:

Task 1--Raw Materials
Task 2--Melting and Casting
Task 3--Crushing
Task 4--Milling and Classifying
Task 5--Powder Storage

Task 6--Mixing Additives
Task 7--Magnetizing and Aligning Powder
Task 8--Pressing
Task 9--Sintering
Task 10--Shaping
Task 11--Magnetizing the Magnets
Task 12--Shipping

Task (1) RAW MATERIALS - Various methods for the preparation of powders for the manufacturing process shall be evaluated. This evaluation shall take into consideration the desired economic and magnetic properties. The results of the contractor's in-house program to evaluate as a starting material for production of traveling wave tube magnets, cobalt-samarium powder produced by the alkaline earth hydride direct reduction of samarium oxide shall be made available to the Air Force.

Task (2) MELTING AND CASTING - An evaluation to determine the best type of process suited for the large-scale alloy melting will be made. The aspects of processes to be evaluated will include: arc melting, induction melting, atmosphere, crucible type, melt practice, mold size and geometry, and cost structure.

Task (3) CRUSHING - Pilot scale facilities at available developmental laboratories will be evaluated to define the most practical and desirable method of crushing.

Task (4) MILLING AND CLASSIFYING - Several techniques will be evaluated to obtain the best method for grinding and classifying. These techniques will include ball milling (plus screening and alternating magnetic field), fluid energy milling, and fluid energy mill classifying.

Task (5) POWDER STORAGE - Various storage practices using the powder to be involved in the manufacturing process, will be examined with respect to both effectiveness in preventing degradation and cost.

Task (6) MIXING ADDITIVES - A determination will be made of the most efficient mixing practices, such as ball milling or tumbling, with consideration to uniformity of mixing, plant investment, maintenance, and cost of operation.

Task (7) MAGNETIZING AND ALIGNING POWDER - An investigation will be carried out to determine the necessity for separate magnetic treatments for premagnetization and for aligning, with an objective of determining the most producible and economical process for obtaining the optimum degree of alignment. The magnitude of the fields to be employed will be evaluated with respect to both economic and feasibility of incorporation into a manufacturing process.

Task (8) PRESSING - Both die pressing and hydrostatic pressing will be evaluated with respect to their manufacturing processes.

Task (9) SINTERING - An evaluation will be directed toward the choice of furnaces and toward their economic operation in a manufacturing process line. Consideration will be given to the optimum time-temperature combination in terms of equipment, maintenance, and reliability. A major emphasis will be placed in the choice of atmosphere control that is most appropriate for manufacturing processing and which is in keeping with the high purity requirements.

Task (10) SHAPING - Consideration will be given to the most economical approach to obtain desired final shapes. Included in these considerations will be (1) sintering to shape and (2) grinding after sintering.

Task (11) MAGNETIZING THE MAGNETS - An evaluation will be made to determine the most economical and effective manner of maintaining the large magnetic fields necessary to fully magnetize Co_5Sm magnets in a production line. Approaches to be considered include: large electromagnets, superconducting coils, and current-pulse magnetization.

Task (12) SHIPPING - The problem of shipping Co_5Sm magnets will be studied with respect to the relative advantages of shipping magnets in a magnetized or in a nonmagnetized condition. Attention will be given to problems of concern both to the magnet manufacturer and to the magnet user.

c. Selection of Microwave Device - The traveling wave tube to be used in the evaluation of the Co_5Sm magnet shall be tube number, Hughes 641H. The performance characteristics of this tube shall be specified.

d. Magnet Characterization

(1) Target Specifications (See Exhibit A-1)

(2) A complete specification of performance capability of the specified Co_5Sm magnet to be produced on this program, both by itself and in a periodic permanent magnet stack arrangement, shall be made at the end of this phase; and submitted as a part of Exhibit B, Sequence Number B001.

2. Phase II--Determination of Manufacturing Process

a. Objective - The objective of this phase is to finalize the processes and techniques that comprise the most economic and reliable manufacturing operation.

b. Criteria and Approach - This determination shall be based on the information obtained in Phase I. Phase I steps shall be reviewed to

optimize each step. Written approval shall be obtained through Procurement, ASNKR-10, for this phase prior to proceeding to Phase III.

3. Phase III--Preproduction Pilot Line

a. Objective - The objective of this phase is to establish a pilot line capable of producing 1000 magnets per month (per 8-hour shift).

b. Criteria and Approach - A production of 250 fully qualified Co_5Sm magnets produced by production personnel shall be delivered to the Air Force Materials Laboratory to demonstrate production line performance. The performance characteristics of production line magnets shall be determined to insure compliance with the performance specification defined in Phase I. Magnet dimensions shall be suitable for incorporation into Hughes 641H traveling wave tubes. Exact size, shape, etc. shall be submitted for approval by AFML-MATE through the Procuring Contracting Officer at completion of Phase II.

4. Phase IV--Microwave Device Application of Co_5Sm Magnets

a. Objective - The objective of this phase is to demonstrate the superior functional characteristics of Co_5Sm traveling wave tubes.

b. Criteria and Approach - A minimum of five (5) Hughes 641H traveling wave tubes shall be obtained for evaluation of the Co_5Sm material, and the performance of these tubes shall be compared with that of other state-of-the-art tubes. To ensure Air Force System applicability, the Co_5Sm TWT's shall be evaluated according to MIL-5400 Class II requirements including:

(1) Humidity	(4) Vibration
(2) Salt Spray	(5) Temperature
(3) Shock	(6) Altitude

5. Static Display--One (1) static display depicting cobalt-samarium magnet manufacturing processes shall be provided.

ATTACHMENT NO. 1

EXHIBIT A

MAGNET CHARACTERISTICS (TARGET SPECIFICATIONS)

Residual Induction (B_r)	> 7500 gauss
Coercive Force (H_c)	> 7500 oersted
Intrinsic Coercive Force (H_c)	> 12000 oersted
Energy Product (BH_{max})	15×10^6 gauss-oersted
Temperature Stability	0.05% per °C
Magnet Life	Flux variation of <5% over 1000 hours at 150°C for a magnet with load line of minus 1.
Curie Point	> 700°C
Mechanical Properties	
Integrity	< 3% weight loss during normal handling (during shipping and assembly of TWTs)
Hardness	$R_c \cong 50$
Impact Strength	Capable of withstanding normal handling, assembly, and operation of TWT tubes consistent with MIL-5400 class II environmental requirements.
Flexural Strength	> 5000 psi
MIL-B-5400 Tests	
Corrosion	None
Temperature Extremes	Within 95° of original (-55°C to 250°C) room temperature properties.

END